Molecular Cloning, *In Vitro* Expression, and Functional Characterization of an Ovine Gastrointestinal Peptide Transporter (oPepT1)

YuanXiang Pan

Dissertation submitted to the Graduate Faculty of the
Virginia Polytechnic Institute and State University
in partial fulfillment of the requirements
for the degree of

DOCTOR OF PHILOSOPHY

in

Animal and Poultry Sciences, emphasis: Animal Nutrition

Dr. E. A. Wong, Co-Chair
Dr. K. E. Webb, Jr., Co-Chair
Dr. J. R. Bloomquist
Dr. B. A. Davis
Dr. D. M. Denbow

February 11, 2000

Blacksburg, Virginia

Key Words: Cloning, Characterization, Ovine, Peptide, Transporter, oPEPT1.

Molecular Cloning, *In Vitro* Expression, and Functional Characterization of an Ovine Gastrointestinal Peptide Transporter (oPepT1)

YuanXiang Pan

(Abstract)

We reported the primary structure, tissue distribution, and *in vitro* functional characterization of a peptide transporter, oPepT1, from ovine intestine. The ovine intestinal oPepT1 cDNA was 2,829 bp long encoding a protein of 707 amino acid residues with an estimated molecular size of 79 kDa, and a pI of 6.57. The cDNA contained a 79-bp 5' untranslated sequence and a 630-bp 3' untranslated sequence. The proposed oPepT1 protein was 77.9, 81.3, and 82.6 percent identical to PepT1 from rabbit, rat, and human, respectively. High stringency northern blot analysis demonstrated that oPepT1 is expressed strongly in the small intestine, at lower levels in the omasum, and at much lower levels in the rumen, but is not expressed in liver and kidney. The presence of the peptide transporter in the forestomach at such levels could provide amino acid nitrogen for the ruminant in a nutritionally significant manner. Transport function of oPepT1 was assessed by expressing oPepT1 in *Xenopus* oocytes using a two-electrode voltage-clamp technique. Overall, the *in vitro* transport characteristics of oPepT1 expressed in oocytes were similar to those of PepT1 from other species. The transport process is electrogenic and pH-dependent, but independent of Na^+, Cl^-, and Ca^{2+}. It displayed a broad substrate

specificity that transported neutral and charged dipeptides and tripeptides. All dipeptides and tripeptides examined evoked inward currents in a saturable manner, with an affinity constant (K_t) ranging from 20 μ*M* to .6 m*M* for dipeptides and .15 to 3.0 m*M* for tripeptides. No responses were detected from tetrapeptides or free amino acids. Although many of the properties displayed by oPepT1 were similar to those of PepT1 from other species, some differences were noted. First, the isoelectric point of oPepT1 was lower than that of others, but the oPepT1 protein appeared to have the same biological activity as that of others at a physiological pH. Second, more potential phosphorylation sites for protein kinases were present in oPepT1. Third, compared with PepT1 from other species, oPepT1 has more negatively charged amino acids at its C-terminus.

Acknowledgements

I would like to express my sincere appreciation to Drs. E. A. Wong and K. E. Webb, Jr., my committee chairs, for their patience, experienced guidance, inspiration and assistance throughout my graduate training and in the preparation of this manuscript. Without their efforts and support, I would never have begun, nor continued, my academic development at Virginia Tech.

I am indebted to Dr. J R. Bloomquist for providing me with the opportunity to study electrophysiology in his lab. His guidance, assistance, comments and discussions of my data allowed me to accomplish my project successfully.

I am grateful to Drs. B. A. Davis and D. M. Denbow for their interest, encouragement, and willingness to serve as my committee members.

I am grateful to Drs. J. C. Matthews and K. Kurima for their assistance, friendship, and many valuable discussions that facilitated my research at Tech.

I especially thank Donald Shaw, Kristin Lee and Martha McCollum for their friendship, technical discussions and support during my research.

I wish to express my deepest appreciation to my wife, Hong Chen, for her support and many sacrifices, which made my graduate program possible.

Table of Contents

List of Tables

Table

List of Figures

Figure

Chapter I

Introduction

In the decade of the 1990s, the application of molecular biotechnology to nutrition and pharmacology research has provided fascinating information on peptide transport processes. The cloning and characterization of both intestinal (PepT1) and renal (PepT2) peptide transporters from different species have had major impacts on the understanding of peptide transport in mammalian species (Fei et al., 1994; Liang et al., 1995; Saito et al., 1995; Miyamoto et al., 1996). The unique structural and functional features shared by these peptide transporter proteins have attracted considerable interest from researchers to examine these systems. Most of the studies have been focused on peptide absorption in the gastrointestinal tract, kidney (Daniel, 1996), liver, and skeletal muscle in human and laboratory animals (Leibach and Ganapathy, 1996). The low affinity peptide transporter, PepT1, is mainly expressed in the small intestine with little expression occurring in liver and kidney (Fei et al., 1994; Liang et al., 1995; Miyamoto et al., 1996). The high affinity peptide transporter, PepT2, is mainly expressed in kidney (Saito et al., 1996). The general structures of the peptide transporter proteins PepT1 and PepT2 are similar in that they both contain 12 transmembrane domains and a large extracellular loop between transmembrane domains 9 and 10 (Fei et al., 1994; Meredith and Boyd, 1995). The amino acid sequences of the 12 transmembrane domains are highly conserved (85% identity), whereas the sequences of the extracellular loops are less conserved (35% identity; Daniel, 1996). These peptide transporters appear to be able to recognize most dipeptide and tripeptide substrates, as well as some pharmacologically active compounds including the

β-lactam antibiotics, angiotensin-converting enzyme (ACE) inhibitors, and the antitumor agent, bestatin (Leibach and Ganapathy, 1996). More recent research in tissues such as the brain, lung, liver, and pancreas expressing peptide transporter mRNA suggest that peptide transport may be a more wide-spread phenomenon in animals. Therefore, the overall physiological importance of peptide transport in animals remains to be investigated.

Although peptide transport is an important physiological process that occurs in tissues of animals (Matthews, 1991), little research has been conducted to identify the system(s) responsible for the absorption of peptides in domestic animals. Early studies from our laboratory indicated that peptides might be absorbed from the ruminant gastrointestinal tract (Koeln et al., 1993) and recent reports demonstrate the existence and tissue distribution of a peptide transporter(s) in sheep, cows, pigs, and chickens (Matthews et al., 1996; Pan et al., 1997; Chen et al., 1999). Expression of mRNA in *Xenopus* oocytes showed that the mRNA present in sheep omasal epithelial tissue was capable of transporting di- to tetrapeptides. Although the size of the mRNA varied among species, the mRNA was present in the small intestine of all animals examined and the omasal and ruminal epithelium of sheep and cows. These results suggest that peptide absorption may be nutritionally important in the ruminant as well as other domestic animals.

Studying the structure, function, capacity, and regulation of the peptide transporter protein(s) in ruminants should not only provide us knowledge of the transport system in these animals, but should also help us understand the role that peptides may play as

sources of amino acids. This knowledge should enhance our ability to manage animal diets for better performance without causing significant nitrogen imbalance. The main objective of this study was to clone and express the ovine peptide transporter and to characterize the function of this transporter *in vitro* by expression in *Xenopus* oocytes.

Chapter II

Review of Literature

Absorption of small peptides makes a significant contribution to meeting protein requirements in animals (Matthews, 1991; Adibi, 1997). cDNA for rabbit (Fei, et al., 1994), human (Liang, et al., 1995) and rat (Saito et al., 1995) intestinal peptide transporters have been cloned. As indicated by functional studies, this cDNA directed proton-coupled absorption of dipeptides and tripeptides, as well as absorption of a number of important clinical drugs, such as β-lactam antibiotics. Therefore, a thorough investigation of peptide transporters has both therapeutic and nutritional applications. The purpose of this review is to describe current information related to the transport of small peptides and the application of knowledge from these studies to a better understanding of the nutritional physiology of animals.

Peptide Transporters and the POT Family

Traditionally, it was believed that proteins and peptides had to be broken down to single amino acids in order to be absorbed into cells in animals. The existence of peptide transport has been documented for years (Matthews, 1991) and the existence of specific carriers for the peptide transport process was proposed more than two decades ago (Matthews and Adibi, 1976). The recent cloning of several cDNA in different species has led to the identification of specific peptide transporters, which are membrane proteins

responsible for selective translocation of small peptides across the cell membrane in all species.

Transporters are a group of membrane proteins responsible for the movement of a large range of substrates across biological membranes into cells. These substrates, in both prokaryotes and eukaryotes, include osmolytes, sugars, amino acids, peptides, neurotransmitters, and drugs. Many transporters have been cloned, sequenced, and functionally expressed in expression systems. Peptide transport across membranes, as a mechanism for acquiring necessary carbon and nitrogen, has been well studied in bacteria (Ames et al., 1990). The ATP-binding cassette (ABC) transporter family is a system found to be involved in the peptide transport processes in bacteria (Tam and Saier, 1993). These transporters utilize ATP directly as the driving force to move substrates across the cell membrane against a concentration gradient. A typical ABC transporter has two nucleotide-binding domains that interact with ATP. A particular ABC transporter accepts only a narrow range of substrates. For instance, some of them transport only dipeptides, some of them transport only tripeptides, and some others recognize larger peptides.

Unlike the ABC transporters, the peptide transporter systems in animals belong to the proton-coupled oligopeptide transporter (POT) family (Paulsen et al., 1994). The POT family members do not have the nucleotide-binding domains that are needed for ATP binding and hydrolysis. The transmembrane proton gradient generated by the Na^+-H^+ exchanger is the driving force for the POT transporters (Figure 2.1). Since the first discovery of the POT family, known members of this family have increased considerably,

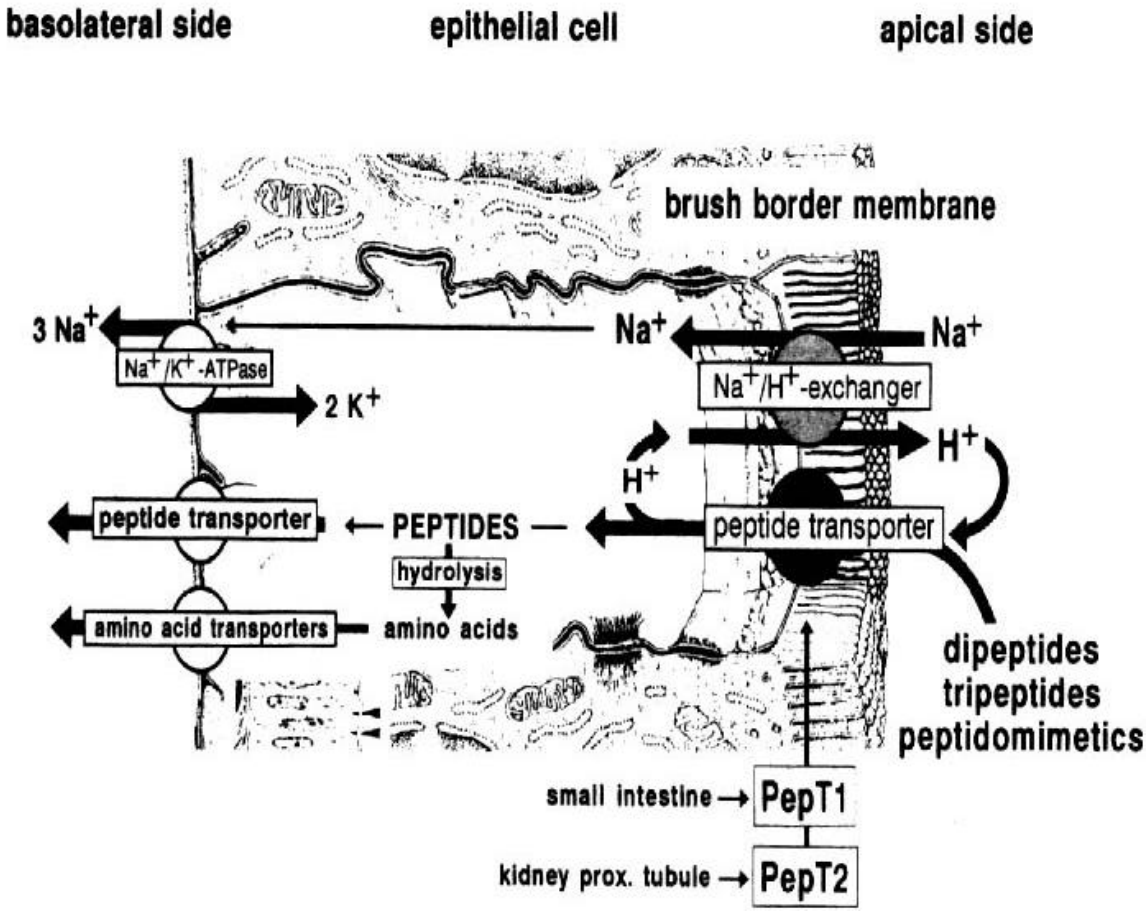

Figure 2.1. A cellular model coupling the peptide transporter and the Na^+-H^+ exchanger (Daniel, 1996).

and now includes members from bacteria, yeast, plants, and animals. The phylogenetic tree for the POT family shows that the sizes of the POT transporter members correlate with their phylogenetic origin (Saier et al., 1999). The transporters in animals have 707 to 786 amino acid residues, the transporters in yeast and plants have 585 to 623 amino acid residues, and the transporters in bacteria have 463 to 500 amino acid residues (Table 2.1). In contrast to the ABC transporters, all of the POT transporters can transport a wide range of dipeptides, tripeptides, and some tetrapeptides, regardless of their MW, composition, hydrophobicity, or charge.

Cloning Methods and Structures of Peptide Transporters

Cloning by Functional Expression. Cloning by functional expression is a method that uses *Xenopus laevis* oocytes for expression of cRNA encoding different genes from various sources. The value of *Xenopus laevis* first became apparent when Gurdon et al. (1971) discovered that the oocyte constitutes an efficient system for translating foreign messenger RNA. The *Xenopus* oocyte is a cell specialized for the production and storage of proteins for later use during embryogenesis. *Xenopus* oocytes at stage V have the complete machinery to translate exogenous RNA faithfully. The most important aspect is that the oocyte expression system can make posttranslational modifications, which preserves the native biological activities of the expressed proteins. Based on the above features, the oocyte expression system has been widely used for functional studies of expressed proteins. To use the system for cloning, mRNA from tissues is isolated and size-fractionated. Injection of pooled mRNA and functional assays narrow down the target mRNA to a particular pool. Using this smaller mRNA pool, a smaller cDNA

Table 2.1. The Proton-dependent oligopeptide transporter (POT) family.

Name	Protein Size (AA)	Phylum	Reference
Rabbit PepT1	707	Animal	Fei et al., 1994
Human PepT1	708	Animal	Liang et al., 1995
Rat PepT1	710	Animal	Saito et al., 1995
Rabbit PepT2	729	Animal	Boll et al., 1996
Human PepT2	729	Animal	Liu et al., 1996
Rat PepT2	729	Animal	Saito et al., 1996
OPT1	737	Animal	Young et al., 1995
KE47	783	Animal	Jack et al., 1996
CG82	786	Animal	Ian et al., 1995
PTR2-A	585	Plant	Garg et al., 1994
PTR2-B	610	Plant	Nusinew et al., 1996
NTR1	584	Plant	Frommer et al., 1994
RCH2	589	Plant	Hutchinson et al., 1996
CHL1	590	Plant	Steiner et al., 1994
PTR2	601	Yeast	Perry et al., 1994
PTR2p	623	Yeast	Mann et al., 1996
YJDL	485	Bacterium	Maeda et al., 1995
YHIP	489	Bacterium	Hama et al., 1994
DTPT	463	Bacterium	Hagting et al., 1994
F493	493	Bacterium	Hasan et al., 1994

library can then be constructed. The reduced size of the expression cDNA library aids in the successful isolation of the target cDNA by subsequently screening the library using functional assays. Information of nucleotide or amino acid sequence of the target gene is not required in this approach. Therefore, this method can be applied to clone any gene as long as the gene encodes a protein that has a functional assay (Daniel, 1996).

Fei et al. (1994) used expression cloning to clone the first peptide transporter from rabbit intestine (PepT1). Rabbit PepT1 was isolated by screening a size-selected rabbit intestinal cDNA library (2.4 to 4.4 **kb**) for the uptake of the [^{14}C]-labelled dipeptide, Gly-Sar. The cDNA (2,746 bp) isolated by functional screening had one consensus polyadenylation site (AATAAA) that was 15 nucleotides upstream from the poly (A) tail, and an open reading frame from 31 to 2,151 nt that encodes a 707-amino-acid protein. Boll et al. used the same strategy to clone rabbit PepT1 (1994) and PepT2 (1996). For PepT1 cloning, injection of size-fractionated poly(A)$^+$ RNA from rabbit intestine into oocytes increased peptidomimetic (cefadroxil) uptake activity about 8-fold in a 2.2 to 5.0 **kb** fraction (Boll et al., 1994). An expression library (2.2 to 5.0 **kb**) was constructed and screened to obtain the single clone. The cDNA clone was 2,756 bp long and the amino acid sequence represented a protein of 707 amino acids. This was identical to the PepT1 cloned by Fei et al. (1994) with differences only in the 5' and 3' untranslated regions (Boll et al., 1994). For PepT2 cloning, size-fractionated poly(A)$^+$ RNA from rabbit kidney cortex were injected and the transport activity was identified in the 3.0 to 5.0 **kb** fractions. This fraction was used for construction of a cDNA library. The cDNA clone isolated by

functional screening was 4,265 bp long and the gene product was a protein of 729 amino acids (Boll et al., 1996).

Cloning by Homologous Screening. Transporters sharing similar functions, such as driving force, electrogenic nature, and substrate specificity, show similar amino acid and nucleotide sequences. Human intestinal PepT1 and renal PepT2, and rat intestinal PepT1 were all cloned by using heterologous probes (Daniel, 1996). The amino acid sequences of the mammalian peptide transporters have much higher homology in the first five transmembrane domains compared with other regions, so cDNA probes are all generated from these regions for screening. Liang et al. (1995) used a .6 **kb** *EcoR* I fragment from the 5' end of the rabbit PepT1 as a probe to screen a human ileal cDNA library under medium stringency conditions. Four positive clones were isolated. The longest insert was a cDNA that had 2,263 bp with an open reading frame of 2,124 bp encoding a protein of 708 amino acids. To clone human PepT2, a human kidney λgt10 cDNA library was screened by plaque hybridization under low stringency conditions. The probe was a 560 bp *Afl* III and *Hind* III fragment excised from the 5' end of rabbit PepT1 cDNA. The full-length PepT2 cDNA was 2,685 bp long with an open reading frame of 2,187 bp encoding a protein of 729 amino acids (Liu et al., 1995).

Degenerate oligonucleotides and RT-PCR can also be used to generate probes for screening cDNA libraries. To clone rat PepT1 (Saito et al., 1995) and PepT2 (Saito et al., 1996), degenerate oligonucleotides were designed based on the cDNA information of rabbit PepT1. The oligonucleotide primers corresponded to amino acid sequences in transmembrane domain 1 (aa 17 to 22) and domain 4 (aa 138 to 143). The rat intestine or

kidney mRNA was reverse transcribed (RT) into cDNA and the cDNA was used as a template for subsequent PCR to generate a DNA fragment for screening the rat kidney λgt22A cDNA library. The isolated rat PepT1 cDNA consisted of 2,921 bp and encoded a protein of 710 amino acids (Saito et al., 1995). Another study from the same lab isolated two PCR products using degenerate primers (Saito et al., 1996). One product was identical to the previous study (Saito et al., 1995) that showed 80% nucleotide identity and another showed 60% nucleotide identity to rabbit PepT1. Using these RT-PCR products as probes to screen the rat kidney λgt22A cDNA library, 3-**kb** and 4-**kb** clones were obtained and designated as rat PepT1 and PepT2, respectively. This 3-kb PepT1 was identical to the rat PepT1 cDNA in the previous study (Saito et al., 1995). The rat PepT2 cDNA contained 3,938 bp and encoded a protein of 729 amino acids.

Cloning by Complementation. Cloning by complementation is a technique that has been used to clone peptide transporters in bacteria (Hagting et al., 1994). A host bacterial strain defective in peptide transport is isolated. This strain cannot grow in a medium that provides the required amino acid only in the form of a peptide. A bacterial cDNA or genomic DNA library that contains the target peptide transporter cDNA is then introduced into the deficient host strain by transformation. The transformants are screened on the selective medium to test whether the introduced gene has corrected the deficient function of the host strain. The transformants that are able to survive on a medium containing the required amino acid in peptide form contain the target peptide transporter gene and therefore can be isolated.

The di- and tripeptide transporter (DtpT) of *Lactococcus lactis* was identified and cloned by complementation of a dipeptide transport-deficient and proline-dependent *Escherichia coli* strain. *L. lactis* chromosomal DNA was partially digested and ligated into the expression vector, pTAQI. The newly created plasmid DNA contained different *L. lactis* genomic DNA fragments. These plasmids were then used to transform the *E. coli* strain E1772, which is a peptide transport-deficient strain. Transformed E1772 were plated on a selective medium containing Pro-Gly as the sole source of proline. Only those bacteria that were functionally complemented by the peptide transporter gene of *L. lactis* would survive on the medium. The cloned DtpT gene was 3.5 **kb** and encoded a protein of 463 amino acids (Hagting et al., 1994).

Structures of Peptide Transporters in Mammals. PepT1 and PepT2 are two distinct peptide transporters that are expressed mainly in the intestine and kidney, respectively. Rabbit PepT1 was the first cloned mammalian peptide transporter cDNA (Fei et al., 1994). This cDNA was 2.7 **kb** and encoded a protein of 707 amino acid residues with an estimated molecular size of 79 kDa and a pI of 7.47. The proposed protein has 12 transmembrane domains that span the plasma membrane. The hydropathy plot using Kyte-Doolittle (1982) methods predicted that the protein had a large 200-amino acid, hydrophilic, extracellular loop between transmembrane domains 9 and 10, and a small 56-amino acid, hydrophilic, intracellular loop between transmembrane domains 6 and 7. The amino acid sequence also indicated that there were three potential N-linked glycosylation sites (N 50, N 439, and N 513), one protein kinase C (PKC) phosphorylation site (S 357), and one cAMP-dependent protein kinase (PKA)

phosphorylation site (T 362; Figure 2.2a). Based on the sequence from rabbit PepT1, human (hPepT1; Liang et al., 1995; Mackenzie et al., 1996) and rat (Saito et al., 1995) were cloned. The proposed human and rat PepT1 structural features were similar to rabbit PepT1 and are presented in Table 2.2 and Figure 2.2.

The human PepT2 cDNA was 2,685 bp long encoding a protein of 729 amino acids with an estimated molecular size of 82 kDa and a pI of 8.26 (Liu et al., 1995). The proposed protein of human PepT2 also had 12 transmembrane spanning domains. The predicted protein structure has a 165-amino acid hydrophilic extracellular loop between transmembrane domains 9 and 10, and two short 53- to 57-amino acid hydrophilic intracellular loops between transmembrane domains 6 and 7, and 10 and 11. The amino acid sequence also indicates that there are three potential N-linked glycosylation sites (N 435, N 472, and N 528), five potential PKC phosphorylation sites (S 262, S 376, S 607, S 640, and S 724), and one PKA phosphorylation site (S 34) (Figure 2.3a). Compared to human PepT2 and other PepT1, the rabbit (Boll et al., 1996) and rat PepT2 (Saito et al., 1996) cDNA were longer, but the encoded proteins are the same size as human PepT2. The proposed rabbit and rat PepT2 structural features are similar to human PepT2 and are presented in Table 2.2 and Figure 2.3.

PepT1 and PepT2 are very similar in their structures. The proposed proteins all have 12 transmembrane domains that span the plasma membrane. The predicted proteins all have a long hydrophilic extracellular loop between transmembrane domains 9 and 10, and a short hydrophilic intracellular loop between transmembrane domains 6 and 7. The amino acid sequences also indicate that there are some potential N-linked glycosylation

Table 2.2. Comparison of sequences and protein characteristics of known mammalian peptide transporters.

Transporter	cDNA	Protein	Structural Features	Ref.
Rabbit PepT1	2.7 kb	707 aa MW 79 kDa pI 7.47	12 Transmembrane domains N-glycosylation sites: 3 (N 50, N 439, and N 513) PKC sites: 1 (S 357) PKA sites: 1 (T 362)	Fei et al., 1994
Human PepT1	3.1 kb	708 aa, MW 79 kDa pI 8.58	12 Transmembrane domains N-glycosylation sites: 7 (N 50, N 404, N 408, N 409, N 509, N 514, and N 562) PKC sites: 2 (S 357, and S 704) PKA sites: none	Liang et al., 1995
Rat PepT1	3.0 kb	710 aa, MW 79 kDa pI 7.39	12 Transmembrane domains N-glycosylation sites: 5 (N 415, N 439, N 510, N 532, and N 539) PKC sites: 1 (S 357) PKA sites: 1 (T 362)	Saito et al., 1995; Miyamoto et al, 1996
Human PepT2	2.7 kb	729 aa MW 82 kDa pI 8.26	12 Transmembrane domains N-glycosylation sites: 3 (N 435, N 472, and N 528) PKC sites: 5 (S 262, S 376, S 607, S 640, and S 724) PKA sites: 1 (S 34)	Liu et al., 1995
Rabbit PepT2	4.2 kb	729 aa MW 82 kDa pI 7.39	12 Transmembrane domains N-glycosylation sites: 5 (N 435, N 472, N 508, N 528, and N 587) PKC sites: 4 (S 264, S 376, S 640, T 724) PKA sites: none	Boll et al., 1996
Rat PepT2	3.9 kb	729 aa MW 82 Kda pI 7.99	12 Transmembrane domains N-glycosylation sites: 4 (N 435, N 448, N 528, and N 587) PKC sites: 3 (S 376, S 640, and T 708) PKA sites: none	Saito et al., 1996
HPT1	3.3 kb	832 aa MW 92 kDa pI unknown	1 Transmembrane domains Others unknown	Dantzig et al., 1994
PTH1	2.7 kb	572 aa MW 65 kDa pI unknown	12 Transmembrane domains N-glycosylation sites: 4 (N 134, N 141, N 220, and N 435) PKC sites: 11 (T 250, T 266, S 271, S 279, S 289, S 293, S 297, S 301, T 307, S 400, and S 482) PKA sites: none	Yamashita et al., 1997

a

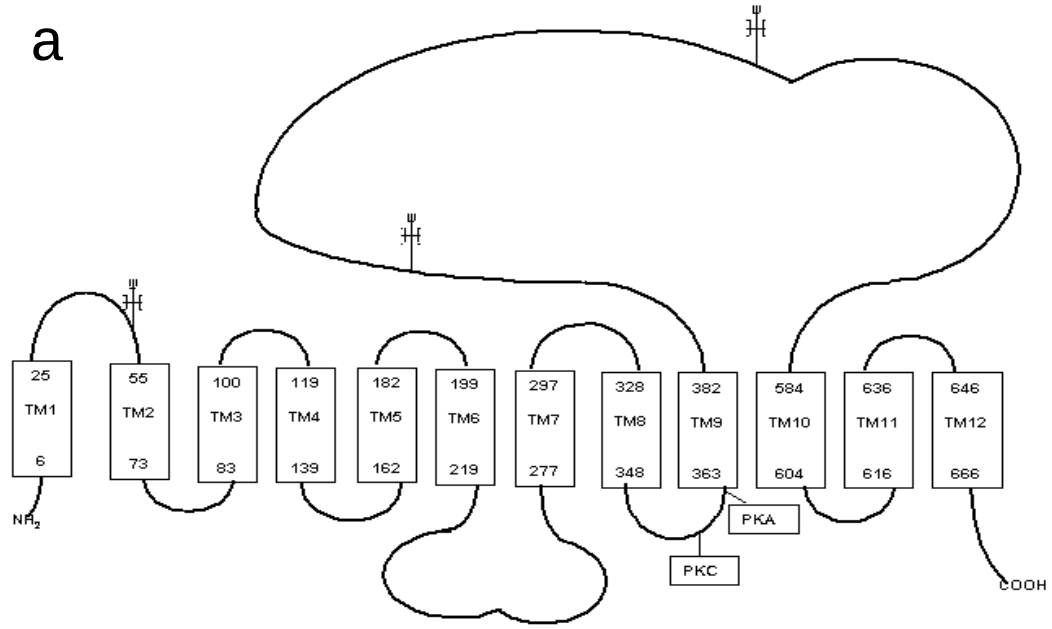
25
TM1
6
55
TM2
73
100
TM3
83
119
TM4
139
182
TM5
162
199
TM6
219
297
TM7
277
328
TM8
348
382
TM9
363
584
TM10
604
636
TM11
616
646
TM12
666
NH2
PKA
PKC
COOH

b

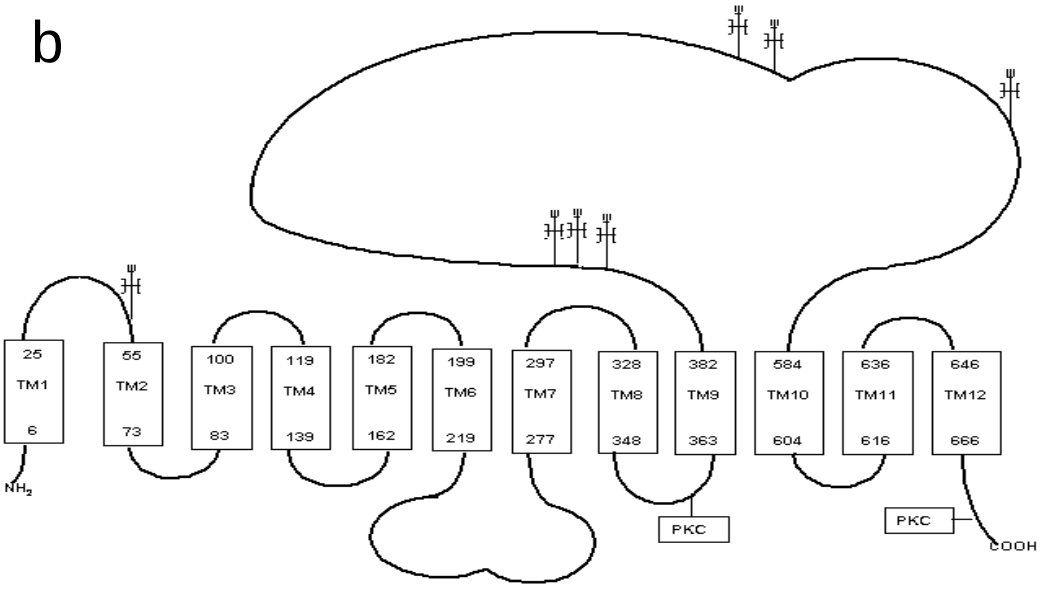
25
TM1
6
55
TM2
73
100
TM3
83
119
TM4
139
182
TM5
162
199
TM6
219
297
TM7
277
328
TM8
348
382
TM9
363
584
TM10
604
636
TM11
616
646
TM12
666
NH2
PKC
PKC
COOH

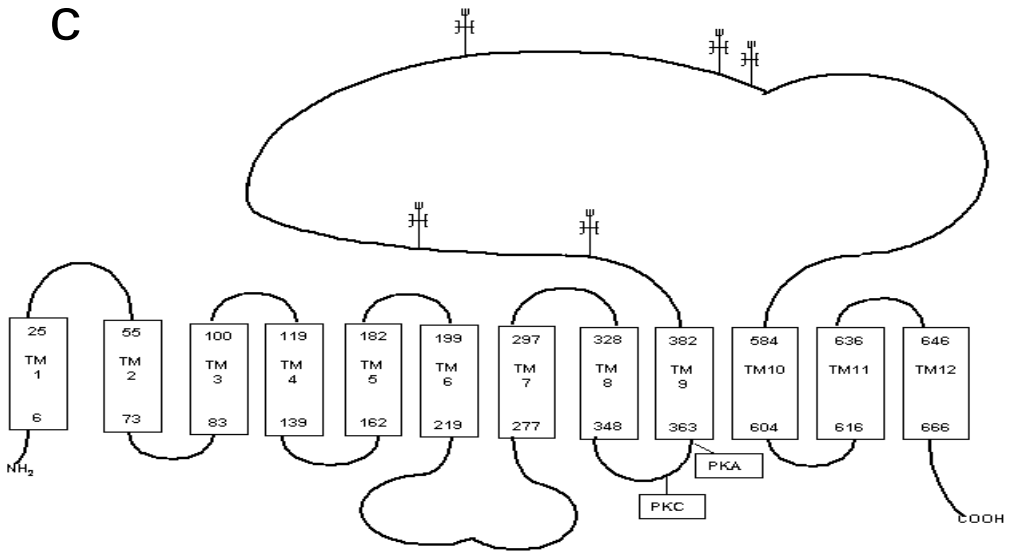

Figure 2.2. Proposed structures of rabbit (a), human (b), and rat (c) PepT1 proteins. TM: transmembrane domain; PKA: cAMP-dependent protein kinase site; PKC: protein kinase C site; N-glycosylation site labeled as (ψ).

a

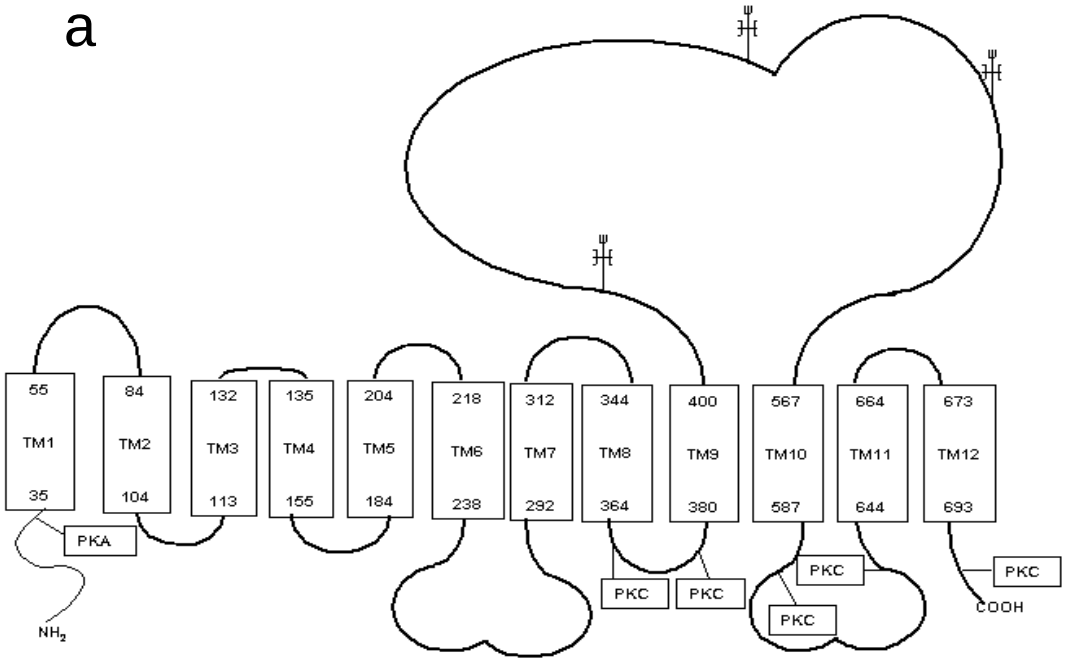
55
TM1
35
84
TM2
104
132
TM3
113
135
TM4
155
204
TM5
184
218
TM6
238
312
TM7
292
344
TM8
364
400
TM9
380
567
TM10
587
664
TM11
644
673
TM12
693
PKA
PKC
PKC
PKC
PKC
PKC
NH2
COOH

b

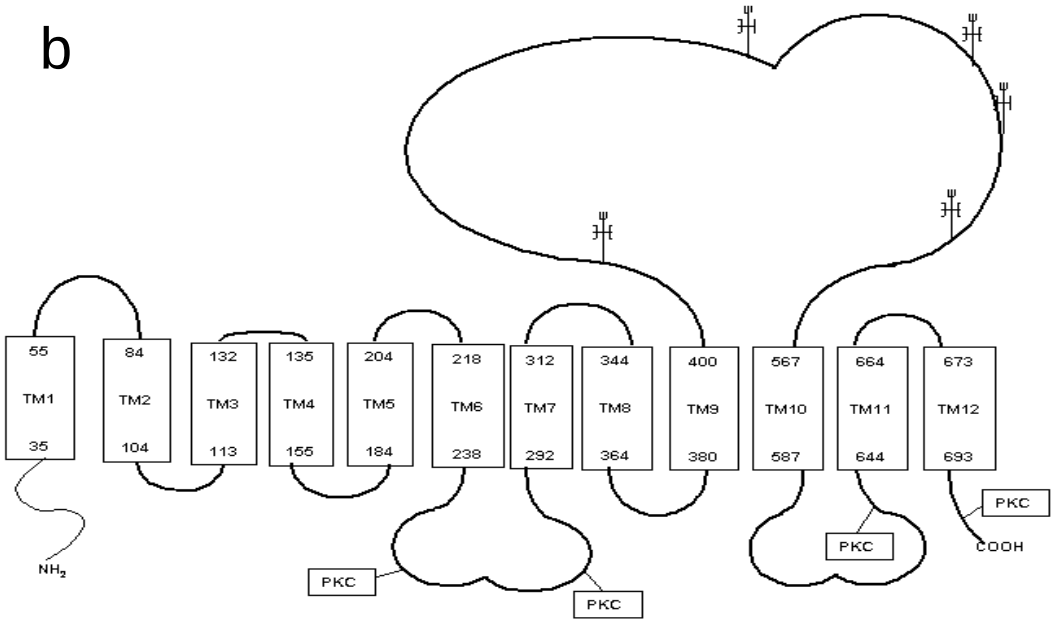
55
TM1
35
84
TM2
104
132
TM3
113
135
TM4
155
204
TM5
184
218
TM6
238
312
TM7
292
344
TM8
364
400
TM9
380
567
TM10
587
664
TM11
644
673
TM12
693
PKC
PKC
PKC
PKC
NH2
COOH

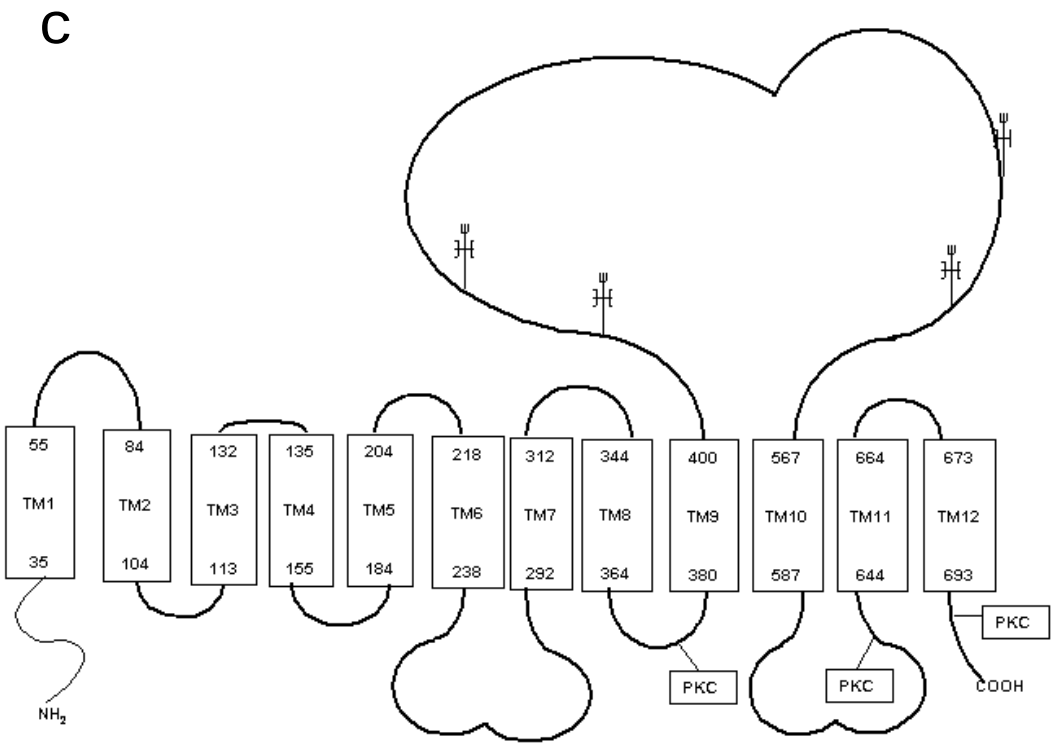

Figure 2.3. Proposed structures of human (a), rabbit (b), and (c) rabbit PepT2 proteins. TM: transmembrane domain; PKA: cAMP-dependent protein kinase site; PKC: protein kinase C site; N-glycosylation site labeled as (ǂ).

sites and some potential protein kinase phosphorylation sites. All PepT1 proteins are highly homologous among themselves (77% to 83%) and all PepT2 proteins are highly homologous among themselves (76% to 83%). But these are two distinctly different transporters. The similarity of amino acid sequence between the two groups is only 30 to 50% and their affinities for peptide substrates are different. PepT1 is a low-affinity transporter, whereas PepT2 is a high-affinity transporter. A more detailed discussion of the transport characteristics of these proteins will be presented later in this chapter.

In 1994, a unique peptide transporter, HPT1, was cloned from a Caco-2 cell cDNA library (Dantzig et al., 1994). The cloned cDNA was 3,345 bp long encoding a protein of 832 amino acid residues with an estimated molecular size of 92 kDa. After transfection of HPT1 cDNA into CHO cells, a pH-dependent transport activity for cephalexin and dipeptides in the transfected cells was detected. Amino acid sequence comparisons of HPT-1 with other peptide transporter members showed no homology with any of the known peptide transporters. Although HPT-1 was 20 to 30% identical to members of the cadherin superfamily of Ca^{2+}-dependent, cell-cell adhesion proteins, HPT-1 lacked a cytoplasmic domain that was required for the cadherin cell-cell adhesion function. The presence of a single transmembrane domain in HPT-1 may indicate that HPT-1 is either the first member of a new class of peptide transporters (Figure 2.4a; Daniel, 1996) or it is just a part of a peptide transporter.

Yamashita et al. (1997) reported the cloning of a peptide/histidine transporter (PHT1) from a rat brain cDNA library using a 55-nt sequence homologous to rabbit

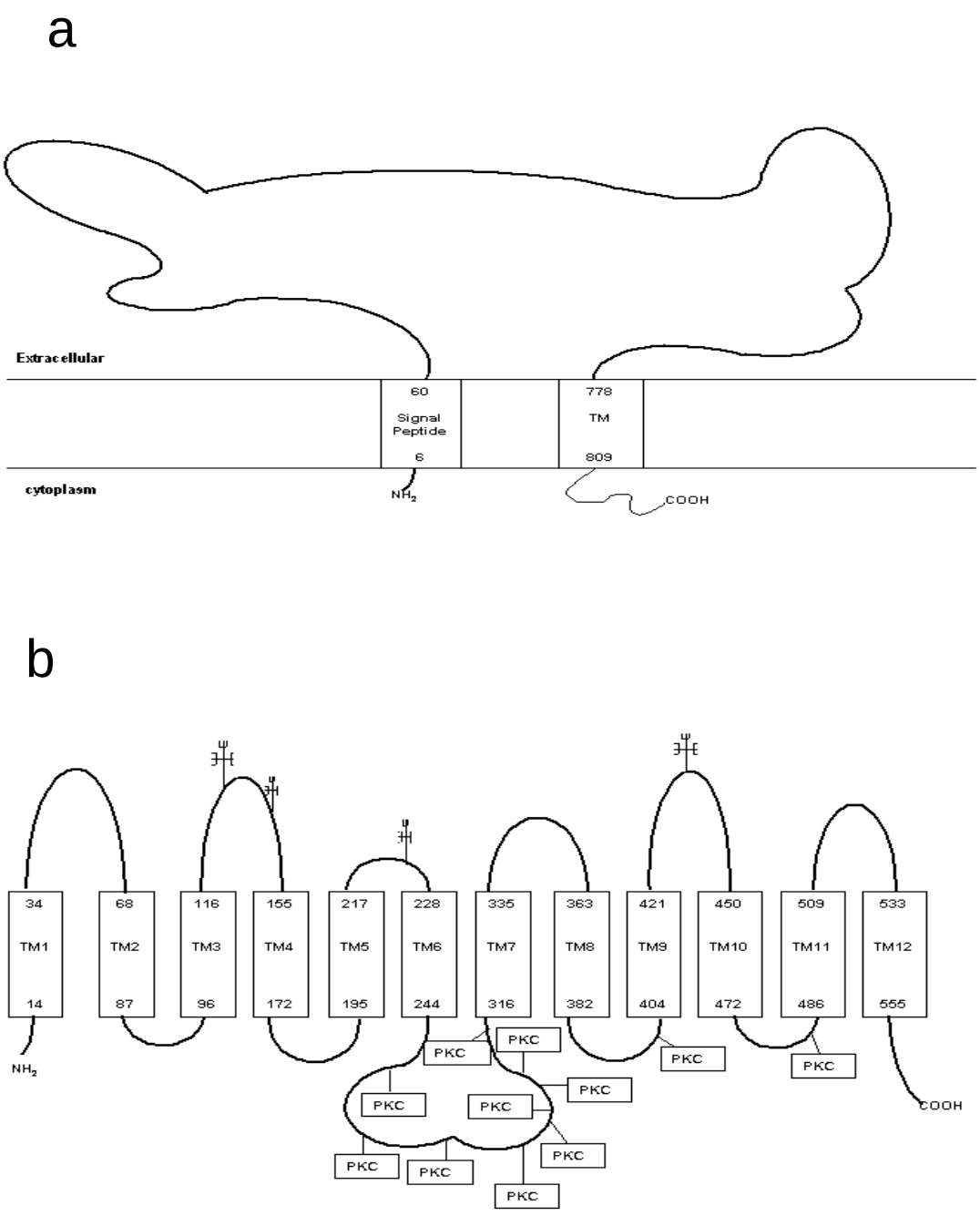

Figure 2.4. New class of peptide transporter: structures of HPT-1 (a) and PHT1 (b) proteins. TM: transmembrane domain; PKA: cAMP-dependent protein kinase site; PKC: protein kinase C site; N-glycosylation site labeled as (Ψ).

PepT1 as a probe under medium stringency conditions. The cloned PHT1 cDNA was 2,751 bp long encoding a protein of 572 amino acid residues with an estimated molecular mass of 64.9 kDa. The predicted protein had 12 transmembrane domains, but only had a short hydrophilic intracellular loop between transmembrane domains 6 and 7 and did not contain the large hydrophilic extracellular loop between transmembrane domains 9 and 10. The amino acid sequence of rat PHT1 indicated that there were four potential N-linked glycosylation sites (N 134, N 141, N 220, and N 435), eleven potential PKC phosphorylation sites (T 250, T 266, S 271, S 279, S 289, S 293, S 297, S 301, T 307, S 400, and S 482), but no site for PKA phosphorylation (Figure 2.4b)**.** The amino acid sequence of PHT1 showed only low similarity with other mammalian peptide transporters (32% similarity and 17% identity with PepT1, 27% similarity and 12% identity with PepT2, and 15% similarity with HPT-1), but showed 50% similarity and 29% identity with the histidine transport protein (NTR1), a peptide transporter from the plant *Arabidopsis thaliana*. Despite the low similarity of PHT1 to other mammalian peptide transporters, PHT1 did transport the dipeptide carnosine as well as the free amino acid histidine in a proton-dependent manner. Interestingly, Wang et al. (1998) screened a rat brain cDNA library using the human PepT2 cDNA as the probe and only a cDNA that is identical to the already cloned rat PepT2 was isolated from rat brain. Therefore, PHT1 is probably the first member of a new class of peptide transporters in mammals.

By photoaffinity labeling with [^{3}H]-cephalexin and photoreactive β-lactam antibiotics and dipeptides, Kramer et al. (1998) identified a 127-kDa protein that was a component of the H^+/oligopeptide transport system in rabbit small intestine brush border

membrane vesicles (BBMV). Peptide transport was found in all segments of the small intestine with the specific labeled protein. By enzymatic deglycosylation of the 127-kDa protein with endoglucosidase F and N-glycanase, two fragments of 116 kDa and 95 kDa were obtained, whereas with endoglucosidase H, only one fragment of 116 kDa was found. This indicated that the 127-kDa protein is a microheterogeneous glycoprotein. It was also found that the solubilized and purified 127-kDa protein showed sucrase and isomaltase activities. With polyclonal antibodies raised against the purified 127-kDa protein, coprecipitation of sucrase activity and the photolabeled 127-kDa beta-lactam antibiotic binding protein occurred. Target size analysis showed a functional molecular mass of 165 kDa for photoaffinity labeling of the 127-kDa protein. These findings suggested that there was a homo- or heterodimeric functional structure of the 127-kDa protein in the brush-border membrane, and that the H^+/oligopeptide binding protein of 127 kDa was closely associated with the sucrase/isomaltase complex in the enterocyte brush-border membrane.

In conclusion, PepT1 and PepT2 have been cloned by functional expression and homologous screening in rabbit, rat and human. PepT1 and PepT2 are very similar in their structures in that they have 12 transmembrane domains and a long extracellular loop. HPT1 and PHT1 are two peptide transporters that are different from both PepT1 and PepT2.

Expression of Peptide Transporter mRNA and Proteins

Expression of peptide transporters among various tissues has been studied by northern blot analysis using specific radiolabeled DNA probes. Using a full-length PepT1

cDNA as the probe for northern blot analysis, Fei et al. (1994) found a 2.9 **kb** mRNA expressed at high levels in the small intestine of the rabbit, at much lower levels in the liver and kidney, and only trace amounts in the brain. No mRNA was detected in the colon, skeletal muscle, heart, spleen, or lung. Human PepT1 mRNA was 3.3 **kb**, and the majority of this PepT1 mRNA was expressed in the small intestine as well as in Caco-2 cells, an intestinal epithelium derived cell line (Liang et al., 1995). Human PepT1 mRNA was also found in kidney, placenta, liver, and pancreas, but not in muscle, brain, or heart. In rats, the mRNA for PepT1 was 2.9 to 3.0 **kb** (Saito et al., 1995; Miyamoto et al., 1996). The majority of this mRNA was expressed in the small intestine and only trace amounts were found in kidney cortex. PepT1 was not detectable in liver.

The tissue-pattern of expression of peptide transporter PepT2 mRNA is different. Using the full-length cDNA of PepT2 for northern blot analysis in the rat, a 4-**kb** mRNA was expressed mainly in the kidney medulla and at lower levels in the kidney cortex (Saito et al., 1996). The mRNA was also found in brain, lung, and spleen, but was not detectable in the heart, liver, or small intestine. In the rabbit, a 4.8-**kb** PepT2 mRNA was found in the kidney cortex as well as in brain, lung, liver, and heart when a complementary RNA fragment (1.24 **kb**) synthesized from PepT2 cDNA was used as the probe for northern blot analysis (Boll et al., 1996). PepT2 mRNA in human tissues was not detectable by northern blot analysis (Liu et al., 1995). Only after using RT-PCR, was the PepT2 mRNA detected in human kidney and small intestine (Liu et al., 1995). The differences in northern blot analysis of the expression of peptide transporter mRNA may be due to differences in protocols employed by different researchers, which could result in different

sensitivities in northern blot analysis. The variations could also be due to differences in the levels and patterns of peptide transporter mRNA expression in different species.

The expression of the peptide transporters among various tissues has also been studied by *in situ* hybridization using a specific radiolabeled DNA probe. Freeman et al. (1995a) studied cellular expression of PepT1 mRNA along the rabbit gastrointestinal tract using *in situ* hybridization. Anti-sense oligonucleotides, synthesized according to the published sequence of PepT1, were radiolabeled and used as probes for *in situ* hybridization. The autoradiographs showed that the mRNA was expressed all along the small intestine and decreased dramatically in the colon. Results also demonstrated that the expression was restricted to only the epithelial surface of the small intestine and there was no expression in deeper tissues, such as the lamina propria, muscularis mucosa, or serosa. PepT1 mRNA was not expressed at detectable levels in the stomach, sacculus rotundus, or cecum. These data are consistent with the results from northern blot analysis of rabbit intestine (Fei et al., 1994). Along the crypt-villus axis in the entire small intestine, the mRNA was expressed only at or above the crypt-villus junction with the maximal expression occurring at about 100 to 200 μm above the junction. The mRNA was not expressed at all in the lower to mid crypt in the entire small intestine. The expression pattern of PepT1 mRNA in the small intestine and along the crypt-villus axis was almost identical with those of villus-specific proteins, such as the plasma membrane Ca^{2+} pump (PMCA1, Freeman et al., 1993) and Na^{+}-glucose cotransporter (SGLT1; Freeman et al., 1995b), both of which have been well studied. The near-identical expression patterns suggested that some common transcription factors might be involved that act on promoter

regions of genes expressed specifically in the villus (Freeman, 1993). A more recent study was conducted by Smith et al. (1998) to evaluate the mRNA expression of rat PepT1 and PepT2 in rat kidney. With RT-PCR and *in situ* hybridization of rat kidney sections, they found that PepT1 mRNA was expressed specifically in early parts of the proximal tubule, whereas PepT2 mRNA was expressed mainly in latter parts of the proximal tubule. All other segments along the nephron showed no expression of PepT1 or PepT2 mRNA. This finding is in conflict with the proposed mechanism (Brandsch et al., 1995; Leibach and Ganapathy, 1996) which is that peptides are immediately reabsorbed in proximal regions by a high-affinity/low-capacity transporter (PepT2), whereas hydrolyzed peptides passing down the tubule are reabsorbed in distal parts of the nephron by a low-affinity/high-capacity transporter (PepT1).

Despite the significant progress in peptide transporter research, few studies have focused on peptide transporter distribution and localization at the level of protein expression. With rabbit antiserum raised against a synthetic peptide corresponding to the carboxyl-terminal amino acids of rat PepT1, PepT1 protein was detected by western blot analysis in brush border membranes prepared from rat small intestine and kidney cortex (Saito et al., 1995). The protein had an apparent molecular mass of 75 kDa. Ogihara et al. (1996) investigated the localization of the transporter protein in the rat digestive tract. A rabbit anti-PepT1 antibody was developed according to the carboxyl-terminal amino acids of rat PepT1 and used to examine the PepT1 protein. Positive immunofluorescence staining for PepT1 indicated the presence of the protein in the small intestine, located mainly on the brush border membrane of the cell. PepT1 was not detected in the

esophagus, stomach, colon, or rectum. The differentiated absorptive epithelial cells in the villi had high expression of PepT1 protein, whereas crypt and goblet cells showed little or no expression. These data were also in agreement with that of *in situ* hybridization (Freeman et al., 1995a). Therefore, mRNA expression and protein expression were coincident.

Shen et al. (1999) used both northern blot analysis and immunolocalization to study the expression of both PepT1 and PepT2 mRNA and protein in rat kidney. Northern blot analyses were performed using two cDNA fragments (547 bp of PepT1 or 561 bp of PepT2) as probes, which corresponded to the partial sequences in the large extracellular loop between transmembrane domains 9 and 10. The results from the northern blots showed that rat PepT1 mRNA was expressed in the superficial cortex and, at lower levels, in the middle cortex, but not at all in the deep cortex, medulla, or papilla. Rat PepT2 mRNA was expressed in the deep cortex and outer medulla, but not in the superficial cortex, inner medulla, or papilla. For immunoblotting and immunolocalization studies, the antisera were generated either against rat PepT1 or PepT2 synthetic peptides corresponding to the carboxyl-terminal region sequences or against fusion proteins containing the sequences in the large extracellular loop between transmembrane domains 9 and 10. Both antisera showed similar patterns with immunoblotting, but antiserum generated against synthetic peptides from the carboxyl-terminal region had much better staining in immunolocalization studies. The protein had an apparent molecular mass of 90 and 85 kDa for rat PepT1 and rat PepT2 from the western blots, respectively. The data were consistent with their predicted molecular weight based on the cDNA clones and

putative glycosylation sites (Miyamoto et al., 1996; Saito et al., 1995 and 1996). Immunolocalization experiments indicated that rat PepT1 proteins were expressed in the convoluted segments of the proximal tubule, whereas PepT2 proteins were restricted to expression in the straight segments. All other nephron segments were negative for PepT1 or PepT2. This finding confirmed the previous studies using RT-PCR and in situ hybridization to evaluate the expression of PepT1 and PepT2 mRNA in rat kidney (Smith et al., 1998). These studies demonstrated that peptides were reabsorbed sequentially in proximal regions of the nephron, first by PepT1, a low-affinity/high-capacity transporter, and then by PepT2, a high-affinity/low-capacity transporter. These data also confirm that PepT1 and PepT2 mRNA and protein expression are parallel in rat kidney.

In conclusion, the mRNA expression of PepT1 and PepT2 among various tissues in rabbit, rat and human has also been studied by both northern blot analysis and *in situ* hybridization. PepT1 is mainly an intestinal peptide transporter, whereas PepT2 is mainly a renal peptide transporter. Immunolocalization of PepT1 and PepT2 proteins confirms that their mRNA and protein expression are coincident.

Regulation of Peptide Transporters

Although the biochemical properties of peptide transporters, such as kinetics, substrate specificity, and stereoselectivity have been studied and reported thoroughly (Leibach and Ganapathy, 1996), very little is known about the molecular mechanisms that regulate peptide transporter function and the mechanisms by which peptide transporters recognize substrates. The function of peptide transporters can be affected by factors that influence protein structure, localization on the membrane, and substrate binding sites.

Because of the experimental difficulty in isolating, purifying, and crystallizing membrane proteins, very little information is available about the structure-function relationship of peptide transporters. A number of factors that can influence peptide transporter activity are described below.

Protein Kinases. Transporters are known to contain consensus sites for phosphorylation by protein kinases (Wright et al., 1992). Protein kinases have been shown to either directly or indirectly regulate the activity of transport proteins (Newton and Johnson, 1998). Direct regulations occur through phosphorylation of the transport proteins, which may change the kinetics of the transporter, such as maximum velocity (V_{max}), substrate affinity (K_t), or turnover number of the transporter. The transport activity of the glutamate cotransporter (GLT-1) was increased by PKC (Rothman, 1994). Mutation of the serine residue that forms part of the consensus phosphorylation site of PKC (Ser-113) eliminated the response to phorbol esters, a PKC activator (Casado et al., 1993). These results demonstrate that the regulation of transporter functions can occur by direct phosphorylation of the protein.

Transport proteins, like all other membrane proteins, are cotranslationally inserted into the endoplasmic reticulum during protein synthesis and processed through the Golgi apparatus (Rothman and Orci, 1992). Vesicles are formed in the Golgi apparatus to deliver the proteins to the plasma membrane, where the vesicles fuse with the plasma membrane and result in increases in the number of transporters. Transport proteins can also be selectively retrieved from the plasma membrane by endocytosis (Rothman, 1994). Protein kinases may, therefore, also indirectly regulate transport activity by regulating the

delivery or retrieval of membrane proteins from the plasma membrane. A study by Brandsch et al. (1994) showed that a proton-dependent peptide transport system expressed in human Caco-2 cells was regulated by PKC. When the cells were treated with phorbol esters, which activate PKC, the transport function was significantly inhibited. Further kinetic analysis showed that the inhibition was due to a decrease in the maximal transport rate (V_{max}) of the transporter whereas the apparent affinity (K_t) was unchanged. In the porcine renal cell line LLC-PK1, transport of dipeptide, Phe-Ala, by PepT2 was decreased by 30 percent when PKC was activated, whereas transport was increased by 60 percent when cells were pre-incubated with PKC inhibitors (Wenzel et al., 1999).

In some cases, it was shown that protein kinases also regulated levels of the transporter mRNA through post-transcriptional regulation of messenger RNA stability. In the renal epithelial cell line LLC-PK1 cells, activation of PKA increased the half-life of the glucose transporter SGLT1 mRNA (Peng and Lever, 1995), whereas PKC activation decreased SGLT1 expression by destablization of the mRNA (Hediger and Rhoads, 1994). Muller et al. (1996) also reported that an increase in the intracellular level of cAMP in Caco-2 cells that expressed PepT1 resulted in a decrease in the ability of these cells to uptake Gly-Sar by 50%. Since cAMP can activate protein kinase C and A in the cAMP pathway, this provides additional evidence that protein kinases C and A are involved in the regulation of peptide transport.

Glycosylation. There are a number of potential N-glycosylation sites in peptide transporters (Fei et al., 1994; Liang et al., 1995; Miyamoto et al., 1996). The presence of *N*-glycosylation sites in all the transporters cloned so far suggests that glycosylation must

play an important role in the function of these proteins. The effect of the disruption of the putative glycosylation sites by site-directed mutagenesis suggested that the carbohydrate moiety of the glycine transporter GLYT1 was necessary for the proper trafficking of the transporter protein to the plasma membrane (Olivares et al., 1995). Moreover, the removal of oligosaccharides by enzymatic methods from a purified glycine transporter affected its transport activity (Nunez and Aragon, 1994). However, the functions of the N-glycosylation sites predicted for the peptide transporters have not been tested.

Histidine. Histidyl residues are critical in several proton-coupled transporter systems because of their ability to act as a proton donor or an acceptor. To study the effects of histidyl residues on endogenous peptide transporter activity, Brandsch et al. (1997) examined the uptake of radiolabeled Gly-Sar after treatment of both Caco-2 cells (expressing PepT1) and SKPT cells (expressing PepT2) with diethyl pyrocarbonate (**DEPC**). DEPC can chemically modify the histidyl residues, making them incapable of acting as a proton donor or acceptor. Uptake of radiolabeled Gly-Sar by DEPC-treated Caco-2 and SKPT cells was significantly decreased as compared with the control cells. DEPC treatment only decreased the V_{max} of Gly-Sar uptake. It had no effect on K_t.

Fei et al. (1997) used site-directed mutagenesis to identify the function of three conserved histidyl residues in both human PepT1 (His-57, His-121, and His-260) and human PepT2 (His-87, His-142, and His-278). Site-directed mutagenesis changed a histidine codon (CAT or CAC) to an asparagine (AAT or AAC) or glutamine codon (CAA) in both human PepT1 and human PepT2. The mutants were expressed in both *Xenopus* oocytes and HeLa cells. Transport activity in both oocytes and HeLa cells was

examined by the measurement of Gly-Sar uptake. Results showed that mutation of His-121 and His-260 in PepT1, and His-142 and His-278 in PepT2 had no effect on the uptake of Gly-Sar compared with wild type, whereas the His-57-mutated PepT1 and His-87-mutated PepT2 failed to show any uptake of the substrate. Therefore, His-57 in PepT1 and His-87 in PepT2 are critical histidyl residues necessary for the uptake function of the peptide transporters. However, Terada et al. (1996) previously reported that His-57 and His-121, which are located in the transmembrane domains 2 and 4, respectively, of rat PepT1, were both involved in substrate binding and were both necessary for the activity of the transporter. The reason for this discrepancy regarding the role of His-121 in rat and human PepT1 remains unknown. Other studies support Terada's conclusion (1996) that at least two histidyl residues are involved in peptide transport activity. Steel et al. (1997) reported that, in human PepT1, one histidyl residue was needed as a cation site for proton coupling and another histidyl residue, located next to the substrate-binding site, was required for determining differently charged dipeptide-H^+ flux coupling ratios.

To clarify the mechanisms involved in the interaction of the substrates with the essential histidyl residues of PepT1 and PepT2, Terada et al. (1998) examined the interaction of dipeptides and β-lactam antibiotics with the histidyl residues of rat PepT1 and PepT2. PepT1 and PepT2 were transfected into the renal epithelial cell line LLC-PK_1. DEPC abolished the uptake of Gly-Sar by both transfectants. Using an excess of dipeptide or aminocephalosporin, the DEPC-induced inhibition of Gly-Sar uptake was decreased. However, anionic cephalosporins without an α-amino group or bestatin with a β-amino group, did not attenuate the DEPC-induced inhibition of Gly-Sar uptake. Various charged

dipeptides prevented the DEPC inactivation of PepT1, which suggests that the failure of anionic cephalosporins without an α-amino group to prevent the DEPC inhibition was not due to their ionic charge. These data suggested that the histidyl residue located in the recognition site was involved in the binding site of the α-amino group of the dipeptides and aminocephalosporins. Because only the unprotonated imidazole ring reacts with DEPC, the imidazole group of the histidine residue located at the recognition site was protonated by the α-amino group of the dipeptides and aminocephalosporins, but not by the peptide-like drugs that did not have an α-amino group. The α-amino group of the substrates might interact with the imidazole ring of the histidine residue of peptide transporters by proton binding. These results were observed for PepT1 and PepT2 in a similar manner, which suggests that the histidyl residue plays the same role in both transporters.

Tyrosine. Tyrosine is another critical amino acid residue present in peptide transporters. Conserved tyrosines have been proposed to be involved in Na^+, Cl^-, and substrate recognition (Pantanowitz et al., 1993; Bismuth, et al., 1997). Yeung et al. (1998) studied the role of tyrosine 167 (Y-167) in peptide transport function by site-directed mutagenesis and dipeptide uptake studies. A computer model of the arrangement of the transmembrane domains identified this particular amino acid to be conserved in the peptide transporters from bacteria, plant, and human. The hPepT1 mutations were generated by changing hPepT1 at tyrosine 167 into alanine (Y167A), phenylalanine (Y167F), serine (Y167S), or histidine (Y167H). Gly-Sar uptake in cells transiently transfected with Y167A-hPepT1 was inhibited completely. However, western blot

analysis and cell surface expression by immunofluorescence microscopy showed that the level of Y167A-hPepT1 expression was similar to those of the wild type. Therefore, the mutation affected peptide transport function, but not the steady-state protein level or trafficking of the transporter to the plasma membrane. Moreover, Gly-Sar uptake in cells transfected with Y167F-, Y167S-, or Y167H-hPepT1 was also inhibited completely. All these findings demonstrate that Y-167 plays an essential role in hPepT1 function.

Substrate-Binding Domain. Recently, Doring et al. (1997) performed a functional analysis of peptide transport by using a chimeric transporter obtained from the intestinal and renal isoforms. The chimeric peptide transporter (CH1Pep) was constructed in such a way that the amino terminus (residues 1-401) was from PepT2, while the carboxyl terminus (402-707) was from PepT1. The function of CH1Pep was studied in oocytes. Results showed that CH1Pep had all the functional characteristics of PepT2 including high affinity, substrate specificity, and dependence on pH. This indicated that the amino terminus determined the phenotype of PepT2. To identify the substrate-binding domain in PepT1 and PepT2 that is responsible for the differing affinities, Fei et al. (1998) constructed a series of PepT1-PepT2 chimeras using an *in vivo* restriction site-independent procedure. The kinetic data for seven different chimeras were compared with those of wild type PepT1 and PepT2. Analysis of these chimeras revealed that the region including the transmembrane domains 7, 8 and 9 of the transporters was the putative substrate-binding site in both PepT1 and PepT2.

Zinc. Using renal brush border membrane vesicles (BBMV), Daniel and Adibi (1995) investigated the role of zinc in the process of peptide transport. Zinc is an essential

trace element that has many fundamental roles in determining the structural motif that regulates the activity of an enzyme. The results of this study showed that incubation of BBMV with zinc sulfate increased the uptake of Gly-Gln, Leu-Tyr, and cephalexin by twofold without changing the diffusion rate of the substrates. Zinc had no effect on the uptake of either Gln or glucose by BBMV. Therefore, zinc might have a selective effect on peptide transport.

Trauma. It was observed that, when amino acids were introduced into the gut lumen as dipeptides and tripeptides, they were absorbed more rapidly than as a mixture of free amino acids (Adibi and Kim, 1981). Compared with amino acid transport, peptide transport in the intestine is relatively resistant to starvation, intestinal diseases, protein-caloric malnutrition, and vitamin deficiency (Grimble and Silk, 1989). To investigate the molecular mechanisms of the resistance of the intestinal peptide transport system to tissue damage, Tanaka et al. (1998) studied the effects of injury induced by the antitumor drug 5-fluorouracil on expression and transport activity of PepT1 in rat intestine. Their data confirmed that the intestinal peptide transport activity was not affected by tissue damage because the levels of PepT1 remained unaffected while the levels of amino acid, glucose, and phosphate transporter were markedly decreased in 5-fluorouracil-treated animals. This resistance might be due to a relative increase in PepT1 synthesis rather than to a change in its kinetic properties.

Dietary Regulation. Intestinal peptide transport activity varies significantly in response to changes in different factors (Buddington and Diamond, 1989). Dietary regulation is one of the most important factors for intestinal peptide transport (Ferraris et

al., 1988; Ferraris and Diamond, 1989). There is strong evidence from experimental models that dietary protein is a regulator of peptide transport activity (Erickson et al., 1995). The effect of different dietary protein levels on the expression of PepT1 was studied by examining mRNA expression along the longitudinal axis of the rat small intestine. Northern blot analysis of mRNA from the intestine of rats on a normal diet (17% casein) showed that mRNA for PepT1 was relatively evenly distributed along the longitudinal axis of the small intestine. Changing the diet from low (4% casein) to high (50% gelatin) protein resulted in a 1.5- to 2-fold increase in the PepT1 mRNA level in the middle and distal small intestine. Therefore, dietary protein levels might have a regulatory effect on the expression of the peptide transporters, at least as indicated by the relative abundance of their mRNA.

The response of the level of human PepT1 expression to dipeptide substrates was investigated in the Caco-2 human intestinal cell line (Walker et al., 1998). After incubating Caco-2 cells for 3 d in a peptide-containing medium (Gly-Gln), V_{max} for uptake of Gly-Sar was increased 1.6-fold. Northern blot analysis of mRNA from Caco-2 cells showed that the increase in substrate transport was accompanied by a parallel increase of 1.9-fold in human PepT1 mRNA. The half-life of human PepT1 mRNA was also increased from 8.9 h to 12.5 h. Human PepT1 protein was also located using an anti-human-PepT1 antibody. PepT1 proteins were increased 1.7-fold due to the peptide-containing medium. This study indicated that a peptide substrate directly upregulated the expression of human PepT1 by both enhancing mRNA stability and increasing transcription rate. The regulation was independent of hormonal or neural control.

By using specific antibodies and a cDNA probe for rat PepT1, Shiraga et al. (1999) analyzed the dietary regulation of this transporter in the rat small intestine. The promoter of the rat PepT1 gene was identified to be within –3.1 **kb** from the transcription start site. Interestingly, an amino acid-responsive element (AARE) was present in the region from –277 to –271 of the promoter. A series of 5'-deleted fragments including –3.1 kb, -1.6 kb, -912 bp, -351 bp, - 171 bp, -97 bp, -50 bp –27 bp, and –13 bp were inserted into a plasmid containing the luciferase gene. Effects of these mutations on amino acid and dipeptide induction of luciferase activity were assayed in transiently transfected cells. The luciferase activities of clone -351 responded to particular amino acids (phenylalanine, arginine, and lysine) and dipeptides (Gly-Sar, Gly-Phe, Lys-Phe, and Asp-Lys). These results suggested that the up-regulation of peptide transport activity by dietary protein was caused by selective amino acids and dipeptides in the diet activating transcription of the PepT1 gene.

Sigma Receptor Ligand. Sigma binding sites are distributed in the brain, peripheral tissues, and in various neuronal and non-neuronal cell lines, and evidence suggests a role for sigma sites in maintenance of cell function (Vilner et al. 1995a, 1995b). Pentazocine is a selective sigma ligand. Fujita et al. (1999) investigated the effects of pentazocine on the uptake of Gly-Sar in the human intestinal cell line Caco-2 expressing PepT1. Caco-2 cells were treated with different concentrations of pentazocine and semi-quantitative RT-PCR revealed that treatment of pentazocine increased PepT1 mRNA in Caco-2 cells in a concentration-dependent manner. The activity of PepT1 was assessed by measuring the uptake of Gly-Sar in the presence of a H^+ gradient. Results showed that

pentazocine increased the uptake of Gly-Sar in Caco-2 cells mediated by PepT1 in a concentration- and time-dependent manner. Kinetic analyses indicated that pentazocine increased the maximal velocity for Gly-Sar uptake in Caco-2 cells without affecting the affinity constant. These data indicated that pentazocine could up-regulate PepT1 in Caco-2 cells by increasing the levels of PepT1 mRNA, which could cause an increase in the density of the transporter protein in the cell membrane.

Neural Regulation. Intestinal absorption of β-lactam antibiotics, such as cefixime and cephalexin, has been shown to proceed through the dipeptide carrier system (Ganapathy et al., 1995). Nifedipine, an L-type calcium channel blocker, has been reported to enhance the absorption of cefixime in vivo but not in vitro. Neural mechanisms might be involved in the effect of nifedipine (Harcouet et al., 1997). Berlioz et al. (1999) examined the involvement of the nervous system on the intestinal absorption of cephalexin, a test molecule that is only carried by peptide transporters. A single-pass jejunal perfusion technique was used in rats. Nifedipine increased the plasma cephalexin levels in treated rats approximately twofold versus controls. Nifedipine also increased the cephalexin level approximately twofold in portal plasma and increased urinary excretion of cephalexin, which indicated that nifedipine effectively increased cephalexin intestinal absorption. Perfusing high concentrations of dipeptides in the jejunal lumen reduced cephalexin absorption and inhibited the enhancement of cephalexin absorption produced by nifedipine. Atropine, capsaicin, clonidine, and isoproterenol enhanced cephalexin absorption by the same magnitude as nifedipine, whereas hexamethonium and lidocaine inhibited the effect of nifedipine. Therefore, complex neural networks were regulating the

function of the intestinal peptide transporter. Sympathetic noradrenergic fibers, intestinal sensory neurons, and nicotinic synapses might all be involved in the increase of cephalexin absorption induced by nifedipine.

In conclusion, the function of peptide transporters can be affected by many factors including protein kinases, glycosylation, histidine, tyrosine, substrate-binding domain, zinc, trauma, diet, sigma receptor ligand, and neurons.

Functional Characteristics of Peptide Transporters

Stoichiometry and Proton-Dependence of Peptide Transporters. Peptide transporters are dependent on the presence of protons for transport activity. Four hydrolysis-resistant dipeptides (Phe-Ala, Phe-Glu, Phe-Gln, and Phe-Lys) were used to investigate the effects of net charge on transmural dipeptide transport by isolated jejunal loops of rat small intestine (Lister et al., 1997). At a luminal pH of 7.4, dipeptides with a net charge of -1 (Phe-Glu) and +1 (Phe-Lys) were transported at substantially slower rates than neutral Phe-Ala and Phe-Gln. At a pH of 6.8, transmural transport of Phe-Ala and Phe-Gln was increased by 61% and 49%, respectively. The lower pH increased the rate for negatively charged Phe-Glu by 306% and decreased the rate for positively charged Phe-Lys by 46%. Increasing luminal pH to 8.0 inhibited Phe-Ala transport by 60%, whereas Phe-Lys transport was increased 60%. The transport rate for Phe-Glu or Phe-Gln was not reported at pH 8.0. These results demonstrate that the transport of neutral and negatively charged peptides is linked to the cotransport of protons, whereas that of the positively charged peptide is not.

Brandisch et al. (1997) studied the effect of protons on the affinity and V_{max} of Gly-Sar uptake by Caco-2 (PepT1) and SKPT cells (PepT2). Uptake of Gly-Sar was measured over a concentration range in both cells at an outside pH of either 6.0 or 7.0. In Caco-2 cells, the K_t was 1.0 m*M* at pH 6.0 and 1.2 m*M* at pH 7.0. However, the V_{max} was $13.7 \pm .3$ nmol· 10 min^{-1}· mg^{-1} of protein at pH 6.0 and $5.8 \pm .3$ nmol· 10 min^{-1}· mg^{-1} of protein at pH 7.0. Similar results were obtained with SKPT cells. In both cell types, protons affected only V_{max} but did not affect the affinity of the transporters for the substrates.

Steel et al. (1997) expressed PepT1 in *Xenopus* oocytes to study the stoichiometry and pH dependency of PepT1. They observed a reduction of the pH inside the cell when differently charged peptides (Gly-Glu, Gly-Leu, and Gly-Lys) were transported, suggesting the movement of protons. After calculating the rate at which different dipeptides induced intracellular acidification and the rate of the uptake of peptides and the related charge influxes, the authors suggested a proton-peptide coupling ratio of 1:1, 2:1, and 1:1 for neutral, acidic, and basic dipeptides, respectively. The results also indicated that at a pH of 5.5 to 6.0, PepT1 favored substrates as neutral and acidic forms.

The stoichiometry of peptide transport in rat renal BBMV was variable and depended on the net charge carried by the substrate. The proton-peptide coupling ratio for anionic (Phe-Glu), neutral (Phe-Ala) and cationic (Phe-Lys) dipeptides was reported to be 2:1, 1:1, and 0:1 respectively (Temple et al., 1995). The stoichiometry for neutral (Gly-Ala), and anionic (Gly-Glu) dipeptides has been confirmed in PepT1-expressing *Xenopus* oocytes (Steel et al., 1997). However, Temple (1998) found that the transport

of the cationic peptide (Gly-Lys) was pH-dependent with a coupling ratio of 1:1. The transport of both the anionic dipeptides Phe-Glu and the cationic dipeptides Phe-Lys in renal BBMV was inhibited by both enalapril and captopril (angiotensin-converting enzyme inhibitors) providing evidence that, in this system, both of these charged peptides are transport by PepT1. Enalapril and captopril are not substrates for PepT2 (Boll et al., 1996). Therefore, the reason for the observed difference has yet to be determined, but does not appear to be due to the transport of Phe-Lys by PepT2 in renal BBMV.

The binding and dissociation of ions near the extracellular surface of the human PepT1 is thought to evoke a pre-steady-state current that results in a conformational change and leads to a translocation of the charged empty carrier (Mackenzie et al., 1996). However, results from Nussberger et al. (1997) indicated a symmetry of H^+ binding in response to either intra- or extracellular acidification, which suggested that PepT1 has only one proton binding site that can be accessed from either side of the membrane.

For PepT2, inward currents were qualitatively and quantitatively similar regardless of the net charge of the substrate at a given pH, which indicated the possibility of a variable flux-coupling ratio for H^+/H_3O^+-dependent peptide transport. Amasheh et al. (1997b) showed, for PepT2, that the characteristics of both peptide and proton interaction with the transporter were nearly independent of the net charge of peptides. In the case of PepT1, mainly (or only) the zwitterionic substrate species of a charged peptide was transported by a 1:1 flux-coupling ratio. In the case of PepT2, kinetic analysis of proton-dependent inward currents at saturating substrate concentrations did not provide any evidence for a Hill coefficient significantly greater than 1 for any of the substrates. This

suggested that there were no multiple H^+ binding sites with different affinities, which favored the hypothesis of a fixed coupling ratio for transport of the substrate species carrying no net charge. There is evidence that other solute transporters also have the capability to transport anionic as well as cationic substrates electrogenically with similar kinetics. In the case of PepT2, the weak pH dependence of dipeptide affinities might be due to the high substrate affinities. Even low concentrations of the zwitterionic form of a substrate might quickly cause saturation of binding sites. Therefore, transport rates might be dependent only on membrane potential and proton binding.

Chen et al. (1999a) reported their kinetic analysis of the rat kidney high-affinity peptide transporter PepT2 expressed in *Xenopus* oocytes. Using simultaneous radioactive uptake and current measurements under voltage-clamp conditions, the charge to substrate uptake ratio was found to be close to two for both Phe-Ala (neutral) and Phe-Glu (anionic). This indicated that the H^+:substrate stoichiometry was 2:1 and 3:1 for neutral and anionic dipeptides, respectively. The higher stoichiometry for anionic peptides suggested that they were transported in the protonated form. For cationic peptide Phe-Lys, the charge to uptake ratio was 2.4:1. This suggested that Phe-Lys was transported across the membrane via PepT2 either in its deprotonated (neutral) or its positively charged form with an average stoichiometry of 1.4:1. These findings led to the conclusion that PepT2 coupled transport of one peptide molecule to two H^+. This is in contrast to the low-affinity transporter PepT1 that couples transport of one peptide to one H^+. Meanwhile, Fei et al. (1999) studied the interaction of rat PepT2 with neutral, anionic, and cationic dipeptides using both electrophysiological and radioactive uptake methods. Phe-

Gln (neutral), Phe-Glu (anionic), and Phe-Lys (cationic) were chosen as representative peptide substrates. All three peptides induced H^+-dependent inward currents in *Xenopus laevis* oocytes expressing rat PepT2. The H^+:peptide stoichiometry was 1:1 in each case. A simultaneous measurement of radiolabeled peptide influx and charge transfer in the same oocyte indicated that the transfer of one net positive charge into the oocyte coupled with the transfer of one peptide molecule in each case irrespective of the charged nature of the peptide. This suggested that the zwitterionic peptides were preferentially recognized by PepT2 as transportable substrates and that the proton:peptide stoichiometry was 1:1 for the transport process. The reason for the observed differences between these two studies has yet to be determined.

Substrate Specificity of Peptide Transporters. Transport studies have shown that cloned peptide transporters are capable of taking up a broad range of di- and tripeptides and peptidomimetics. At a pH of 7.5, two charged dipeptides (Phe-Glu, -1, and Phe-Lys, +1) were transported slower than the neutral dipeptides (Phe-Gln and Phe-Ala). At a pH of 6.8, transport rate for the negatively charged Phe-Glu and the neutral peptides (Phe-Gln and Phe-Ala) increased, whereas transport rate for the positively charged Phe-Lys decreased. Increasing the pH to 8.0 inhibited the uptake of the neutral peptide Phe-Ala, but increased the uptake for Phe-Lys (Lister et al., 1997). These results suggested that the peptide transporter preferred neutral substrates compared with charged peptides under physiological pH conditions.

Substrate specificity of rabbit PepT1 was examined in *Xenopus* oocytes injected with rabbit PepT1 cRNA (Amasheh, et al. 1997b). The uptake of differently charged

substrates was determined by measuring the inhibition of [^{3}H]-Phe-Ala uptake upon addition of substrates at a pH of 8.0, 7.4, 6.5, or 5.5. Greater inhibition means more absorption of the unlabled substrate by the transporter. The glycyl peptides studied included Gly-Gln (zwitterionic), Gly-Asp (anionic), and Gly-Lys (cationic). At each pH, Gly-Gln strongly inhibited the uptake of [^{3}H]-Phe-Ala. The Gly-Asp inhibited the uptake of [^{3}H]-Phe-Ala at a pH of 7.4 or lower. Gly-Lys inhibited uptake only when the pH was at or higher than 6.5. These results suggest that, under physiological conditions, the affinity of PepT1 for the zwitterionic or anionic substrates is greater than for cationic substrates.

Results from the examination of the transport of the anionic cefixime and zwitterionic cefadroxil in *Xenopus* oocytes expressing rabbit PepT1 and in Caco-2 cells have been reported (Wenzel et al., 1996). In both oocytes and Caco-2 cells, zwitterionic cefadroxil was transported more rapidly at a pH equal to or higher than 6.0. The anionic cefixime was absorbed more efficiently when the pH was equal to or lower than 6.0 (Wenzel et al., 1996). The authors calculated the percentage of the charged or zwitterionic forms of the substrates at each pH. For instance, the relative proportion of the neutral form of cefixime increased as the pH was lowered below 6.0. These results again indicate that the zwitterionic form of the substrate is preferred by the peptide transporters under physiological conditions.

In a study conducted by Ganapathy et al. (1997), the anionic peptidomimetics cephalosporins (cefixime, ceftibuten, and cefdinir) were used as substrates to study substrate interactions with PepT1 and PepT2. At pH of 6.0, cefixime and ceftibuten are

dianionic, and cefdinir is monoanionic. The human intestinal cell line, Caco-2, which only expresses PepT1 (Ganapathy et al., 1995) and rat kidney cell line, SKPT, which only expresses PepT2 (Brandsch et al., 1995) were used. Uptake of [^{14}C]-Gly-Sar in both cell lines was inhibited significantly by cephalosporins in the order of ceftibuten > cefixime > cefdinir. The same results were obtained when PepT1 and PepT2 were expressed in Hela cells. In a subsequent study, *Xenopus laevis* oocytes were injected with PepT1 mRNA. Oocytes incubated with the negatively charged ceftibuten at pH 7.5 showed a small outward current. At a pH of 6.0, addition of ceftibuten (dianionic) to the buffer induced a huge inward current. These results provide further evidence that the zwitterion is the preferred form.

Functions of Peptide Transporters. The function of the peptide transporter in different tissues is under intensive investigation. The different expression patterns of PepT1 and PepT2 among tissues actually reflect their functions in animals. The expression of PepT1 in the small intestine and the kidney of animals is of nutritional and pharmacological importance. The transport of peptides not only contributes to the body nitrogen needs (Matthews, 1991), but also participates in the absorption of many therapeutically active peptides, including peptide-like antibiotics, anti-cancer drugs (Inui et al., 1992), and angiotensin-converting enzyme inhibitors (Swaan et al., 1995). It might also serve as a pathway for the absorption of some metals that are required by the animal (Tacnet et al., 1993) and reabsorption of peptides in the kidney (Smith et al., 1998). Bockman et al. (1997) showed for the first time that an H^+/peptide cotransporter was located in nuclei of vascular smooth muscle cells and Schwann cells and in lysosomes of

the exocrine pancreas. It is likely that the transporter moved small peptides from the lysosome to the cytoplasm following intralysosomal protein degradation. The function of the transporter in the nucleus remains unclear. Peptide signaling molecules may be transmitted between the nucleus and cytoplasm using a peptide transporter.

Although PepT2 is mainly expressed in the kidney and is responsible for reabsorption of peptide forms of amino nitrogen (Daniel and Herget, 1997), PepT2 is also expressed in the brain (Boll et al., 1996; Saito et al., 1996). A new study using nonisotopic *in situ* hybridization was performed to analyze the distribution of PepT2 mRNA in rat brain, retina and peripheral ganglia (Berger and Hediger, 1999). The results showed that PepT2 was expressed in rat brain by astrocytes, ependymal cells, subependymal cells, and the epithelial cells of the choroid plexus. PepT2 mRNA was also expressed by retinal Muller cells and peripheral satellite cells. The expression levels of PepT2 were below average in distinct areas in the ventral forebrain compared to astrocytes. Other glial cells or neurons did not express PepT2. These results suggested that it is astrocytes that remove small peptides from the extracellular fluid. It was also shown that PepT2 was expressed in astroglia-rich primary cultures and that this might be responsible for the uptake of Cys-Gly in the cultures (Dringen et al., 1998). The peptide transporter, PHT1, was also isolated from rat brain. PHT1 was expressed in both neurons and glial cells in *in situ* hybridization studies (Yamashita et al., 1997), and it likely also participates in the removal of small peptides.

Traditionally, it was believed that only free amino acids entered the portal blood from intestinal epithelial cells (Matthews, 1991). However, recent studies demonstrated

that ~50% of circulating plasma amino acids were peptide bound, and the majority were in the form of di- and tripeptides (Seal and Parker, 1996), suggesting the existence of a basolateral peptide transporter in the small intestine. Terada et al. (1999) used Gly-Sar to examine the transport system of the basolateral peptide transporter in Caco-2 cells. The apical PepT1 and basolateral peptide transporter in human intestinal Caco-2 cells were functionally compared by characterization of [^{14}C]-Gly-Sar transport. The Gly-Sar uptake via the basolateral peptide transporter was less sensitive to medium pH and was not transported against a concentration gradient as was uptake via PepT1. Comparison of the inhibition constant values of various β-lactam antibiotics for PepT1 and the basolateral peptide transporter suggested that PepT1 had a higher substrate affinity than the basolateral peptide transporter. DEPC, a histidine residue modifier, inhibited Gly-Sar uptake by both transporters, and the inhibitory effect was greater on PepT1 than the basolateral peptide transporter. These findings suggest that a different peptide transporter is expressed at the basolateral membranes of Caco-2 cells and that PepT1 and the basolateral peptide transporter cooperate in the efficient transepithelial transport of small peptides and peptide-like substrates.

In conclusion, PepT1 and PepT2 are proton-dependent peptide transporters. PepT1 couples transport of one peptide to one H^+, whereas PepT2 couples transport of one peptide molecule to two H^+. However, both PepT1 and PepT2 prefer the zwitterionic form of the substrate under physiological conditions. The expression of PepT1 in the small intestine and PepT2 in the kidney is of nutritional and pharmacological importance.

Recognition Patterns of Substrate by Peptide Transporters

Peptide transporters can recognize a broad range of natural substrates for the maintenance of protein nutrition (Matthews, 1991). To understand the structure-function relationships and the specificities of the peptide transporters, different forms of peptide-like substrates were used to investigate how peptide transporters recognize different substrates. These studies using peptide-like substrates to examine transport capabilities of peptide transporters have provided some valuable information to help us understand how peptide transporters function.

Beta-Lactam Antibiotics. The structure of most of the β-lactam antibiotics resembles the backbone of tripeptides with the second peptide bond incorporated into a lactam ring (Figure 2.5). The peptide substrates of the peptide transport system and cephalexin share certain structural features such as a peptide bond with an α-amino group and a terminal carboxylic acid group. This structural similarity is apparently the basis for the molecular mimicry, enabling the peptide transporters to accept cephalexin as a substrate. The two organs, the small intestine and the kidney, in which the peptide transporters are primarily expressed, play an important role in the therapeutic efficacy of β-lactam antibiotics. The intestinal peptide transport system is responsible for the absorption of these orally administrated drugs. The renal peptide transport system, which functions in the reabsorption of these drugs from the glomerular filtrate, enhances the half-life of these drugs in the circulation. Therefore, detailed studies on the interaction of β-lactam antibiotics with the peptide transporters in these two organs are vital to the understanding of the pharmacodynamics of these drugs.

Ganapathy et al. (1995) examined the differences in the recognition of β-lactam antibiotics by the intestinal and renal peptide transporters, PepT1 and PepT2. PepT1 was studied in the human intestinal cell line Caco-2, which expresses PepT1 but not PepT2. PepT2 was studied in the rat proximal tubule cell line SKPT, which expresses PepT2 but not PepT1. The substrate recognition pattern of PepT1 and PepT2 was studied with cefadroxil (a cephalosporin) and cyclacillin (a penicillin) as model substrates for the peptide transporters that were constitutively expressed in Caco-2 cells (PepT1) and SKPT cells (PepT2). Cyclacillin was ninefold more potent than cefadroxil in competing with Gly-Sar for uptake by PepT1, whereas, cefadroxil was 13-fold more potent than cyclacillin in competing with the dipeptide for uptake by PepT2. The substrate recognition pattern of PepT1 and PepT2 was also studied using cloned human peptide transporters functionally expressed in HeLa cells. Expression of PepT1 or PepT2 in HeLa cells was found to induce H^+-coupled cephalexin uptake in these cells. Similarly, the peptide uptake induced by PepT1 cDNA in HeLa cells was inhibited more potently by cyclacillin than by cefadroxil, and the peptide uptake induced by PepT2 cDNA in HeLa cells was inhibited more potently by cefadroxil than by cyclacillin. Thus, the recognition of β-lactam antibiotics as substrates between the intestinal and renal peptide transporters was markedly different.

To investigate whether multiple peptide transporters mediate absorption of β-lactams carrying different charges (the anionic cefixime and the zwitterionic cefadroxil) at physiological pH, Wenzel et al. (1996) used Caco-2 cells and *Xenopus laevis* oocytes expressing the cloned rabbit PepT1. Both cefixime and cefadroxil were taken up into both

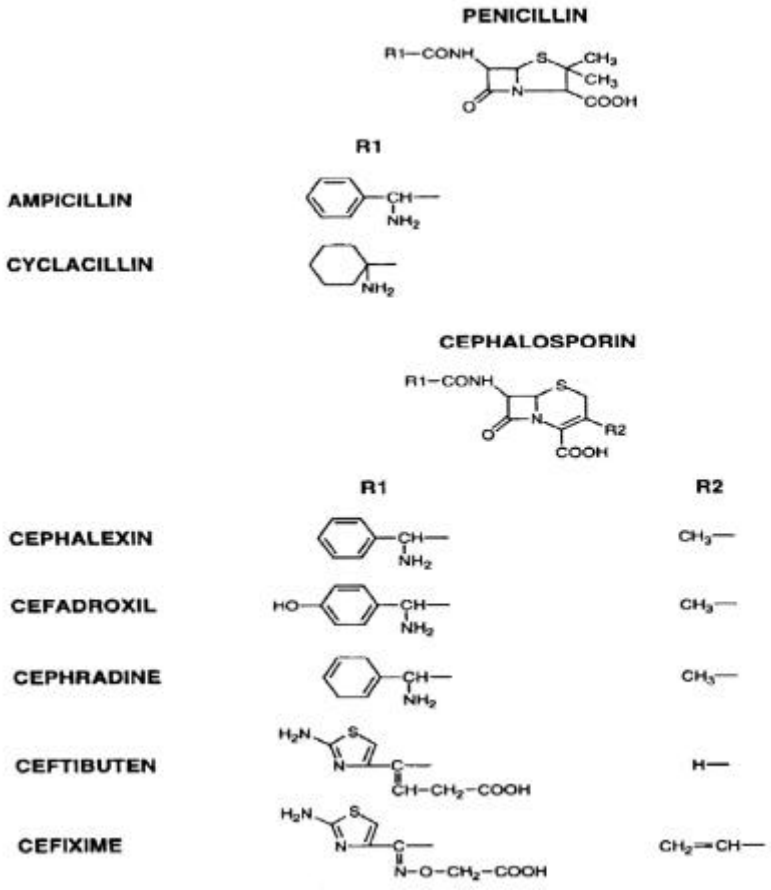

Figure. 2.5. Chemical structures of some β-lactam antibiotics (Ganapathy et al., 1995).

Caco-2 cells and oocytes expressing PepT1 in a pH-dependent and saturable transport manner. Mutual inhibition suggested that acidic and zwitterionic substrates might share a common transporter. Cefixime and cefadroxil caused a significant decline in intracellular pH because of proton coupled substrate influx. Uptake of cefixime and cefadroxil into oocytes expressing PepT1 was electrogenic, which indicated that transport of both cefixime and cefadroxil was associated with movement of net positive charge. Compared to cefadroxil uptake, a more acidic pH was required for cefixime uptake in both cell systems, and intracellular acidification was faster. This indicated that cefixime was taken up only in its nonionized form with an additional proton being cotransported. Thus, a single peptide transport system can mediate electrogenic uptake of the neutral form of all β-lactam antibiotics into intestinal epithelial cells.

Terada et al. (1997) compared the recognition of β-lactam antibiotics by LLC-PK_1 cells stably transfected with PepT1 or PepT2 cDNA. Cyclacillin and ceftibuten (Figure 2.5) showed inhibitory effects on the Gly-Sar uptake in the PepT1-expressing cells. Other β-lactams, such as cephalexin, cefadroxil, and cephradine (Figure 2.5), inhibited modestly the PepT1-mediated Gly-Sar uptake. All β-lactams, except for ceftibuten, showed much more potent inhibition of Gly-Sar uptake by PepT2 than by PepT1. Comparison of the inhibition constant values between cefadroxil and cephalexin indicated that the hydroxyl group at the NH_2-terminal phenyl ring increased affinity for both PepT1 and PepT2. Therefore, PepT2 had a much higher affinity for β-lactam antibiotics having an α-amino group than PepT1, and substitutes at the NH_2-terminal side chain of these drugs were involved in the recognition by both peptide transporters. These findings were similar to

those reported for the human PepT1 and PepT2, suggesting the differential recognition of β-lactam antibiotics (Ganapathy *et al.*, 1995). By evaluating the inhibitory potencies of the antibiotics against Gly-Sar transport, the interactions of β-lactam antibiotics with peptide transporters in rat renal brush-border membranes were examined (Takahashi et al., 1998). Western blot analysis showed that PepT1 and PepT2 with apparent molecular masses of 75 and 105 kDa, respectively, were expressed in the renal brush-border membranes. Two transport systems with high affinity (K_m of 50 μ*M*) and low affinity (K_m of 1.2 m*M*) appeared to mediate Gly-Sar uptake. The inhibition constants of the antibiotics for Gly-Sar uptake were more closely correlated with those in LLC-PK_1 cells stably transfected with rat PepT2 rather than PepT1 cDNA. The β-lactam antibiotics with an α-amino group showed *trans*-stimulation effects on Gly-Sar uptake. This indicated that these amino-β-lactam antibiotics and Gly-Sar shared a common peptide transporter. The antibiotics lacking an α-amino group failed to show the *trans*-stimulation effect. The amino-β-lactam antibiotics were shown to interact predominantly with PepT2 localized in the brush-border membranes of rat kidney.

ACE Inhibitor. The angiotensin converting enzyme (ACE) inhibitors (Figure 2.6) captopril and enalapril, but not lisinopril, were substrates for the intestinal peptide transporter PepT1 (Boll, et al., 1994). However, the renal peptide transporter PepT2 was more selective. Substrates lacking an α-amino group (captopril and enalapril) appeared to not be transported by PepT2 (Boll et al., 1996). Akarawut et al. (1998) subsequently reported that quinapril was capable of non-competitively inhibiting the uptake of Gly-Sar by PepT2 in rabbit renal BBMV. Because of the close structural similarity between

quinapril and enalapril, Lin et al. (1999) examined the inhibitory potential of enalapril and other ACE inhibitors on Gly-Sar transport, and its mechanism of inhibition. Their kinetic analysis demonstrated that enalapril inhibited the uptake in a competive manner (K_i = 6 m*M*). Fosinopril and zofenopril had the greatest inhibitory potency, whereas the other ACE inhibitors showed low-affinity interaction with PepT2. Overall, the inhibitory potency of tested ACE inhibitors was as follows: fosinopril > zofenopril > ramipril ≈ quinapril > quinaprilat > enalapril > captopril > lisinopril > enalaprilat. In the absence of enalapril, quinaprilat, and quinapril, ACE inhibitor affinity for PepT2 had a very strong correlation with the lipophilicity of the drugs ($r = .98$, $p < .001$). For all ACE inhibitors, the correlation was still strong ($r = .94$, $p < .001$).

Valacyclovir. Valacyclovir is a prodrug of acyclovir that does not contain a peptide bond in its structure (Figure 2.6). Acyclovir is used to treat a variety of viral infections including cytomegalovirus infections, an AIDS opportunistic infection (Beauchamp et al., 1992). Valacyclovir is derived from acyclovir by esterifying valine to the hydroxyl group of acyclovir. Its bioavailability is three to five times higher than that of acyclovir in humans. Studies characterizing the intestinal absorption mechanisms of valacyclovir suggest the involvement of multiple transporters, including the peptide transporter (Sinko and Balimane, 1998). Ganapathy et al. (1998) studied the interaction of valacyclovir with the peptide transporters in the human intestinal cell line Caco-2 and the rat kidney proximal tubular cell line SKPT that differentially express peptide transporters PepT1 and PepT2. The activity of the peptide transporters was examined by measuring the uptake of radiolabeled Gly-Sar in the presence of a H^+ gradient.

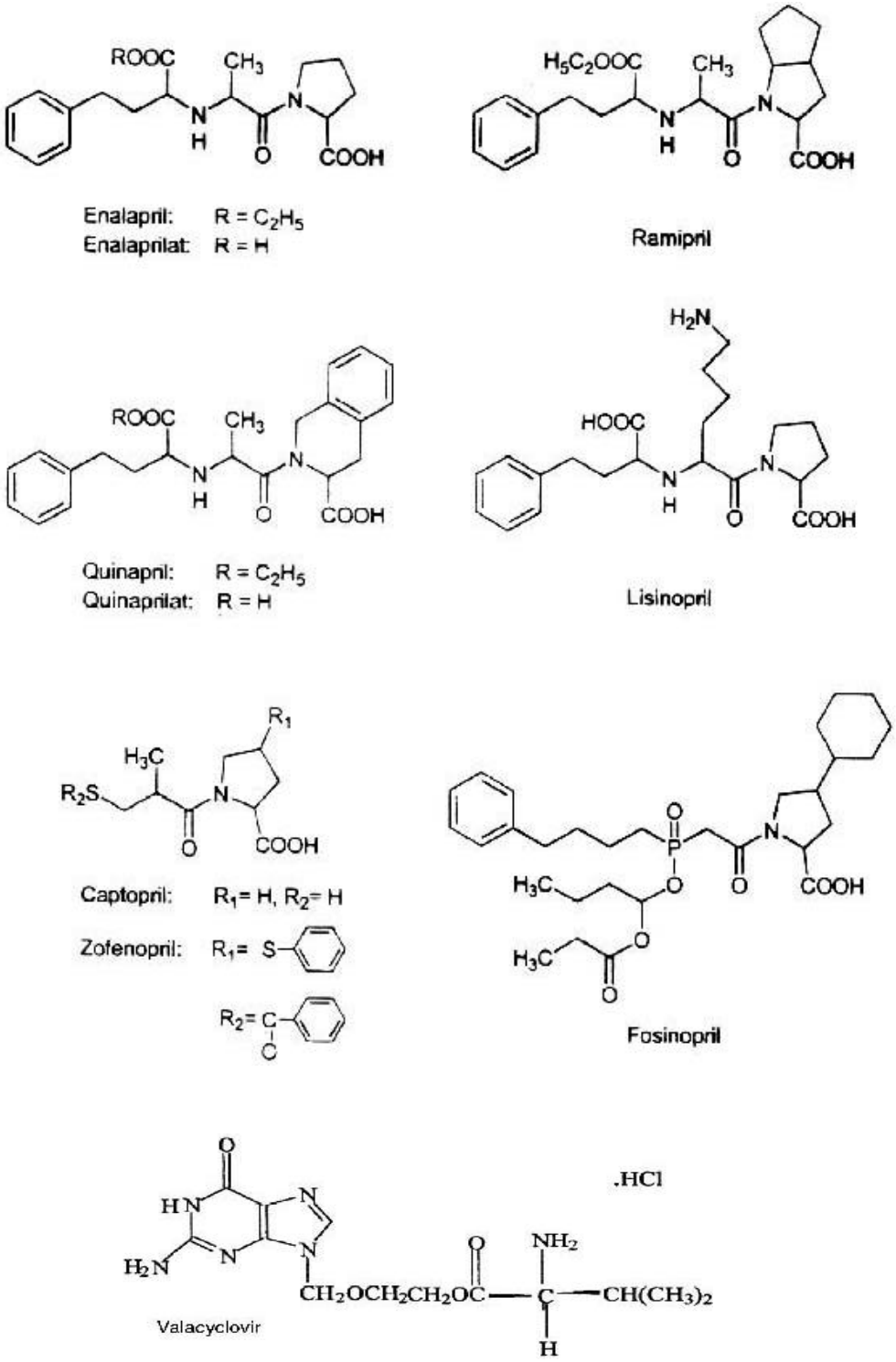

Figure. 2.6. Chemical structures of angiotensin converting enzyme (ACE) inhibitors (Lin et al., 1999) and valacyclovir.

Valacyclovir inhibited the uptake of Gly-Sar with an inhibition constant (K_i) of .49 ± .04 mM in Caco-2 cells and .17 ± .01 mM in SKPT cells in a competitive manner. Acyclovir, however, did not interact with the peptide transporters. Similar results were obtained with heterologously expressed human PepT1 and rat PepT2. It was concluded that valacyclovir was a substrate for the peptide transporters PepT1 and PepT2 and that a peptide bond was not a prerequisite for recognition as a substrate by the peptide transporters.

Guo et al. (1999) characterized the interaction of valacyclovir and hPepT1 using Chinese hamster ovary (CHO) cells that overexpressed the hPepT1 gene. Valacyclovir uptake was significantly greater in CHO cells transfected with hPepT1 than in cells transfected with only the vector. The optimum pH for valacyclovir uptake was pH 7.5. Proton cotransport was not observed in hPepT1/CHO cells, consistent with previous results in tissues and Caco-2 cells (Ganapathy et al., 1998). A very similar K_m value was obtained in hPepT1/CHO cells and in rat and rabbit tissues and Caco-2 cells, indicating that hPepT1 dominated the intestinal transport of valacyclovir in vitro. Valacyclovir uptake was also markedly inhibited by various dipeptides and β-lactam antibiotics. These findings confirmed that valacyclovir was a substrate for the human PepT1 in hPepT1/CHO cells. Although transport was pH dependent, proton cotransport was not necessary.

Using stable transfectants, Sawada et al. (1999) examined the transport mechanisms of the L-amino acid ester compounds with rat PepT1 and PepT2 using stable transfectants. Valacyclovir, competitively inhibited [^{14}C]-Gly-Sar uptake in the LLC-PK_1-rPEPT1 and LLC-PK_1-rPEPT2 cells, respectively. The inhibition constants (K_i) of

valacyclovir were 2.7 and .22 m*M* for rPepT1 and rPepT2, respectively. These results indicated that rPepT2 had higher affinity for valacyclovir. L-Valine methyl ester (Val-OMe) competitively inhibited [^{14}C]-Gly-Sar uptake. K_i values of 3.6 and .83 m*M* for rPepT1 and rPepT2, respectively, indicated that Val-OMe was also a high-affinity substrate for rPepT2. Val-OMe showed the most potent inhibitory effect among the several L-amino acid methyl esters examined. These results suggested that L-valine could be a desirable L-amino acid for the esterification of poorly permeable drugs to enhance their oral bioavailability to intestinal PepT1.

Delta-Aminolevulinic Acid. Delta-aminolevulinic acid (ALA) is the precursor of porphyrin synthesis and has been recently used in vitro and in clinical studies in the treatment of various tumors. Doring et al. (1998a) demonstrated that ALA used the intestinal and renal apical peptide transporters for entering into epithelial cells. Kinetics and characteristics of ALA transport were determined in *Xenopus laevis* oocytes and *Pichia pastoris* yeast cells expressing either PepT1 or PepT2. By using radiolabeled ALA and electrophysiological techniques in these heterologous expression systems, it was shown that PepT1 and PepT2 translocate [^{3}H]-ALA by saturable and pH-dependent transport mechanisms. Di-/tripeptides and ALA, but not GABA or related amino acids, also competed at the same substrate-binding site of the transporters. Reverse transcriptase-PCR analysis using specific primers for PepT1 and PepT2 in rabbit tissues demonstrated that the PepT2 mRNA was expressed in a variety of other tissues including lung, brain, and mammary gland, which had been shown to accumulate ALA. This indicated that these tissues could take up ALA through peptide transporters, providing the

endogenous photosensitizers for efficient treatment. Also for the first time, this study showed that a molecule not possessing a peptide bond was transported as a high affinity substrate by both epithelial peptide transporters. However, a structurally related analogue, γ-aminobutyric acid, which had a shorter backbone than ALA, was not transported by PepT1 and PepT2. This indicated that four or more carbon units in the backbone of the substrates between the amino- and carboxy-terminal groups for the substrates were needed for transport. This corresponded to the backbone length in normal dipeptides. The peptide bond in a dipeptide could be replaced by a ketomethylene function, as present in ALA, without loss of substrate affinity for the peptide transporter by use of arphamenins (Daniel and Adibi, 1994). Similarly, arphamenin A was also shown to serve as a substrate for PepT1 in human Caco-2 cells (Enjoh et al., 1996). Therefore, transport of ALA by PepT1 and PepT2 indicated that, besides the amino and carboxy groups, the carbonyl function at the γ-carbon of ALA was sufficient for recognition as a substrate. This carbon corresponds to the position of the carbonyl function in a normal dipeptide. The side chains present in normal dipeptides might not be important for the interaction with the substrate-binding sites.

Amino Acid Aryl Amides. Transport of amino acid aryl amides by PepT1 was studied in Caco-2 cells and in *Xenopus* oocytes expressing human PepT1 (Borner et al., 1998). In Caco-2 cells, Ala-4-nitroanilide, Phe-4-nitroanilide and Ala-4-phenylanilide were accepted as substrates with equal or higher affinity than natural Ala-containing dipeptides. Ala-anilide, Ala-7-amido-4-methylcoumarin, Ala-4-chloroanilide and Ala-4-methylanilide were also recognized by PepT1 as substrates with lower affinity than natural

Ala-containing dipeptides. In contrast, alanine, Ala-amide, Phe-amide, Ala-methyl ester, Ala-4-nitrobenzyl ester and Ala-methylamide were not recognized as substrates by PepT1. In oocytes, transport of Ala-4-nitroanilide, Ala-7-amido-4-methylcoumarin, Ala-4-methylanilide and Ala-anilide was associated with transfer of positive charge and the currents were saturable with respect to substrate concentration. The data suggested that PepT1 accepted amino acid aryl amides as substrates with different affinity constants.

Dopa-Derivative. Dopa is a metabolite that is structurally similar to the amino acid phenylalanine, and is normally absorbed from the small intestine by amino acid transporters. L-Dopa (L-3,4-dihydroxyphenylalanine) is effective for treatment of Parkinson's disease. However, because of instability and low permeation rate, the bioavailability of L-Dopa is very low. In rat intestinal BBMV, a dipeptide-mimetic, α-methyldopa-Phe, was recognized and transported by the peptide transporter (Tsuji et al., 1990). Another peptidyl-mimetic, phenylglycine-α-methyldopa was also recognized and taken up in rat intestinal BBMV (Wang et al., 1996). Based on these findings, Tamai et al. (1998) used Caco-2 cells and *Xenopus* oocytes expressing human PepT1 to determine whether PepT1 could be used to improve dopa absorption. The dipeptidyl-mimetic derivative of dopa, dopa-Phe, inhibited the uptake of Gly-Sar by Caco-2, but did not inhibit the uptake of dopa. In oocytes expressing PepT1, it was confirmed that dopa-Phe was transported by PepT1. The amount of dopa-Phe crossing the Caco-2 cell monolayer was 40-fold greater than that of dopa.

N-Acetyl Aspartyl Glutamate. N-acetyl aspartyl glutamate (NAAG), a dipeptide derivative, is present in high concentrations in the mammalian brain. This peptide has been

suggested to function as a neurotransmitter (Moffett et al., 1990). Wang et al (1998) reported the functional characteristics of PepT2 expressed in the two mammalian cell lines, HeLa (a human cervical epithelial cell line) and SK-N-SH (a human neuroblastoma cell line), as well as in *Xenopus* oocytes. Normally, PepT2 exhibited much higher affinity (micromolar range) for its substrates than did PepT1 (Ramamoorthy et al., 1995). The results demonstrated that NAAG was a substrate for PepT2, which was also expressed in the brain. However, the K_t for NAAG with PepT2 was in the low millimolar range, which indicated that the blocking of the α-amino group by acetylation might reduce the affinity. Nonetheless, the observed values may be physiologically relevant. NAAG is present in the mammalian nervous system at very high concentrations (Fuhrman et al., 1994). The concentration of NAAG was in the range .2-4.5 mM in different regions of the nervous system. Another interesting finding with respect to the interaction of NAAG (net charge, −3) and the other three peptides (net charges, −1, +1, and 0) with PepT2 was that the transport process induced inside-negative currents irrespective of the net charge of the peptide. However, the proton-to-peptide stoichiometry was still 1:1 in all cases. Amasheh et al. (1997b) reported similar findings for PepT2 cloned from rabbit kidney. A simple transport model assigning the charge translocation during the transport cycle solely to the movement of the peptide substrate and proton could not explain the observed findings. PepT1 was known to contain essential histidyl residues (Terada et al., 1996; Fei et al., 1997) that could exist either in a protonated form or in a nonprotonated form in the pH range 5.0-7.0, depending on the microenvironment of the involved histidyl residue. Similarly, PepT2 also possessed essential histidyl residues that were obligatory for the

transport function (Fei et al., 1997). Nussberger et al. (1997) proposed a model for the operational mechanism of PepT1. This model predicted the translocation of proton and peptide and the association of the transport process with inward negative currents irrespective of the net charge of the translocated peptide substrate. This model suggests the involvement of differently charged amino acids in the substrate-binding site of the PepT1 protein.

Substrate Structure Requirements for Peptide Transporters. Considering the wide distribution of peptide transporters throughout nature and their nutritional as well as pharmacological importance, identification of the minimal structural requirements of substrates affecting their affinity and capacity for transport would greatly advance our understanding of peptide transporters. Understanding the substrate structure requirement is very important in the design of new specific substrates for the peptide transporters. Swaan and Tukker (1997) tried to use computer-aided conformational analysis to characterize the recognition site of PepT1 based on studies of substrates with rigid backbones. Conformational analysis and calculations were used to determine the lowest energy conformation of transporter substrates, as well as the conformations of compounds that displayed common recognition site geometry, such as inhibitors, and inactive structural analogs. Substrate groups were classified into three interaction classes: substrates that were transferred across the membrane by transporters, inhibitors that showed affinity for the peptide transporter but were not transferred across the membrane, and other compounds that contained the recognition site geometry but showed no affinity for the carrier. The analysis indicated that there were three ways to diminish or abolish the

affinity of substrates for the peptide transporter: introduction of a second negative group into the substrates, esterification of the free carboxyl group of the substrates, or use of either side chains with a positively charged nitrogen function or groups capable of hydrogen bond formation to block the free carboxylic acid.

Based on data derived from competition studies in renal BBMV, Daniel and Herget (1997) proposed a simplified model of substrate requirements for PepT2 (Figure 2.7). In this model, PepT2 showed stereoselectivity that preferred all substrates built with L-enantiomers of amino acids. For high substrate affinity, a high hydrophobicity of side chains was required. Peptide bonds in the substrates could also be replaced without loss of binding affinity. Ketomethylene functions in the region of the first peptide bond or a cyclization in the region of the second bond could be used to replace peptide bonds. For example, replacing a rigid lactam ring structure has no effect on the capability and high affinity of a variety of β–lactam antibiotics interacting with the binding sites.

Using comparative molecular field analysis (CoMFA), a three-dimensional approach towards building quantitative structure-activity relationships, Swaan et al. (1998) examined the relationship between chemical structure (steric and electrostatic fields) and affinity for PepT1. Various biological activity parameters (K_t, J_{max}, P_c) and molecular descriptors (CoMFA fields, isobutylalcohol/water distribution coefficients) were examined. The results indicated that carrier permeability (P_c, calculated as the ratio of K_t), and the maximal carrier flux (J_{max}), were sensitive to composition, size and hydrophobicity of the substrates. The best model obtained predicted a high correlation between carrier permeability (P_c) and the steric (76.3% contribution) and electrostatic (23.7%

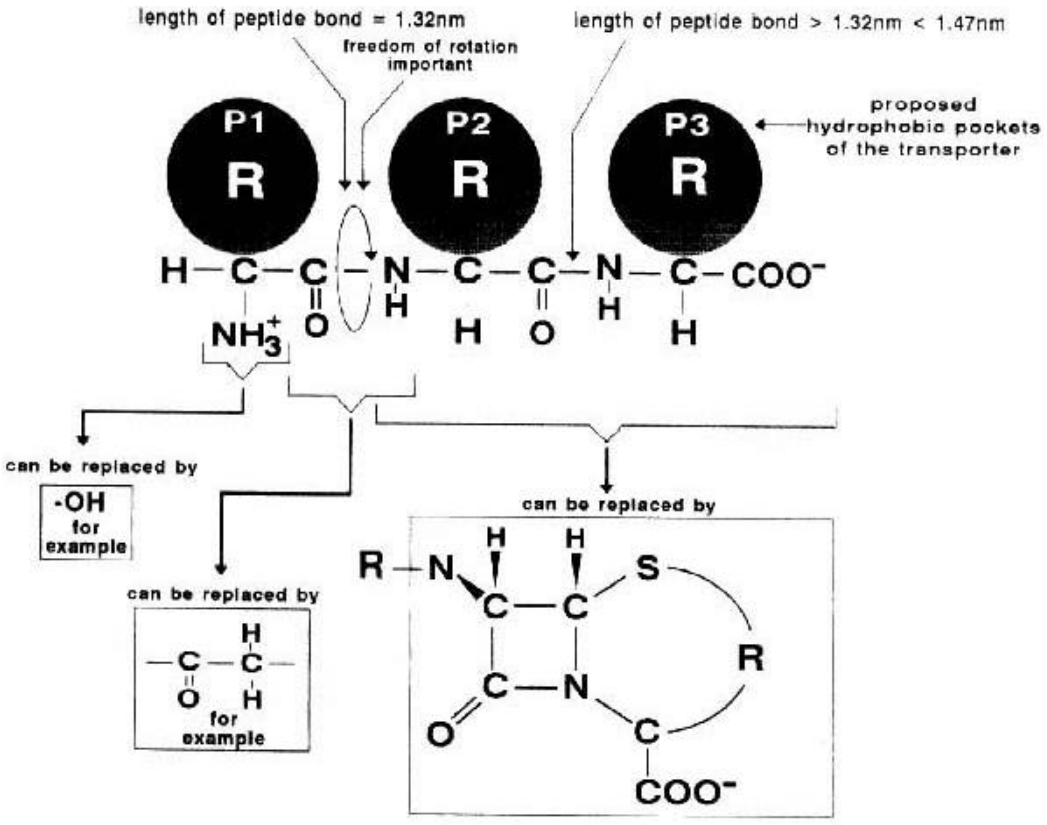

Figure 2.7. Proposed structural requirements for substrate recognition by PepT2. R: the side chains of amino acids. P1, P2, and P3: proposed hydrophobic pockets in the substrate-binding sites of PepT2 (Daniel and Herget 1997).

contribution) molecular fields with a correlation coefficient of .754. The model fit the experimental data with a correlation coefficient of .993 and a standard error of .041. These results could lead to a better understanding of the molecular requirements for optimal substrate-carrier interactions with the intestinal peptide transporter. This method offered a useful tool for designing new structures with affinity for PepT1.

It has been shown that 4-aminophenylacetic acid (4-APAA), a peptide mimic lacking a peptide bond, interacted with a proton-coupled oligopeptide transporter using a number of different experimental approaches. In addition to inhibiting transport of labeled peptides, these studies showed that 4-APAA is self-translocated (Temple *et al.* 1998). Transport of 4-APAA across the rat intact intestine was stimulated 18-fold by luminal acidification to pH 6.8 in enterocytes isolated from mouse small intestine. The intracellular pH was reduced on addition of 4-APAA, as shown with the pH indicator, carboxy-SNARF. Peptide transport was *trans*-stimulated by 4-APAA in brush-border membrane vesicles isolated from rat renal cortex. In *Xenopus* oocytes expressing PepT1, 4-APAA produced *trans*-stimulation of radiolabeled peptide efflux, and as determined by HPLC, 4-APAA was a substrate for translocation by this transporter. These results with 4-APAA showed that the presence of a peptide bond is not a requirement for translocation through PepT1. Interestingly, Meredith et al., (1998) reported that 4-aminomethylbenzoic acid (4-AMBA) competitively inhibited peptide influx in both *Xenopus* oocytes expressing rabbit PepT1 and through PepT1 in rat renal brush border membrane vesicles. 4-AMBA is a molecule that mimics the spatial configuration of dipeptides and is structurally similar to 4-APAA. However, 4-AMBA was not translocated through PepT1 as measured by

direct HPLC analysis in oocytes expressing PepT1. 4-AMBA also failed to trans-stimulate labelled peptide efflux through PepT1 in oocytes and in renal membrane vesicles. In oocytes expressing PepT1, efflux experiments were carried out with and without external peptide substrates as a function of 4-AMBA concentrations. When there was no peptide present, increasing 4-AMBA concentration had no effect on the efflux rate. The inhibitory ability of 4-AMBA was reduced with an increase in peptide concentration. This suggested that the substrate and inhibitor competitively bound at the same site. Therefore, 4-AMBA was the first molecule reported to be a non-translocated competitive inhibitor of peptide transport and thus might be particularly useful as an experimental tool.

Snyder et al., (1997) prepared 47 analogs of loracarbef and cephalexin to evaluate the structural features necessary for uptake by this peptide transporter. Loracarbef and cephalexin are derivatives of two β-lactams that contain a phenylglycine side chain. Analogs modified with a cyclopropyl or a trifluoromethyl group at the 3 position of cephalexin and loracarbef inhibited cephalexin uptake. Compounds with lipophilic groups on the primary amine of the side chain inhibited cephalexin uptake, retained activity against gram-positive bacteria but lost activity against gram-negative bacteria. Analogs lacking an aromatic ring in the side chain inhibited cephalexin uptake, but lost all antibacterial activity. Although the transporter preferentially transported the L stereoisomer, these analogs lacked antibacterial activity and were hydrolyzed intracellularly in Caco-2 cells. Substitution of the phenylglycyl side chain with a phenylacetyl side chain did not change the results. Thus, the phenylglycyl side chain is not absolutely required for uptake.

Both *cis* and *trans* conformers can be found in peptides and proteins due to the partial double bond character of the peptide bond. Whether peptide transporters are able to differentiate between *cis* and *trans* conformers of di- and tripeptides has not yet been shown. However, Daniel *et al.* (1992) had proposed that isomerization at the peptide bond might be responsible for the measured 4- to 12-fold lower affinities of Gly-Pro and Gly-Sar, compared with Gly-Gly and Gly-Ala at the renal peptide transporter. To study the structural requirements for substrates, Bransdsch et al. (1998) investigated the influence of the substrate backbone dynamics caused by peptide bond *cis/trans* isomerization on the intestinal peptide transport. Using Ala-ψ [CS-N]-Pro as a substrate in their investigation, the first direct evidence was provided for the conformational specificity of peptide transport. Ala-ψ [CS-N]-Pro is a modified dipeptide derivative where the peptide bond was replaced by the isosteric thioxo peptide bond. The Ala-Pro derivative, Ala-ψ [CS-N]-Pro, existed as a mixture of *cis* and *trans* conformation in aqueous solution and was characterized by a low *cis/trans* isomerization rate. Ala-ψ [CS-N]-Pro was recognized by PepT1 with high affinity. In solution with 96% *trans* conformation, the K_i value of Ala-ψ [CS-N]-Pro for the inhibition of the uptake of radiolabeled Gly-Sar in Caco-2 cells was .30 ± .02 m*M*. In contrast, in solution with 62% *trans* conformer, the K_i value was increased to .51 ± .02 m*M*. Therefore, only the *trans* conformer interacted with the transport system. Uptake of Ala-ψ [CS-N]-Pro was also studied by analyzing the intracellular content of Caco-2 cells following transport, as well as the composition of the extracellular medium using capillary electrophoresis. The percentage of *trans* conformer was 62% in the uptake medium, which increased to 92%

inside the cells. This was the first direct evidence that a H^+/peptide cotransport system selectively bound and transported the *trans* conformer of a peptide derivative.

PepT1, like its nonmammalian counterparts, transports almost all possible dipeptides, tripeptides, and numerous peptidomimetics. Free amino acids appear not to be accepted as substrates. Although transport of peptides and peptidomimetics occurs in a stereospecific manner (Wenzel et al., 1995), the transporter discriminates possible substrates only by differences in affinity for binding and maximal transport capacity. Because the ω-amino fatty acids (ω-AFA) represent simple structures, a modeling of their possible conformations could be performed (Doring et al. 1998b). Using the ω-AFA in combination with the modeling of these novel substrates that possessed only two functional groups and a hydrocarbon backbone, Doring et al. were able to define the minimal molecular requirements for substrate transport by PepT1. The capability of PepT1 for transport of ω-AFA was demonstrated in two different expression systems by using a radiolabeled ω-AFA as well as by measuring substrate-induced inward currents in voltage clamped *Xenopus* oocytes expressing PepT1. By employing computational analysis of possible substrate conformations in combination with transport assays using transgenic yeast cells and *Xenopus laevis* oocytes expressing PepT1, the minimal structural requirements for substrate binding and transport were determined. Based on a series of medium chain fatty acids bearing an amino group as a head group (ω-amino fatty acids, ω-AFA), transport by PepT1 required, as a minimum, the two ionized head groups separated by at least four methylene groups. Also, a distance of greater than 500 pm but less than 630 pm between the two charged centers (carboxylic carbon and amino nitrogen) was

needed for substrate to be recognized and transported. Additional groups in the ω-AFA backbone that provide more hydrogen bonding sites seemed to increase substrate affinity, but were not essential. Removal of either the amino group or the carboxyl group in ω-AFA maintained the affinity of the substrate for interaction with the transporter but abolished the capability for electrogenic transport.

In conclusion, the β-lactam antibiotics with an α-amino group are preferred by both PepT1 and PepT2. The lipophilicity of the ACE inhibitors has a strong correlation with affinity for PepT2. A peptide bond is not required for the transport by both PepT1 and PepT1, but four or more carbon units in the backbone of the substrates between the amino- and carboxy-terminal groups are needed for transport. PepT1 can selectively bind and transport the *trans* conformer of a peptide derivative.

Summary

The expansion of molecular biotechnology to nutrition and pharmacology research has led to the identification of a class of peptide transporters. Cloning and in vitro expression of these transporters have revealed the molecular structures and mechanisms of action of these peptide transporters. This review has concentrated on recent efforts to characterize the peptide transporters and their functions. Expression of transporter mRNA and transporter functional characteristics are two well-studied aspects. PepT1 and PepT2 are very similar in their structures that have 12 transmembrane domains and a long extracellular loop. HPT1 and PHT1 are two peptide transporters that are different from both PepT1 and PepT2. PepT1 is mainly an intestinal peptide transporter, whereas PepT2 is mainly a renal peptide transporter. Immunolocalization of PepT1 and PepT2 proteins

confirms that their mRNA and protein expression are coincident. More recent studies have focused on regulation of peptide transporters and recognition patterns of substrates by peptide transporters. The function of peptide transporters can be affected by many factors, such as protein kinases, glycosylation, histidine and tyrosine residues, substrate-binding domain, zinc, trauma, diet, sigma receptor ligand, and neurons. PepT1 and PepT2 are proton-dependent peptide transporters. PepT1 couples transport of one peptide to one H^+, whereas PepT2 couples transport of one peptide molecule to two H^+. However, both PepT1 and PepT2 prefer the zwitterionic form of the substrate under physiological conditions. A peptide bond is not required for the transport by both PepT1 and PepT2, but four or more carbon units in the backbone of the substrates between the amino- and carboxy-terminal groups are needed for transport. PepT1 can selectively bind and transport the *trans* conformer of a peptide derivative.

Most of the information that has been obtained regarding the ability of tissues to transport peptides has been in laboratory animals. The relative contribution of peptide transport may vary among animals because of the differences in their physiological conditions and metabolic status. Overall, little is known about the magnitude of peptide absorption and the metabolic significance of this phenomenon in domestic animals. Therefore, further studies on the identification of peptide transporters in different tissues and animals are needed in order for us to fully understand this absorption phenomenon.

Chapter III

Objectives

In recent years, the utilization of peptides as sources of amino acids and nitrogen has been recognized to be an important biological process in living species from micro-organisms to animals and plants (Payne and Smith, 1994; Meredith and Boyd, 1995). Much information has been obtained regarding the ability of the intestine (Leibach and Ganapathy, 1996) and tissues such as liver (Lochs et al., 1986), kidney (Daniel and Herget, 1997), and skeletal muscle (Roth et al., 1988) to use peptides. Overall, little is known about the magnitude of peptide absorption and the metabolic significance of this phenomenon in ruminants. Using an expression system, the data from injection of poly(A)$^+$ RNA isolated from omasal epithelia into *Xenopus laevis* oocytes (Matthews et al., 1996; Pan et al., 1997) indicated that mRNA encoding a transport protein(s) that is capable of dipeptide absorption exists in sheep omasal epithelium. However, the four-strata structure of all forestomach epithelia makes it difficult to purify and further characterize the transporter protein(s) using conventional procedures. With the success of cloning techniques in other species, the identification and characterization of peptide transporter protein(s) in ruminants becomes possible. Therefore, the objectives of this research were:

I. To obtain a full-length ovine peptide transporter cDNA by constructing and screening a cDNA library from sheep gastrointestinal epithelial tissues

with a 446-bp RT-PCR fragment cloned from sheep omasal epithelial total RNA (Chen et al., 1999b) as the probe.

II. To determine the sequence of the peptide transporter cDNA and compare the structural features with peptide transporters from other species.

III. To characterize the function of the sheep peptide transporter expressed in *Xenopus* oocytes following injection of *in vitro* synthesized cRNA.

IV. To survey the distribution of the peptide transporter mRNA in sheep using the full-length cDNA as the probe.

Chapter IV

Molecular Cloning, *In Vitro* Expression, and Functional Characterization of an Ovine Gastrointestinal Peptide Transporter (oPepT1)

Abstract

We report the primary structure, tissue distribution, and *in vitro* functional characterization of a peptide transporter, oPepT1, from ovine intestine. The ovine intestinal oPepT1 cDNA is 2,829 bp long encoding a protein of 707 amino acid residues with an estimated molecular size of 79 kDa, and a pI of 6.57. The cDNA contains a 79-bp 5'- untranslated sequence and a 630-bp 3'- untranslated sequence. The proposed oPepT1 protein is 77.9, 81.3, and 82.6 percent identical to PepT1 from rabbit, rat, and human, respectively. High stringency northern blot analysis demonstrated that oPepT1 is expressed strongly in the small intestine, at lower levels in the omasum, and at much lower levels in the rumen, but is not expressed in liver and kidney. The presence of the peptide transporter in the forestomach at such levels could provide amino acid nitrogen for the ruminant in a nutritionally significant manner. Transport function of oPepT1 was assessed by expressing oPepT1 in *Xenopus* oocytes using a two-electrode voltage-clamp technique. Overall, the *in vitro* transport characteristics of oPepT1 expressed in oocytes are similar to those of PepT1 from other species. The transport process is electrogenic and pH-

dependent, but independent of Na^+, Cl^-, and Ca^{2+}. It displays a broad substrate specificity that transported neutral and charged dipeptides and tripeptides. All dipeptides and tripeptides examined evoked inward currents in a saturable manner, with an affinity constant (K_t) ranging from 20 μ*M* to .6 m*M* for dipeptides and .15 to 3.0 m*M* for tripeptides. No responses were detected from tetrapeptides or free amino acids. Although many of the properties displayed by oPepT1 were similar to those of PepT1 from other species, some differences were noted. First, the isoelectric point of oPepT1 is lower than that of others, but the oPepT1 protein appears to have the same biological activity as that of others at a physiological pH. Second, more potential phosphorylation sites for protein kinases exist in oPepT1. Third, compared with PepT1 from other species, oPepT1 has more negatively charged amino acids at its C-terminus.

Key Words: Ovine, Peptide, Transport, Molecular cloning, Expression, Characterization

Introduction

The cloning and characterization of peptide transporters from different species has provided valuable information about peptide transport in mammalian species (Fei et al., 1994; Liang et al., 1995; Saito et al., 1995; Miyamoto et al., 1996). The unique structural and functional features shared by these peptide transporter proteins have attracted considerable attention from researchers to examine these systems. Most of the studies have been focused on peptide absorption in the gastrointestinal tract, kidney (Daniel, 1996), liver, and skeletal muscle in human and laboratory animals (Leibach and Ganapathy, 1996). The peptide transporter, PepT1, is mainly expressed in the small intestine with little expression occurring in liver and kidney (Fei et al., 1994; Liang et al., 1995; Miyamoto et al., 1996). Another peptide transporter, PepT2, is mainly expressed in kidney (Saito et al., 1996). The general structures of PepT1 and PepT2 proteins are similar in that they both contain 12 transmembrane domains and a large extracellular loop between transmembrane domains 9 and 10 (Fei et al., 1994; Meredith and Boyd, 1995). The amino acid sequences of the 12 transmembrane domains are highly conserved (85% identity), whereas the sequences of the extracellular loop are less conserved (35% identity; Daniel, 1996). These peptide transporters appear to be able to recognize most dipeptide and tripeptide substrates, as well as some pharmacologically active compounds including β-lactam antibiotics, angiotensin-converting enzyme (ACE) inhibitors, and the antitumor agent, bestatin (Leibach and Ganapathy, 1996).

Peptide transport is an important physiological process that occurs in tissues of animals (Matthews, 1991). However, little research has been conducted to identify the

system(s) responsible for the absorption of peptides in domestic animals. Early studies from our laboratory indicated that peptides might be absorbed from the ruminant gastrointestinal tract (Koeln and Webb, 1982) and recent reports demonstrate the existence and tissue distribution of a peptide transporter(s) in sheep, cows, pigs, and chickens (Matthews et al., 1996; Pan et al., 1997; Chen et al., 1999). Expression of mRNA in *Xenopus* oocytes showed that the mRNA present in sheep omasal epithelial tissue was capable of transporting di- to tetrapeptides. Although the size of the mRNA varied among species, the mRNA was present in the small intestine of all animals examined and the omasal and ruminal epithelium of sheep and cows. These results suggest that peptide absorption may be nutritionally important in the ruminant as well as other domestic animals.

Studying the structure, function, capacity, and regulation of the peptide transporter protein(s) in ruminants should not only provide us knowledge of the transport system in these animals, but should also help us understand the role that peptides may play as sources of amino acids. This knowledge should enhance our ability to manage animal diets for better performance without causing any nitrogen imbalance. The purpose of this study was to clone and express the ovine peptide transporter and to characterize the function of this transporter *in vitro* by expressing its cRNA in *Xenopus* oocytes.

Materials and Methods

Materials. All chemicals, substrates, and reagents were of either molecular biology or cell culture tested chemical grades. The ZAP Express cDNA synthesis system and ZAP Express cDNA Gigapack III cloning kit were purchased from Stratagene (La Jolla, CA). Restriction enzymes were from New England BioLabs (Beverly, MA). Magna Nylon transfer membranes were purchased from Micron Separation, Inc. (MSI, Westboro, MA). The RNA transcription kit, mMESSAGE mMACHINE, for synthesis of cRNA was obtained from Ambion (Austin, TX). *Xenopus laevis* frogs were purchased from Nasco (Fort Atkinson, WI) or Xenopus One (Ann Arbor, MI). Collagenase A was purchased from Boehringer Mannheim Corporation (Indianapolis, IN). Streptomycin, penicillin, diethyl pyrocarbonate, and eighteen peptides (dipeptides to tetrapeptides), were purchased from Sigma Chemical Co. (St. Louis, MO). All peptides tested are listed in Table 4.4.

Extraction and Purification of Poly(A)+ RNA from Animal Tissue. A modification (Matthews et al., 1996) of the method of Puissant and Houdebine (1990) was used to extract total RNA from tissues of crossbred sheep (average BW 60 kg). Briefly, tissues were collected and homogenized (10 cm diameter probe, PT 10/35 polytron, Brinkman Instrument, Wesburg, NY) in 50 mL polypropylene tubes containing 4 *M* guanidine thiocyanate, 25 m*M* sodium citrate, pH 7.0, 100 m*M* β-mercaptoethanol, and .5% N-laurylsarcosinate. Homogenates were then pooled into 250 mL centrifuge bottles and 2 *M* acetic acid (pH 4.1), water-saturated phenol (pH 4.2, Amresco, Solon, OH), and

water-saturated chloroform were sequentially added to centrifuge bottles and the contents were mixed well after each addition. After standing for 40-min in an ice-bath at 4°C, the mixture was centrifuged at 12,000 × *g* at 4°C for 20 min. The resulting supernatants were transferred to new bottles and RNA was precipitated by addition of an equal volume of isopropanol followed by storage at -20°C for 12 to 16 h. After centrifugation for 20 min at 4,000 × *g* at 4°C, the pellets were washed in 4 *M* LiCl and centrifuged at 4,000 × *g* at room temperature (~21°C) for 20 min. The RNA pellets were pooled again in 10 m*M* Tris·HCl (pH 7.6), 1 m*M* EDTA, .5% sodium lauryl sulfate (**SDS**), and an equal volume of chloroform was added. The solutions were transferred to two 30 mL Corex tubes and were then centrifuged at 12,000 × *g* at 4°C for 20 min. The supernatants containing total RNA were transferred to new tubes and stored at -80°C in the presence of .2 *M* sodium acetate (pH 5.0) and isopropanol. When needed, RNA was collected by centrifugation at 12,000 × *g* at 4°C for 20 min, washed in 70% ethanol, and suspended in diethyl pyrocarbonate (**DEPC**)-treated water. The absorbance was measured at both 260 and 280 nm (Model U-2000, Spectrophotometer, Hitachi Instrument Inc, Japan) to check RNA concentration and purity. The integrity of total RNA was examined by denaturing 1% agarose-formaldehyde gel electrophoresis and visualization using ethidium bromide staining.

Poly(A)$^+$ RNA was purified from total RNA by chromatography on oligo(dT) cellulose following established procedures (Sambrook et al., 1989). Briefly, total RNA was recovered by centrifugation at 12,000 × *g* at 20°C for 30 min, and was then dissolved

in DEPC-treated water and quantified at both 260 and 280 nm. Typically, 200 mg of oligo(dT) cellulose (Type 7, Phamacia Biotech, Piscataway, NJ) was used to make one large column (Type QS-GS, Isolab, Inc., Akron, OH), with a volume of ~ 1 mL. The column was prepared by washing sequentially with 1.5 mL of .1 *N* NaOH, 1.5 mL of DEPC-treated water, and 4.5 mL of column loading buffer (20 m*M* Tris-HCl, pH 7.6, 1 m*M* EDTA, .5 *M* NaCl, and .1% N-laurylsarcosinate) until the pH was less than 8.0. Approximately 10 mg of total RNA were loaded on the column. After washing the column with column loading buffer to eliminate nonspecific binding, elution buffer (10 m*M* Tris-HCl, pH 7.6, and 1 m*M* EDTA) was added to elute the poly(A)$^+$ RNA from the column. Normally, a second round of chromatography was performed on a column which contained 80 mg of oligo(dT) cellulose to further purify the poly(A)$^+$ RNA. For both rounds, the final RNA eluate was precipitated with an equal volume of isopropanol at -80°C in the presence of .2 *M* sodium acetate in a 1.5 mL ultracentrifuge tube. To recover the poly(A)$^+$ RNA, the precipitate was centrifuged (Model Optima TL, Beckman Instruments, Inc., Palo Alto, CA) at 80,000 $\times$ *g* at 4°C for 30 min.

Construction of a Directional Ovine cDNA Library. A cDNA library was constructed using poly(A)$^+$ RNA isolated from sheep omasal or jejunal tissue according to the manufacturer's protocol with minor modifications. The ZAP Express cDNA synthesis system was employed for this purpose. This system was chosen because the cDNA inserts could be directionally cloned into the ZAP Express vector so that the inserts were under the control of the T3 promoter in the vector. This feature was essential for functional expression of the cloned cDNA using the *Xenopus laevis* expression system. In the first

strand synthesis reaction, a 50-nucleotide primer (linker-primer, 5' – GAG AGA GAG AGA GAG AGA GAA CTA GTC TCG AGT TTT TTT TTT TTT TTT TT – 3') with poly(dT) and a *Xho* I site was used. The poly(dT) region bound to the 3' poly(A) tail of the poly(A)$^+$ RNA template, and MMLV-RT was used to synthesize the first-strand cDNA. Briefly, in a 1.5 mL RNase-free microcentrifuge tube were added 5 μL of 10 × first strand buffer, 3 μL first-strand methyl nucleotide mixture, 2 μL of linker-primer (1.4 μg/μL), 1 μL of RNase inhibitor, and 27.5 μL of DEPC-treated water. This combination was then mixed well. Five micrograms of poly(A)$^+$ RNA were added to bring the volume to 48.5 μL. After incubation at room temperature for 10 min to allow the primer to anneal to the template, 1.5 μL of MMLV-RT (50 U/μL) were added to make the final volume of 50 μL and incubated at 37°C for 1 h. After a 1-h incubation, the reaction tube was placed on ice and second strand synthesis was started by adding 20 μL of 10 × second strand buffer, 6 μL of second-strand dNTP mixture, 111 μL of sterile distilled water, 2 μL of RNase H (1.5 U/μL), and 11 μL of DNA polymerase I (9 U/μL) and followed by incubation at 16°C for 2.5 h. The water bath was checked during incubation to make sure the temperature stayed below 16°C. After second strand synthesis, the tube was immediately put on ice and 23 μL of blunting dNTP mix and 2 μL of cloned *Pfu* DNA polymerase (2.5 U/μL) were added to blunt the cDNA termini at 72°C for 30 min. The template was purified by phenol/chloroform extraction and ethanol precipitation according to standard procedures. The tube was centrifuged at 12, 000 × *g* for 1 h at 4°C, and the pellet was resuspended in 9 μL of EcoR I adapters (5' –OH-AAT TCG GCA CGA G –

3') and incubated at 4°C for at least 30 min. Addition of 1 μL of 10 × ligase buffer, 1 μL of 10 m*M* rATP, and 1 μL of T4 DNA ligase (4 U/μL) were followed by incubation at 4°C for 2 d. After the ligase was heat inactivated in a 70°C water bath for 30 min, 1 μL of 10 × ligase buffer, 1 μL of 10 m*M* rATP, 6 μL of sterile water, and 1 μL of T_4 polynucleotide kinase (10 U/μL) were added to the tube to phosphorylate the adapter ends for 30 min at 37°C. The kinase was then heat inactivated for 30 min at 70°C. Twenty-eight μL of *Xho* I buffer supplement and 3 μL of *Xho* I (40 U/μL) were added to the tube and the tube was incubated for 1.5 h at 37°C. The *Xho* I digestion removed the *EcoR* I adapter from the 3' end of the cDNA to generate double-stranded cDNA with *EcoR* I and *Xho* I termini for unidirectional cloning.

Prior to ligation to the ZAP Express vector, cDNA was size-fractionated by gel filtration chromatography (spin column with Sephacryl S-400HR). Only the fractions containing cDNA of a size larger than .5 kb were used for library construction. The cDNA was then ligated into the *EcoR* I/*Xho* I-digested ZAP Express vector by mixing 2.5 μL of resuspended cDNA (~100 ng, quantitated by ethidium bromide plate assay), .5 μL of 10 × ligase buffer, .5 μL of 10 m*M* rATP (pH7.5), 1 μL of the ZAP Express vector (1 μg/μL), and .5 μL of T_4 DNA ligase and incubation at 4°C for 2 d. Vector-ligated cDNA was packaged with Gigapack III Gold packaging extract according to the manufacturer's packaging protocol. The packaging extract (25 μL) was quickly thawed by holding the tube between the fingers and 2.5 μL of the vector-ligated cDNA (0.5 μg) were added immediately to the packaging extract. After incubating the tube at room temperature

(~21°C) for 2 h, 500 μL of SM buffer and 20 μL of chloroform were added to the tube. The supernatant containing the phage was titered and then introduced into the *Escherichia coli* strain XL1-Blue MRF'. To plate the packaged phage, 2 μL of the supernatant were mixed with 200 μL of XL1-Blue MRF' cells (OD_{600} of .5) at 37°C for 15 min to allow the phage to attach to the cell before plating onto NZY agar plates. The primary library packaged *in vitro* by packaging extract was very unstable; therefore, the library was plated out immediately on a series of large 150 mm NZY agar plates to perform plaque lifts for screening of the library.

Screening of the cDNA Library. Positive clones were identified by plaque hybridization of the cDNA library transferred from NZY agar plates to MSI Magna nylon transfer membranes by plaque lifts according to the manufacturer's protocol. For the primary screening, the library was divided into ten pools of about 50,000 plaques each. The cDNA probe used for screening was a 446-bp fragment cloned from sheep omasal epithelial total RNA by RT-PCR (Chen et al., 1999b). The cDNA probe was labeled with [α-^{32}P] dATP (ICN Pharmaceutical, Costa Mesa, CA) by nick translation using DNA polymerase I/DNase I (Life Technologies, Gaithersburg, MD) and purified by Sephadex G-25 spin column chromatography. Hybridization was carried out for 16 h at 42°C in a solution containing 50% formamide, 5 × Denhardt's solution (5 × Denhardt's = .1% Ficoll, .1% polyvinylpyrrolidone, and .1% BSA), 6 × saline-sodium phosphate-EDTA (SSPE, 1 × SSPE = .15 *M* NaCl, 10 m*M* NaH_2PO_4, and 1 m*M* EDTA), .5% SDS and 10 μg/mL denatured salmon sperm DNA. Post-hybridization washing was done under high-

stringency conditions, which involved washing twice in 5 × SSC, .5% SDS at room temperature for 15 min, twice in 1 × SSC, .5% SDS at 37°C for 15 min, and twice in .1 × SSC, 1% SDS at 65°C for 15 min. Positive clones were identified after primary screening. Secondary, tertiary and quaternary screenings were performed with the same conditions. On the autoradiographs from the final screening, 100% of the plaques showed positive hybridization, which confirmed the purity of the phage.

Excision of the Phagemid from the ZAP Express Vector. The ZAP Express vector is designed to have the f1 bacteriophage "origin of replication" subcloned into the vector. The ZAP Express vector contains all sequences of the pBK-CMV phagemid vector containing the insert cDNA, and the site of initiation and the site of termination for DNA synthesis that are recognized by the helper proteins from M13 phage. The helper proteins make a circular DNA molecule containing the pBK-CMV vector between the initiator and terminator when a strain of *E. coli* is infected with both the lambda vector and the M13 helper phage. When using the ZAP Express vector for sequencing or transcription, *in vivo* excision was performed on the isolates to obtain the insert-containing the pBK-CMV phagemid vector. Briefly, a positive plaque identified after screening of the cDNA library was cored from the agar plate and transferred to a 1.5 mL microcentrifuge tube with 500 µL SM buffer and 20 µL chloroform to release the phage particles overnight at 4°C. In a 14 mL polypropylene tube, 250 µL of the phage stock (containing 1 x 10^5 phage particles) were mixed with 200 µL of XL1-Blue MRF' cells (OD_{600} of 1.0) and 1 µL of the ExAssist helper phage (1 x 10^6 pfu/µL). After the tube was incubated at 37°C for 15 min, 3 mL of NZY broth were added and the tube was incubated for 3 h at 37°C with shaking. Then

the tube was heated at 65°C for 20 min and was centrifuged at 1,000 × *g* for 15 min. The supernatant was decanted into a 14 mL sterile polypropylene tube and this stock contained the excised pBK-CMV phagemid vector packaged as phage particles. To plate the excised phagemids, 200 μL of freshly grown XLOLR cells (OD_{600} = 1.0) were mixed with 10 μL of the phage supernatant in a 14 mL polypropylene tube and the tube was incubated at 37°C for 15 min without shaking. Then, 300 μL of NZY broth were added to the tube and the tube was incubated at 37°C for an additional 45 min. After incubation, 200 μL of the cell mixture were plated on LB-kanamycin (50 μg/mL) agar plates and the plates were incubated overnight at 37°C. Colonies appearing on the plate after incubation contained the pBK-CMV phagemid vector with the cloned DNA insert. To maintain the pBK-CMV phagemid, the colony was streaked on a new LB-kanamycin agar plate.

Sequencing of the Full-Length cDNA Insert. The pBK-CMV phagemid was selected from LB-kanamycin agar plates, cultured in a 200-mL LB-medium overnight, and purified by cesium chloride density gradients. Sequencing by the dideoxynucleotide chain termination method was performed manually using a Sequenase version 2.0 DNA sequencing kit (U. S. Biochemical Corp., Cleveland, OH). Both sense and antisense strands of the cDNA were sequenced by primer walking. Internal regions of the cDNA were sequenced using 17- to 19-mer primers. Sequencing reactions were run on 7% polyacrylamide gels. Analysis of nucleotide and amino acid sequence was performed using Lasergene, a sequence analysis software from DNAStar, Inc (Madison, WI). Data base searches were done using the GenBank™ Program BLAST (Benson et al., 1996).

Northern Analysis. Tissue distribution of oPepT1 mRNA transcripts was determined by northern blot. Poly(A)$^+$ RNA was isolated and purified as described above from sheep tissues (liver, kidney, omasum, rumen, abomasum, duodenum, jejunum, ileum, cecum, colon, longissimus muscle, and semitendinous muscle). Poly(A)$^+$ RNA samples (10 μg) from these tissues were denatured and size-fractionated on a 1% agarose gel containing 2.2 *M* formaldehyde and stained with ethidium bromide. The size of the mRNA bands was determined by an RNA ladder (.24 to 9.5 **kb**; Life Technologies, Gaithersburg, MD). The size-fractionated RNA was then transferred onto a nylon membrane (MSI, Westboro, MA) by capillary transfer overnight and cross-linked with UV light for 30 s. The blot was probed with the full-length sheep PepT1 cDNA. The probe was labeled with [α-^{32}P]-dATP (ICN Pharmaceutical, Costa Mesa, CA) by nick translation using DNA polymerase I/DNase I (Life Technologies, Gaithersburg, MD) and purified by Sephadex G-25 spin column chromatography. The blot was prehybridized for 1 to 2 h at 42°C in hybridization solution containing 50% deionized formamide, 5 × Denhardt's solution, 6 × SSPE, .2% SDS, and 10 μg/mL yeast tRNA. The blot was hybridized and washed under high stringency conditions according to the manufacturer's protocol. Blots were hybridized overnight at 42°C for 16 to 18 h and washed twice with 5 × SSPE, .5% SDS at room temperature for 30 min, twice with 1 × SSPE, .5% SDS at 42°C for 30 min, and twice with .1 × SSPE, .1% SDS at 65°C for 30 min. The blot was then exposed to Kodak XAR-5 film with an intensifying screen at –80°C.

In Vitro Transcription of cRNA. Sense cRNA was synthesized using the RNA transcription kit, mMESSAGE mMACHINE, according to the manufacturer's protocol.

Phagemid containing the cDNA insert were linearized using *Sma* I which cleaves distal to the T_3 promoter and after the cDNA insert. A typical digestion reaction would use 20 μg of phagemid DNA with 10 μL of 10 × NEB buffer 4, 1 μL of *Sma* I (40 U/μL, New England Biolabs, Beverly, MA), and water to bring the final volume to 100 μL. After restriction enzyme digestion at room temperature (~21°C) for 2 h, the template was purified by phenol/chloroform extraction and ethanol precipitation according to standard procedures, and dissolved in water at a concentration of .5 μg/μL. The transcription reaction was mixed in order with 2 μL of 10 × transcription buffer, 10 μL of 2 × ribonucleotide mix, 2 μL of cDNA template (.5 μg/μL), 2 μL of 10 × enzyme mix, and RNase-free water to bring the final volume to 20 μL and then incubated at 37°C for 2 h in a cabinet incubator to prevent condensation. The cDNA insert was transcribed *in vitro* by T_3 RNA polymerase in the presence of an RNA cap analog (both in enzyme mix). Template DNA was removed by adding 1 μL of RNase-free DNase I (2 U/μL) to the reaction. The reaction was stopped by adding 115 μL of RNase-free water and 15 μL of ammonium acetate. The resultant cRNA was purified by multiple extractions with phenol/chloroform (1:1) and precipitated with ethanol. The cRNA was recovered by centrifugation at 12,000 × *g* at 4°C for 30 min and resuspended in nuclease-free water at a concentration of 1 μg/μL and stored frozen at -80°C in aliquots. Concentration was determined by UV spectrophotometry and the integrity of the cRNA verified by denaturing 1% agarose-formaldehyde gel electrophoresis and visualization using ethidium bromide staining.

Antisense cRNA was synthesized according to the protocol of Alting-Mees et al. (1992). Phagemid containing the cDNA insert was linearized using *Sal* I, which cleaves distal to the T_7 promoter and after the cDNA insert. A typical digestion reaction would use 20 μg of phagemid DNA with 1 μL of 100 × BSA (1 μg/mL), 10 μL of 10 × NEB buffer for *Sal* I, 1 μL of *Sal* I (50 U/μL, New England Biolabs, Beverly, MA), and water to bring the final volume to 100 μL. After restriction enzyme digestion at 37°C for 3 h, the template was purified by phenol/chloroform (1:1) extraction and ethanol precipitation according to standard procedures, and dissolved in water at a concentration of .5 μg/μL. The typical transcription reaction used 1 μg of *Sal* I-digested DNA template in a nuclease-free 1.5 mL microfuge tube with 4 μL of 2.5 m*M* rNTPs, 1 μL of .75 *M* dithiothreitol, 1 μL of RNasin (40 U/μL, Promega, Madison WI), 5 μL of 5 × transcription buffer (200 m*M* Tris, 40 m*M* $MgCl_2$, 10 m*M* spermidine, 250m*M* NaCl), 1 μL T7 RNA polymerase (20 U/μL, Promega, Madison WI), and RNase-free water to bring the final volume to 25 μL. The reaction was incubated at 37°C for 2 h in a cabinet incubator to prevent condensation. Template DNA was removed by adding 1 μL of RNase-free DNase I (2 U/μL) to the reaction and the reaction was incubated an additional 15 min at 37°C. The resultant cRNA was purified by multiple extractions with phenol/chloroform (1:1) and precipitated by the addition of .1 vol of 3 *M* sodium acetate (pH 5.2) and 2.5 vol of 100% ethanol. The cRNA was recovered by centrifugation at 12,000 × *g* at 4°C for 30 min and resuspended in nuclease-free water at a concentration of 1 μg/μL and stored frozen at -80°C in aliquots. The cRNA concentration was determined by UV spectrophotometry,

and the integrity of the cRNA was verified by denaturing 1% agarose-formaldehyde gel electrophoresis and visualization using ethidium bromide staining.

Oocyte Preparation and Microinjection. Female *Xenopus laevis* frogs were kept in water tanks at 15 to 16°C in de-chlorinated water on an 8 h light and 16 h dark cycle and fed at least two times a week with a complete diet (Frog Brittle, Nasco, Fort Atkinson, WI). To obtain oocytes, mature frogs were anesthetized by immersion in ice water supplemented with .15% ethyl-m-aminobenzoate (MS222 from Sigma) as described by Goldin (1992). A small incision was made in the lower abdominal quadrant and a few lobules of ovarian tissue, containing up to 500 oocytes, were removed and placed in Ca^{2+}-free medium (in m*M*: 96 NaCl, 2 KCl, 1 $MgCl_2$, 5 HEPES titrated with NaOH to pH 7.5). The wound was closed in two layers and the frog was allowed to recover from the anesthesia in a separate tank containing .01% penicillin-G in water overnight, then it was returned to the colony.

The ovarian material was separated into pieces and treated at room temperature (~21°C) with Collagenase A at a concentration of 2 mg/mL in Ca^{2+}-free medium for about 40 min. Oocytes at stages V or VI (1 to 1.2 mm in diameter) were collected after the surrounding follicle tissue layers were peeled off with watch-maker's forceps (Size 5, George Tiemann and Company, Plainfield, NY). Defolliculated oocytes were stored again for at least 1 h in Ca^{2+}-free medium. After washing, oocytes were incubated at 18°C in a culture solution (in m*M*: 96 NaCl, 2 KCl, 1 $MgCl_2$, 1.8 $CaCl_2$, 5 HEPES titrated with NaOH to pH 7.5) supplemented with 2.5 m*M* sodium pyruvate, 100 units/mL penicillin-G, and 100 μg/mL streptomycin to recover overnight before injection.

Only healthy oocytes with a resting membrane potential (V_m) more negative than -30 mV one day after removal of follicle tissue were used for injection. The oocytes were placed in injection buffer (in m*M*: 96 NaCl, 2 KCl, 1 $MgCl_2$, 1.8 $CaCl_2$, 5 HEPES titrated with NaOH to pH 7.5) in a tissue culture dish under a stereomicroscope. Before injection, cRNA samples were heated at 65°C for 2 min. Using a microinjection system (Matthews et al., 1996a), 50 ng of either sense cRNA or antisense cRNA were injected into each oocyte in the vegetal pole, near the polar interface. Antisense cRNA solution was used as a control. The injected oocytes were returned to the culture solution and then incubated at 18°C for 1 to 7 d. The culture solution was changed daily and damaged oocytes, as indicated by misshapen and ruptured oocytes, were discarded.

Electrophysiology. The two-electrode voltage-clamp technique (TEVC) was used to characterize the induced peptide transport activity in oocytes injected with sense cRNA or antisense cRNA. All responses were monitored by a two-electrode voltage-clamp amplifier (TEV-200, Dagan Corporation, Minneapolis, MN), and analyzed by a MacLab (AD Instruments, Milford, MA), which is an analog-digital converter and software system that uses an Apple Macintosh computer for performing data acquisition (Soderlund et al., 1989). In this technique, the membrane potential of the oocytes was clamped at –60 mV. Under voltage-clamp conditions, command potentials were controlled by the Macintosh computer via Chart (version 3.0), a software product from AD Instruments (Milford, MA). One electrode was used to monitor the real time membrane potential and the second electrode was used to pass current into the oocyte so that the membrane potential

stayed at –60 mV by utilizing a feedback circuit. The quantity of current passing through the second electrode was used as a measure of peptide transport activity.

Normally, electrophysiological measurements in sense-cRNA- or antisense-cRNA-injected oocytes were carried out 4 to 7 d after injection. Conventional microelectrodes were pulled from borosilicate glass filament tubing of 1.0 mm outer diameter and .6 mm inner diameter (World Precision Instruments, Inc., Sarasota, FL) using a horizontal puller (Stoelting, model APP-1, Wooddale, IL). Microelectrodes were filled with 2 *M* KCl to yield a tip resistance of 5 to 10 MΩ. A single oocyte was placed in a recording chamber (200 μ*L*) in the presence of measurement buffer (in m*M*: 96 NaCl, 2 KCl, 1 $MgCl_2$, 1.8 $CaCl_2$, 5 HEPES) at pH 5.5. Oocytes were maintained in this pH 5.5 buffer for at least 10 min before impalement. Oocytes were always impaled to enable measurement of the resting V_m before the current electrode was inserted. This was followed by a 10-min period for stabilization before the start of the experiment. In all cases, the electrodes were inserted into the dark, animal pole for better visualization of the two electrodes. Although oocyte resting V_m was found to range from –20 to –70 mV, it was relatively constant for all oocytes from the same frog. Only oocytes at stage V with a resting V_m more negative than -30 mV were used in the experiments.

All peptide substrate solutions were prepared by dissolving the peptides in the appropriate measurement buffer. Changes in pH of the solutions resulting from dissolving peptides were adjusted with NaOH or HCl. An oocyte was perfused continuously with measurement buffer with or without peptide at a rate of 1.2 mL/min using a gravity feed perfusion system (Model BPS4, Ala Scientific Instruments, Inc., Westburg, NY). The

oocytes were thoroughly washed with fresh buffer before exposure to the next testing substrates, and several consecutive treatments were applied to the same oocytes. Under these conditions, oocytes could be kept under voltage clamp for periods as long as 2 h. The experiments were repeated in at least five independent oocytes for data analysis. All experiments were performed at room temperature (~21°C).

Computational Analysis. A hydrophobicity plot of oPepT1 was constructed according to the Kyte-Doolittle (1982) hydropathy analysis using a window of 21 amino acid residues via the TMpred service program from European Molecular Biology Network. The TMpred program makes a prediction of membrane-spanning regions and their orientation. The algorithm is based on the statistical analysis of TMbase, a database of naturally occuring transmembrane proteins (Hofmann and Stoffel., 1993).

Protein phosphorylation/dephosphorylation sites of oPepT1 were predicted based on the consensus amino acid sequences as substrate specificity determinants for protein kinases and phosphatases (Kennelly and Krebs, 1991). The consensus amino acid sequences for cAMP-dependent protein kinase (cAMP-PK or PKA) site prediction are R-R/K-X-S/T, R-X_2-S/T, or R-X-S/T. The consensus amino acid sequences for protein kinase C (PKC) site prediction are (R/K_{1-3}, X_{2-0})-S/T-(X_{2-0}, R/K_{1-3}), S/T-(X_{2-0}, R/K_{1-3}), or (R/K_{1-3}, X_{2-0})-S/T. The consensus amino acid sequence for N-linked glycosylation site prediction is N-X-T/S (X=any amino acid).

Calculations and Statistics. The kinetic parameters, the Michaelis-Menten constant, K_t, and the maximal velocity, I_{max}, and all other calculations (linear as well as nonlinear regression analysis) were performed by using PRISM (GraphPAD, LA, CA).

The experiments were generally carried out with five to six oocytes from at least two batches of oocytes, and results are presented as the mean ± SEM. Comparative analysis of transport parameters for the different substrates was performed in the same batch of oocytes.

Data were evaluated using one way analysis of variance (ANOVA) for the significance of differences. Data were also analyzed by regression analysis to investigate the form of the relationship between transport affinity constant and peptide characteristics. The REG procedure of SAS (1989) was used in this study for regression analysis.

Results

Molecular Cloning of the oPepT1 cDNA

Isolation of the Full-Length cDNA from a Sheep cDNA Library. Earlier studies from our laboratory have demonstrated the presence of a poly(A)$^+$ RNA that encodes for a peptide transporter(s) in sheep intestinal and forestomach epithelium (Matthews et al., 1996; Pan et al., 1997; Chen et al., 1999b). Therefore, with the intention to clone this transporter from sheep tissues, two ovine cDNA libraries were constructed separately with poly(A)$^+$ RNA from sheep omasal and jejunal epithelia. The first omasal cDNA library was very unstable. When the library was plated out 6 d after packaging, the titer of the primary library was only 2 x 10^5 pfu. This low titer cDNA library was amplified to 1.2 x 10^8 pfu and screened with a 446-bp fragment cloned from sheep omasal epithelial total RNA by RT-PCR (Chen et al., 1999b). Ten potential positive plaques were detected after the primary screening, but they all were negative after the secondary screening.

A sheep jejunal cDNA library was made next and plated out immediately after packaging to perform plaque lifts for screening of the library. Screening of the jejunal primary cDNA library (6.1 x 10^7 pfu) using the same 446-bp fragment cloned from sheep omasal epithelial as the probe led to the identification of 300 potential positive clones. Among these 300 positive clones identified in the primary screening, 20 clones were picked and rescreened under the same conditions. Twelve clones were still positive after the secondary screening and were carried on to the tertiary screening. Ten clones were still positive after the tertiary screening and the quaternary screening further purified 10

positive clones obtained in the tertiary screening. On the quaternary autoradiographs, 100% of the plaques showed positive hybridization, which confirmed the purity of the phage.

All of these positive phage from the jejunal cDNA library were excised *in vitro* using the single-clone excision protocol to isolate the pBK-CMV vector DNA containing the cDNA inserts. Single colonies containing pBK-CMV phagemids were selected from LB-kanamycin agar plates and cultured in 200-mL LB-medium overnight. The phagemid was purified by cesium chloride density gradients. The cloned inserts were excised by digestion with *EcoR* I/*Xho* I restriction enzymes and the sizes of the inserts were analyzed on 1% agarose gels. Double digestion of the pBK-CMV DNA with *EcoR* I and *Xho* I yielded three fragments, one 4.5 kb fragment, one 2.2 kb fragment, and one .1 to .6 kb fragment (Figure 4.1A). When the cDNA library was constructed, the cDNA was ligated into *EcoR* I/*Xho* I-digested ZAP Express vector. Therefore, the *EcoR* I/*Xho* I digestion pattern combined with other digestion indicated that there was only one internal *EcoR* I site in the cDNA insert and no internal *Xho* I site in the cDNA insert. Southern blot analysis using the same cDNA probe (446 bp) confirmed that both the 2.2 kb fragment and the .1 to .6 kb fragments can hybridize to the probe (Figure 4.1B). Restriction enzyme digestion showed that the cDNA inserts had no internal sites for *BamH* I, *Not* I, *Sal* I, *Sma* I, and *Xba* I, only one internal site for *Sac* I and *Pst* I, and 2 internal sites for *Kpn* I. Using the data provided by agarose gel electrophoresis, restriction maps for the cDNA inserts were constructed (Figure 4.1C). Partial sequence analysis of both 5' and 3' ends of all positive clones indicated that these clones were cDNAs with different sizes

resulting from truncations of the 5' end (Figure 4.1D). Two of these clones, designated as oPepT1-38 and oPepT1-39, were approximately 2.8 kb long, and they were chosen for further sequence and structure analysis. Both sense and antisense strands of the cDNA were sequenced by primer walking. Internal regions of the cDNA were sequenced using 17- to 19-mer primers (Figure 4.2).

Structural Features of the Ovine Intestinal PepT1 cDNA. The ovine intestinal oPepT1-39 cDNA is 2,829 bp long with an open reading frame of 2,121 bp (from nucleotides 80 to 2,201, Figure 4.3). The open reading frame is flanked by a 79 bp 5'UTR and a 630 bp 3' UTR. The initiation codon is consistent with the Kozak consensus sequence, GCCGCCAGCATGG (Kozak, 1987). At the 3' end, the cDNA has a polyadenylation signal (AATAAA) 12 nt preceding the polyA tail. The encoded protein is predicted to have 707 amino acids. The amino acid sequence of oPepT1-39 is given in (Figure 4.3). The predicted molecular mass of the protein is 78 kDa and the isoelectric point (pI) is 6.57. The sequence of oPepT1-38 cDNA indicates that this cDNA is 40 bp shorter than oPepT1-39 cDNA (Figure 4.3). Comparison of amino acid sequence of oPepT1-38 and 39 showed that these two cDNA encode the same protein. However, their nucleic acid sequences match 99.8% with differences at 5 positions (Figure 4.3). Compared with the oPepT1-39 sequence, the oPepT1-38 has a G instead of A at position 121 (TTG → TTA, Leu), an A instead of G at position 253 (ACG → ACA, Thr), a G instead of T at position 400 (ACT → ACG, Thr), a G instead of A at position 448 (GCA → GCG, Ala), and a C instead of T at position 1960 (GTT → GTC, Val). All these

substitutions did not result in a change in the encoded amino acids. Further study is needed to confirm whether this is a cloning artifact or real polymorphisms.

Hydrophobicity analysis using the algorithm of Kyte and Doolittle (1982) and with 19 to 21 amino acid residues per membrane spanning domain indicated that the ovine PepT1 has 12 putative transmembrane domains (TM) like human rabbit and rat PepT1 (Figure 4.4). The model also shows that both the amino terminus and the carboxyl terminus are on the cytoplasmic side of the membrane (Figure 4.5). The model predicts a long extracellular loop (200 amino acids) between transmembrane domains 9 and 10, which contains five potential N-linked glycosylation sites at positions Asn 404 (N-N-S), Asn 434 (N-L-S), Asn 438 (N-I-S), Asn 508 (N-V-S), and Asn 513 (N-A-S). There is also an additional putative N-linked glycosylation site at position Asn 117 (N-I-S) in the short extracellular loop between transmembrane domains 3 and 4. The predicted protein also contains four potential sites for protein kinase C-dependent (PKC) phosphorylation in putative intracellular loops between transmembrane domains 6 and 7 (Ser 252, S-K-K; Ser 266, S-E-K), 8 and 9 (Ser 357, S-L-K), and 10 and 11 (Ser 611, S-N-M-K). The predicted protein also contains three potential sites for cAMP-dependent protein kinase (PKA) phosphorylation in putative intracellular loops between transmembrane domains 6 and 7 (Ser 249, R-I-S; Ser 275, R-L-I-S), and between transmembrane domains 8 and 9 (Thr 362, K-M-T).

Tissue Distributions of oPepT1 mRNA. The tissue distribution of oPepT1 mRNA transcripts was examined by northern blot analysis of poly(A)$^+$ RNA isolated from several sheep tissues, with the full-length oPepT1 as the probe. A 2.8 kb poly(A)$^+$ RNA was

detected from rumen, omasum, and small intestine tissues (Figure 4.6). Among these tissues, poly(A)$^+$ RNA from the omasal and duodenal tissues showed less hybridization with the probe than poly(A)$^+$ RNA from the jejunal and ileal tissues. The ruminal poly(A)$^+$ RNA showed only minimal hybridization indicating that this mRNA is present in low abundance in ruminal epithelium. The poly(A)$^+$ RNA from other tissues, including the liver, kidney, abomasum, cecum, colon, longissimus muscle, and semitendinous muscle, showed no detectable hybridization with the probe in this study at both high and low stringency.

Functional Expression and Characterization

Preliminary Experiments. To demonstrate that the ovine PepT1 (oPepT1-39) cDNA cloned from the sheep jejunal cDNA library encodes a functional peptide transporter, oPepT1-39 cRNA was synthesized using the RNA transcription kit, mMESSAGE mMACHINE. Oocytes were injected with 50 ng of oPepT1-39 cRNA or with antisense (control) and incubated for 4 d at 18°C. The expression of the peptide transporter was monitored 4 d after injection by measuring the inward current of oocytes using the two-electrode voltage-clamp technique when oocytes were clamped to –60 mV and perfused with 1 m*M* dipeptide Gly-Sar at pH 5.5 (Figure 4.7). Inward currents were detected in oPepT1-injected oocytes when Gly-Sar was perfused. Control oocytes (water injected) did not show any response in current to perfusion with the substrate Gly-Sar. The results confirmed the functionality of oPepT1.

To determine the optimal amount of cRNA and optimal time of cRNA expression to conduct experiments, oocytes were injected with sense or antisense (control) oPepT1

cRNA at different concentrations (25ng, 50ng, 100ng, 150ng) and then incubated for a varying number of days. The inward current induced in both sense and antisense cRNA-injected oocytes was measured. The inward current induced in sense cRNA-injected oocytes increased over a time period of 4 d after which there was a relatively steady response through d 7 (Figure 4.8). On the contrary, the inward current in antisense cRNA injected oocytes was not detectable over the time period of 7 d. Oocytes injected with 25 ng and 50 ng sense cRNA had higher levels of inward current than oocytes injected with 100 ng and 150 ng sense cRNA. Also mortality of oocytes injected with 100 ng and 150 ng cRNA was higher than that of oocytes injected with 25ng and 50 ng cRNA. Therefore, 50 ng of cRNA was chosen for all oocyte expression experiments.

Influence of Ions on the Transport Process. To determine the influence of different ions on peptide transport, oocytes were injected with 50 ng of oPepT1 sense cRNA or antisense cRNA and incubated for 4 to 7 d at 18°C. The inward currents of oocytes were measured using the two-electrode voltage-clamp technique when oocytes were clamped to –60 mV and perfused with 1 m*M* dipeptide Gly-Sar in standard measurement buffer (in m*M*: 96 NaCl, 2 KCl, 1 $MgCl_2$, 1.8 $CaCl_2$, 5 HEPES) at pH 5.0, pH 5.5, pH 6.0, pH 6.5, and pH 7.0 (Figure 4.9). Control oocytes (antisense cRNA injected) did not show any response to perfusion with the substrate. Inward currents detected in sense oPepT1 cRNA-injected oocytes when 1 m*M* Gly-Sar was perfused were 41 ± 4 nA at pH 5.0, 43 ± 5 nA at pH 5.5, 42 ± 4 nA at pH 6.0, 32 ± 5 nA at pH 6.5, 20 ± 6 nA at pH 7.0. Therefore, in an environment with a lower H^+ concentration (pH 6.5 and

pH 7.0), the inward currents that indicated peptide transport in oocytes was lower ($P < 0.01$) compared with the presence of a higher H^+ concentration at pH 5.0, 5.5 and 6.0.

Na^+-free and Cl^--free buffers were prepared by replacing 96 m*M* NaCl with choline chloride, or sodium gluconate, and Ca^{2+}-free buffer was prepared by replacing 1.8 m*M* $CaCl_2$ with choline chloride in standard measurement buffer, respectively. Substitution of ions did not have any effect on peptide transport activity of oPepT1 at any pH (Figure 4.9). The inward currents in the standard measurement buffer induced by oPepT1 at pH 5.0 to pH 6.0 (42 ± 4 nA) were similar to the values obtained in the absence of Na^+ (42 ± 4 nA), Cl^- (41 ± 5 nA), or Ca^{2+} (42 ± 3 nA). Similar profiles of the inward currents at pH 6.5 and 7.0 were obtained in all four solutions, which showed that the inward currents that were indicative of peptide transport into oocytes decreased ($P < 0.01$) compared with pH 5.0, 5.5 and 6.0, but there was no significant difference among solutions. Therefore, the data indicated that peptide transport activity of oPepT1 was driven by an inwardly directed H^+ gradient and was independent of Na^+, Cl^-, or Ca^{2+}.

Current Responses to Substrates Carrying Different Net Charges. Current responses to the presence of peptides carrying different net charges were recorded in oocytes injected with 50 ng of oPepT1 sense cRNA or antisense cRNA. Oocytes were incubated for 4 to 7 d at 18°C after injection. Oocytes were clamped to –60 mV using the two-electrode voltage-clamp technique and perfused with 10 m*M* (saturating substrate concentrations) dipeptides (Gly-Sar, Met-Met, Glu-Glu, or Lys-Lys) in standard measurement buffer at pH 5.0, pH 5.5, pH 6.0, pH 6.5, and pH 7.0 (Figure 4.10). Control oocytes (antisense cRNA injected) did not show any response to perfusion with any

substrate. Currents generated in sense cRNA-injected oocytes by 10 m*M* zwitterionic and anionic substrates Gly-Sar, Met-Met, and Glu-Glu increased as buffer pH decreased from 7.0 (Gly-Sar, 20 ± 5 nA; Glu-Glu, 15 ± 4 nA; Met-Met, 10 ± 6 nA;) to 5.0 (Gly-Sar, 42 ± 4 nA; Glu-Glu, 45 ± 6 nA; Met-Met, 40 ± 5 nA). The cationic peptide, Lys-Lys, evoked the highest inward currents at pH 7.0 (35 ± 5 nA), but currents were reduced by almost 50% at pH 5.0 (15 ± 4 nA). Thus, the inward current values for sense cRNA-injected oocytes are differentially affected by charged peptides at different pH.

Inward Currents in Oocytes Clamped to Different Membrane Potentials. The effects of different membrane potentials to the current responses were determined in cRNA-injected oocytes. Oocytes were injected with 50 ng of oPepT1 sense cRNA or antisense cRNA and incubated for 4 to 7 d at 18°C. Oocytes were then clamped to different command potentials using the two-electrode voltage-clamp technique and perfused with 1 m*M* dipeptides (Gly-Sar, Met-Met, Glu-Glu, or Lys-Lys) in standard measurement buffer at pH 5.5. Control oocytes (antisense cRNA injected) did not show any response to perfusion with the substrate. As shown in Figure 4.11A, when the membrane potential was clamped to –40 mV, –60 mV, –80 mV, or –100 mV, currents (I) evoked by different peptides were almost identical.

Currents in Response to Combined Dipeptide Perfusion. To determine whether peptide-evoked inward currents were generated by the same substrate binding site on oPepT1, oocytes were injected with 50 ng of oPepT1 sense cRNA and were then clamped to –60 mV using the two-electrode voltage-clamp technique and perfused with 5 m*M* dipeptides Met-Met, Glu-Glu, and Lys-Lys in standard measurement buffer at pH 5.5.

The three peptides at 5 m*M* evoked similar currents (40 ± 6 nA) at pH 5.5. Perfusion of all three peptides alone, or together, or addition of one peptide to ongoing perfusion of any other peptide did not show any additional responses to the inward current. For instance, evoked current by perfusion of 5 m*M* Met-Met was not affected when Glu-Glu, or Lys-Lys was added in the perfusion (Figure 4.11B).

Current Responses as a Function of Substrates and Their Concentrations. In order to determine kinetic features of oPepT1, current responses for the different peptides or amino acids at different substrate concentrations were recorded in oocytes injected with 50 ng of oPepT1 sense cRNA or antisense cRNA and incubated for 4 to 7 d at 18°C. Oocytes were clamped to –60 mV using the two-electrode voltage-clamp technique and perfused with 0.01, 0.05, 0.25, 0.5, 1.0, 2.5, and 5.0 m*M* di-, tri-, or tetrapeptides in standard measurement buffer at pH 5.5. Control oocytes (antisense cRNA injected) did not show any response to perfusion with the substrate. Perfusion of 1 m*M* of the amino acids, Gly, Met, Glu, or Lys, also did not show any response. All di- and tripeptides examined were able to evoke inward currents in a saturable manner **(**Figure 4.12), resulting in an affinity constant (K_t) range of 20 μ*M* to .61 m*M* for dipeptides and .15 to 3.0 m*M* for tripeptides. No responses were detected from tetrapeptides in this perfusion study (Table 4.1). All peptides examined constitute a variety of substrates differing from their molecular weight, electrical charge, and hydrophobicity. However, for all peptides, no correlation was found between affinity constant and MW or net charge or hydrophobicity. Therefore, oPepT1 seems to be able to transport peptides regardless of their MW, net charge, or hydrophobicity. For five N-terminus methionine-containing

dipeptides, no correlation was found between affinity constant and the nature of the C terminal amino acid. The dipeptides, Leu-Val and Val-Leu, had similar affinity constants suggesting that they were recognized by oPepT1 in a similar manner. However, tripeptides with a more positive hydrophobic value had a lower affinity constant value.

Discussion

In recent years, several members belonging to the peptide transporter systems of the proton-coupled oligopeptide transporter (POT) family have been cloned and characterized. The first member to be cloned was PepT1 from rabbit, human and rat, which is expressed primarily in the small intestine (Fei et al., 1994; Liang et al., 1995; Saito et al., 1995; Miyamoto et al., 1996). Subsequently, human, rabbit and rat PepT2 were cloned, which are expressed mainly in the kidney and brain (Liu et al., 1995; Boll et al., 1996; Saito et al., 1996). Recently, Yamashita et al. (1997) reported the cloning of a brain peptide/histidine transporter (PHT1) from rat brain, which probably represents a new family of mammalian peptide transporters. Here, we report the cloning and characterization of the first intestinal peptide transporter from ruminant animals. Functional expression in *Xenopus laevis* oocytes and tissue distribution of the transporter are also reported.

PepT1 from Sheep Belongs to the POT Family. In the present study, a peptide transporter cDNA, oPepT1, was cloned from sheep small intestine. The full-length intestinal oPepT1 cDNA is 2,829 bp long with an open reading frame of 2,121 bp. The open reading frame is flanked by a 79 bp 5'-UTR and a 630 bp 3'-UTR. All previously cloned PepT1 cDNA have approximately the same size open reading frames as observed with the sheep (rabbit 2,121 bp; human 2,124 bp; rat 2,130 bp). The sizes of their 5'- and 3'-UTR are slightly different. The sizes of the 5' UTR for rabbit, human, and rat are 31, 57, and 52 bp, respectively. All these cDNA contain an initiation codon consistent with the Kozak consensus sequence. The sizes of the 3' UTR for rabbit, human, and rat are

595, 976, and 848 bp, respectively (Fei et al., 1994; Liang et al., 1995; Miyamoto et al., 1996). The DNA sequence similarity in this region is low compared to the coding region. The overall DNA sequence identity of oPepT1 to rabbit, human, and rat PepT1 is 76, 70, and 58 percent, respectively, whereas identity in the coding region is 80, 83, and 79 percent, respectively. The DNA sequence identity of the oPepT1 3' UTR compared to rabbit, human, and rat PepT1 is only 52, 44, and 18 percent, respectively.

One mechanism for modification of transport activity occurs through regulation of the cellular content of transporter protein by alteration of transcript stability. The 5'- and 3'-UTR are responsible for the stability of the transcript (Henize, 1991). Regulated mRNA decay has been shown to play an important role in control of post-transcriptional gene expression (Sachs, 1993). Recent work from several labs has focused on sequence motifs within the 3'-UTR of the glucose transporter (GLUT1) mRNA that serve as destabilizing or stabilizing elements (Chen and Pekala, 1999). There is no information available at the present on how the stability of peptide transporters is affected by their 5'- and 3'-UTR sequences. However, it is interesting to note that, both human and rat PepT1 have longer 3'-UTR (976 and 848 nt) and these cause greater inducible currents when expressed *in vitro* in *Xenopus* oocytes than do rabbit or sheep PepT1 which have shorter 3'-UTR (595 and 630 nt).

The oPepT1-encoded protein is predicted to be composed of 707 amino acids with a predicted molecular mass of 79 kDa and an isoelectric point (pI) of 6.57. All cloned PepT1 including oPepT1 have 12 putative transmembrane domains based on hydrophobicity analysis (Figure 4.4). Depending on the program and plotting parameters

used in each case, there are slight variations in the predicted location of the different membrane domains, but 12 transmembrane-domain seem to be the common structure in the POT family (Saier, 1994). The model also shows that both the amino and the carboxyl termini are on the cytoplasmic side of the membrane. The model predicts a long extracellular loop (~200 amino acids) between transmembrane domains 9 and 10. There are also a number of potential N-glycosylation sites and some protein kinase recognition sites (Fei et al., 1994; Liang et al., 1995; Miyamoto et al., 1996). The presence of *N*-glycosylation sites in all the transporters cloned so far suggests that glycosylation must play an important role in the function of these proteins. The effect of the disruption of the putative glycosylation sites by site-directed mutagenesis suggested that the carbohydrate moiety of the glycine transporter, GLYT1, was necessary for the proper trafficking of the protein to the plasma membrane (Olivares et al., 1995). Moreover, the removal of oligosaccharides by enzymatic methods from a purified glycine transporter affected transport activity (Nunez and Aragon, 1994).

A comparison (Corpet, 1988) of the amino acid sequence of oPepT1 with the published models of several cloned transporters indicated that oPepT1 showed significant similarity to all known PepT1. Alignment results showed that the predicted amino acid sequence of oPepT1 was 83, 81, and 78 percent identical to human, rat, and rabbit PepT1, respectively (Figure. 4.13). Alignment results also showed that the predicted amino acid sequence of oPepT1 was only 30, 27, and 25 percent identical to human, rat, and rabbit PepT2, respectively (data not shown). There is no significant similarity between oPepT1 protein and the HPT1 protein (21 % identity; Dantzig et al., 1994) or the PTH-1 protein

(Yamashita et al., 1997). The sequences of oPepT1 and other PepT1 proteins were most conserved in the regions corresponding to the putative 12 transmembrane domains (Table 4.2).

Histidyl residues are known to be essential for the catalytic function of the proton-dependent peptide transporters (Fei et al., 1997). There are three conserved histidyl residues in both human PepT1 (His-57, His-121, and His-260) and human PepT2 (His-87, His-142, and His-278). Site-directed mutagenesis studies indicated that His-57 in PepT1 and His-87 in PepT2 are the most critical histidyl residues for transport function. The predicted amino acid sequence of oPepT1 showed that His-57 and His 121 are located in the second and fourth transmembrane domains. These two His residues are near the extracellular surface, which are similar topological positions in other PepT1 proteins. His-260 was also present in oPepT1 in the large intracellular loop between transmembrane domains 6 and 7. All the structural features indicated that oPepT1, like other PepT1, belongs to the POT family.

Expression of oPepT1 mRNA. The oPepT1 transcript appeared to be expressed predominantly in the small intestine and to a lesser extent in the omasum and much less in the rumen as determined by northern blot analysis. The expression pattern of poly(A)$^+$ RNA in these tissues appears to be consistent with those from a previous study in our laboratory (Chen et al. 1999b). The small intestine appears to be the primary site of expression of oPepT1 mRNA transcripts. This pattern is in agreement with the studies that the major site of absorption of protein digestion products (e.g., amino acids) is the small intestine in ruminant animals (Phillips et al., 1979; Wilson and Webb, 1990). In

addition to the small intestine, the rumen and omasum are recognized for their absorptive activity of large quantities of volatile fatty acids and ammonia. The hybridization of the probe with mRNA from the omasal tissue was much stronger than that with mRNA from ruminal tissue. This suggests that the omasum has higher absorptive activity of peptides than the rumen if the presence of mRNA is indicative of expression of the transport protein. Although the expression of oPepT1 mRNA is lower in the omasum and rumen compared with the small intestine, the oPepT1 protein certainly could contribute to the absorption of small peptides in the forestomach of sheep. Matthews (1991) also reported that compared to the ruminal epithelium, more dipeptides were absorbed and transferred by the omasal epithelium. Previous reports from our lab showed that rat myogenic cells (C_2C_{12}) and ovine myogenic satellite cells can utilize exogenous methionine-containing peptides as sources of methionine for protein synthesis, and in some cases, the peptides were better than methionine (Pan et al., 1996; Pan and Webb, 1998). We were unable to detect any hybridization under high or medium stringency conditions in mRNA from longissimus muscle or semitendinous muscle. The possible presence of one or more peptide transport protein(s) in muscle cells other than oPepT1, or that cultured cells can utilize peptides via mechanisms other than peptide transporters cannot be discounted. Other studies reported the presence of PepT1 mRNA in the liver and kidney of the rabbit, rat, and human (Fei et al., 1994; Liang et al., 1995; Miyamoto et al., 1996). In the present study, the hybridization of the full-length oPepT1 cDNA probe to mRNA from liver and kidney was not detected. This may indicate a different pattern of expression for the peptide transporter mRNA in ruminant animals.

Structural Differences Between oPepT1 and Other PepT1. Despite the similarity of oPepT1 to other PepT1, there are some noticeable differences. First, the isoelectric point (pI) of oPepT1 (6.57) is lower than that of others (rat PepT1, pI 7.39; rabbit PepT1, pI 7.47; human PepT1, pI 8.58). There may be a physiological reason for this difference. In the intestines, bicarbonate is the principle buffer that is secreted by mucosal cells throughout the small and large intestinal tract and is also provided in pancreatic and biliary secretions (Caple and Heath, 1975). The bicarbonate provided in pancreatic and biliary secretions is to neutralize stomach acid and to provide a more favorable intestinal pH for enzymatic breakdown of feed components and absorption of nutrients. The pH of the unstirred water layer in the intestinal lumen of monogastric animals is 5.5 to 6.0 (Ganapathy and Leibach, 1983). In ruminants, pancreatic and biliary secretions appear inadequate to handle the acid load delivered from the stomach to the small intestine. Bicarbonate concentration in sheep pancreatic secretions is 15 to 30 meq/L (Taylor, 1962) compared to 120 to 130 meq/L in human pancreatic secretions and 150 meq/L in dog pancreatic secretions (Oser, 1965). Also, pancreatic secretory rate is .0067 mL kg^{-1} min^{-1} in sheep compared to .08 mL kg^{-1} min^{-1} in dog. Thus, both bicarbonate content in pancreatic secretions and pancreatic secretory rate in sheep are considerably lower than in dogs, and this may result in a lesser capacity for neutralization of stomach acid in sheep compared with dogs. The pH of the duodenum and upper jejunum in sheep is rather acidic ranging from 2.5 to 4.5 and it is not until the lower jejunum that the intestinal pH reaches near 6 (Ben Ghedalia et al., 1974). However, the titration curves (Figure. 4.14) of all PepT1 proteins show that at pH 4.5 to 5.0, oPepT1 has the same charge as other

PepT1 at pH 5.5 to 6.0, which means that under physiological conditions, oPepT1 protein may have the same functional conformation as other PepT1 proteins.

Second, significant differences exist in the phosphorylation sites for protein kinases. The predicted oPepT1 protein contains four potential sites for protein kinase C-dependent (PKC) phosphorylation in the putative intracellular loops between transmembrane domains 6 and 7, 8 and 9, and 10 and 11 (Figure 4.5). The predicted oPepT1 protein also contains three potential sites for cAMP-dependent protein kinase (PKA) phosphorylation in putative intracellular loops between transmembrane domains 6 and 7, and 8 and 9 (Figure 4.5). Rabbit PepT1 has only one PKC phosphorylation site, and one PKA phosphorylation site (Fei et al., 1995; Table 4.3). Human PepT1 has two PKC phosphorylation sites, but no site for PKA phosphorylation (Liang et al., 1995; Table 4.3). Rat PepT1 has one PKC phosphorylation site, and one PKA phosphorylation site (Miyamoto et al., 1996; Table 4.3). With reference to phosphorylation sites, oPepT1 appears to be more like PepT2. Human PepT2 has five PKC phosphorylation sites, and one PKA phosphorylation site (Liu et al., 1995; Table 4.3). Rabbit PepT2 has four PKC phosphorylation sites, but no site for PKA phosphorylation (Boll et al., 1996; Table 4.3). Rat PepT2 has three PKC phosphorylation sites, but no site for PKA phosphorylation (Saito et al., 1996; Table 4.3). The PTH-1 protein isolated from rat brain has as many as 11 PKC phosphorylation sites (Yamashita et al., 1997).

Protein kinases in different cells are involved with a number of cellular reactions, indicating that they play a key role in many aspects of cellular growth and metabolism. Protein kinases have also been shown to either directly or indirectly regulate the activity of

transport proteins (Newton, 1998). Direct regulation occurs through phosphorylation of the transport proteins, which may change the kinetics of the transporter, such as maximum velocity (V_{max}), substrate affinity (K_t), or turnover rate of the transporter. The transport activity of the glutamate cotransporter, GLT-1, was increased by PKC (Rothman, 1994). Mutation of the serine residue that forms part of the consensus phosphorylation site of PKC (Ser-113) eliminated the response to phorbol esters, a PKC activator (Casado et al., 1993). These results suggest that the regulation of transporter functions occurred by direct phosphorylation of the protein.

Like all other membrane proteins, transport proteins are cotranslationally inserted into the endoplasmic reticulum during protein synthesis and processed through the Golgi apparatus (Rothman and Orci, 1992). Vesicles are formed in the Golgi apparatus to deliver the proteins to the plasma membrane, where the vesicles fuse with the plasma membrane and result in increases in the number of transporters. Transport proteins can also be selectively retrieved from the plasma membrane by endocytosis (Rothman, 1994). Protein kinases may, therefore, also indirectly regulate transport activity by regulating the delivery or retrieval of membrane proteins from the plasma membrane. Results from a study of Brandsch et al. (1994) showed that a H^+-dependent peptide transport system expressed in human Caco-2 cells was regulated by PKC. When the cells were treated with phorbol esters, which activate PKC, transport function was significantly inhibited. Further kinetic analysis showed that the inhibition was due to a decrease in the maximal transport rate (V_{max}) of the transporter, whereas the apparent affinity (K_t) was unchanged.

Therefore, it seems reasonable to speculate at this juncture that oPepT1 may be regulated by protein kinases.

Analysis of charge distribution shows that oPepT1 has a negatively charged cluster from 672 to 691 (VNPAEIE AQFDEDD KEDDLE). Compared with PepT1 from other species, oPepT1 has more negatively charged amino acids in this cluster (Figure 4.15). No information is available at the moment as to how the negatively charged cluster at the C-terminal end of the peptide transporter affects the function of the transport system. Functional analysis of a chimeric peptide transporter derived from PepT1 and PepT2 showed that the large extracellular loop and the C-terminal end were not responsible for the kinetic characteristics of the transport system (Doring et al., 1997). It is likely that this region is important for the peptide transporter protein trafficking inside the cells or for regulating the transport function because of the potential PKC site located at the C-terminus. Thus, the negatively charged C-terminal end may also change oPepT1 transport activity by altering the rate of oPepT1 protein insertion into the plasma membrane, which would ultimately change the expression level of the protein.

Comparison of Functional Characteristics Between oPepT1 and Other PepT1. The expression of oPepT1 by *Xenopus* oocytes from cRNA took approximately 3 d to be detected and expression increased until d 4, after which it plateaued. This is in agreement with other studies from our laboratory (Matthews et al., 1996) and other reports (Miyamoto et al., 1991; Saito et al., 1993). Protein synthesis, processing, delivery, and fusion with plasma membranes required approximately 3 d in oocytes. The capacity of oocytes to translate injected cRNA has been reported to have a clear dose-response

relationship between expression and the amount of message injected (Boll et al., 1996). The expression was almost linearly propotional to the amount injected up to 10 ng of cRNA, and plateaued at 25 ng. When large amounts of cRNA were injected into oocytes in our study, there was no longer an increase in expression. Oocytes injected with 25 ng and 50 ng sense cRNA had higher levels of inward current than oocytes injected with 100 ng and 150 ng sense cRNA. Oocytes injected with 50 ng sense cRNA had a better overall expression compared with oocytes injected with 25 ng sense cRNA. One explanation for this saturation is that oocytes possess a finite translational capacity that can only provide for the translation of a limited number of messages and any injected message exceeding this number will not be translated. The foreign nucleic acid may simply interfere with the normal cycle of oocytes and may interrupt their normal functions. Therefore, injections of 50 ng cRNA seems to be optimal conditions for routine work on expression of cRNA.

The influence of different ions on peptide transport in oPepT1-injected oocytes indicated peptide transport activity of oPepT1 was driven by an inwardly directed H^+ gradient and was independent of Na^+, Cl^-, or Ca^{2+}. These data agree with other reports that a H^+ gradient is critical for the transport process but Na^+, Cl^-, and K^+ are not (Fei et al., 1994; Mackenzie et al., 1996). Proton-dependence is the most important feature of the POT transporter family (Leibach and Ganapathy, 1996). This feature is physiologically relevant because there always is an inwardly directed proton gradient across the membrane of intestinal cells at physiological pH in all species. In the canine renal cell line, MDCK cells, transport activity of a PepT1-like transporter was affected by Ca^{2+} and calmodulin-dependent processes (Brandsch, et al., 1995). Transport of

dipeptides in the porcine cell line, LLC-PK1 cells, by PepT2 was also shown to be altered by Ca^{2+}, but not through a calmodulin-specific pathway (Wenzel et al., 1999).

The pH had a dramatic effect on the transport process of charged peptides. Current responses were observed in oocytes expressing oPepT1 for saturating concentration (10 m*M*) of Gly-Sar, Met-Met, Glu-Glu, and Lys-Lys at different pH ranging from 5.0 to 7.0. Zwitterionic and anionic substrates (Gly-Sar, Met-Met, and Glu-Glu) were transported via oPepT1 with a pH optimum of 5.0, whereas for the cationic substrate, Lys-Lys, the pH optimum was 7.0. However, at pH 5.5, Lys-Lys still caused inward currents. This finding shows that at physiological pH in the intestine, which is approximately pH 4.5 to 5.0 for ruminant animals, oPepT1 is capable of transporting all peptide substrates, regardless of their charges. But zwitterionic and anionic peptides are probably transported faster than cationic peptides. These data agree with a published report indicating that at physiological pH (5.5 to 6.0), rabbit PepT1 preferred neutral and acidic peptides as its substrates (Steel et al., 1997). In their studies, the pH dependence of the current evoked by Gly-Leu, Gly-Glu, Gly-Lys, and Ala-Lys was markedly different. Their highest currents were observed at pH values of 5.0, 5.0, 6.5, and 6.0 for Gly-Leu, Gly-Glu, Gly-Lys, and Ala-Lys, respectively, and lowest currents were recorded at pH values of 7.0, 7.0, 5.0, and 5.0 for Gly-Leu, Gly-Glu, Gly-Lys, and Ala-Lys, respectively. Amasheh et al. (1997a) also reported, at pH 5.5 to 6.0 for human and rabbit PepT1, currents evoked by anionic and zwitterionic peptides Glu-Glu, Gly-Asp, and Gly-Gln were greater than that at any other pH (6.5 to 8.0), and also greater than currents evoked by the cationic peptide, Gly-Lys. The dicationic peptide Lys-Lys did not cause any detectable

currents at pH 5.5, which indicated at physiological pH, human and rabbit PepT1 did not transport dicationic peptides. Transport of charged peptides mediated by PepT2 had a different pattern when transported at different pH (Wang et al., 1998). Although the net charge of the three dipeptides, Ala-Val, Ala-Glu, and Ala-Lys, was different, the relationship between inward current and external pH was similar in all three cases. They found transport of all three peptides, indicated by inward currents, was greatest at pH 5.0, but smallest at pH 6.0.

For oPepT1, we also observed that combined perfusion of saturating concentrations of the dipeptides, Met-Met, Glu-Glu, and Lys-Lys, had no additive responses compared with perfusion of these peptides alone. This indicated that all peptides were interacting at one common binding site on the transporter. Using seven chimeric peptide transporters of human PepT1 and rat PepT2, Fei et al. (1998) identified one putative substrate binding site in the peptide transporter which was located in the region comprised of transmembrane domains 7, 8 and 9. Another study by Doring et al. (1997) suggested that the large extracellular loop between transmembrane domains 9 and 10 was not a major determinant of the affinity constant for PepT1 and PepT2. The finding that the brain peptide/histidine transporter, PHT-1, which lacks the large extracellular loop, transports histidine (Yamashita et al., 1997) raises the question of the function of the loop. What would happen if the loop were removed from the protein? Further studies are needed to determine whether the loop is the real determinant of protein tertiary conformation that controls access to substrates.

When the voltage dependence of peptide transport by oPepT1was examined, we observed that peptide transport, as indicated by substrate-evoked inward currents, was almost completely independent of voltage in the range –100 to –40 mV. Although Fei et al. (1994) reported that Gly-Sar transport by rabbit PepT1 was independent of voltage, other studies showed that peptide transport by PepT1 was voltage-dependent. Boll et al. (1994) and Mackenzie et al. (1996b) found transport of both Gly-Sar and cefadroxil via PepT1 was electrogenic. Evoked currents were voltage-dependent over the range tested (-150 to +50 mV). It is not clear why there are different results from the present study, the study of Fei et al. (1994), and those of Boll et al. (1994) and Mackenzie et al. (1996). In both the present study and the study of Fei et al. (1994), currents generated by substrates were considerably smaller than those observed by Boll et al. (1994) and Mackenzie et al. (1996), which could make it difficult to detect any changes in the evoked current.

We found that all 14 dipeptides and tripeptides transported by oocytes expressing oPepT1 obeyed Michaelis-Menten-type kinetics (Figure 4.12). An affinity constant, K_t, of 0.40 m*M* for Gly-Sar has been reported in our laboratory using poly(A)$^+$ RNA-injected oocytes (Matthews et al., 1996). The K_t of cloned oPepT1 for Gly-Sar in the present study was .61 m*M* at –60 mV at pH 5.5, which is similar to the previous report and to the K_t for human PepT1 (.7 m*M* at –50 mV, at pH 5.5), and somewhat lower than the K_t of 1.9 m*M* (at –60mV, pH 5.5) for rabbit PepT1 (Mackenzie et al., 1996b; Fei et al., 1994). In contrast, human PepT2 had a K_t of 70 μ*M* for Gly-Sar (Ramamoorthy et al., 1995). PepT1 is generally categorized as a low-affinity transport system. Fei et al. (1994)

reported that K_t of rabbit PepT1 for Gly-Leu, Ala-Asp, Gly-Sar, Gly-Gly, and Gly-Gly-Gly were 81 μ*M*, 143 μ*M*, 1.9 m*M*, 2.5 mM, and 5.1 m*M*, respectively. Steel et al. (1997) observed that the K_t of rabbit PepT1 for Gly-Leu, Ala-Asp, Gly-Glu, Ala-Lys, Phe-Glu, Gly-Sar, Gly-Lys, Gly-Gly, and Gly-Gly-Gly were 80 μ*M*, 140 μ*M*, 220 μ*M*, 300 μ*M*, .94 m*M*, 1.9 m*M*, 2.4 m*M*, 2.5 m*M*, 5.1 m*M*, respectively. Apparently, the K_t of PepT1 has a wide range from 80 μ*M* to 5.1 m*M*. PepT2 is categorized as a high-affinity transport system with K_t generally 40 times less than PepT1 (Boll et al., 1996). They reported that the apparent K_t of rabbit PepT2 was ≤ 50 μ*M*, whereas the apparent K_t of rabbit PepT1 was ≥ 1 m*M*. Chen et al. (1999a) reported that K_t of rat PepT2 for Gly-Leu, Gly-Glu, Phe-Glu, Gly-Lys, Phe-Ala, and Phe-Lys was 4.4 μ*M*, 16 μ*M*, 48 μ*M*, 51 μ*M*, 75 μ*M*, and 135 μ*M*, respectively. Apparently, the K_t of PepT2 has a narrower range (4.4 μ*M* to 135 μ*M*) at low micromolar concentration for all dipeptides tested. A K_t range of 20 μ*M* to .61 m*M* for dipeptides and .15 to 3.0 m*M* for tripeptides was observed in the present study. The relatively wide range of affinities for the majority of peptides suggests that oPepT1 is also a low-affinity transporter, just like PepT1 from other species. Larger peptides (Met-Gly-Met-Met, Pro-Phe-Gly-Lys, Val-Gly-Asp-Glu, and Val-Gly-Ser-Glu) and free amino acids (Gly, Met, Glu, and Lys) were not recognized as substrates for oPepT1.

We reported previously that poly$(A)^+$ RNA from sheep omasal epithelium could induce expression of a peptide transport protein(s) in oocytes (Pan et al., 1997). In that study, the tetrapeptides (Met-Gly-Met-Met, Val-Gly-Asp-Glu, and Val-Gly-Ser-Glu) were reported to cause depolarization of the oocytes, which indicated that those substrates were

being transported, whereas Pro-Phe-Gly-Lys did not. However, in oocytes expressing cloned oPepT1, we did not detect any transport of tetrapeptides. There are several possibilities for the differences. First, the previous study used poly(A)$^+$ RNA from sheep omasal epithelium for expression. It is possible that the peptide transporter in sheep omasum is slightly different from intestinal oPepT1, which could cause the changes of transporter substrate specificity. Research has shown substitution mutations of amino acids at some positions in the protein could alter the specificity of the protein, and substitutions appeared to increase the conformational flexibility of the catalytic region, thereby allowing access of the bulkier side chain of the substrates (Guillaume et al., 1997). Second, there might be a peptide transporter(s) present in sheep omasum other than oPepT1 that could be responsible for transporting tetrapeptides. The two primers for PCR amplification of the probe were TGG CTG GG(G/A) AAG TTC AAG AC and CTT CTT GTA CAT (C/T)CC ACT GC (Chen et al., 1999b), which were designed to correspond to nucleotides 259 to 278 and 686 to 705 in rabbit PepT1 (Fei et al., 1994). Therefore, the probe we used to screen the cDNA library did not allow us to detect the presence of peptide transporters other than PepT1-like transporters. Lastly, because poly(A)$^+$ RNA from sheep omasal epithelium included all messages encoding transporters, it is possible that the oocytes used in the previous study also expressed amino acid transporters. Free amino acids because of the impurity or degradation of tetrapeptide solutions could also cause depolarization, which would result in false readings of peptide transport. At this moment, the real reason for the difference between the present study and the previous one is uncertain.

In summary, we have cloned an ovine intestinal peptide transporter, oPepT1, from sheep intestine that encodes for a 707-amino acid protein with a molecular mass of 79 kDa and 12 transmembrane domains. oPepT1 shows high homology to PepT1 from other species. High stringency northern blot analysis demonstrated that oPepT1 is strongly expressed in small intestine, and at lower levels in omasum and much lower in rumen, but not in liver and kidney. The presence of the peptide transporter in the forestomach at such levels may contribute to the provisioning of amino acid nitrogen for ruminants in a nutritionally significant manner. Our studies demonstrate that oPepT1 has been functionally expressed in *Xenopus* oocytes. Characterization of oPepT1 shows that oPepT1 accepts a variety of dipeptides and tripeptides as its substrates, regardless of their physicochemical characteristics, but not tetrapeptides or free amino acids. A K_t range of 20 μ*M* to .61 m*M* for dipeptides and .15 to 3.0 m*M* for tripeptides were observed in this study. The transport process is electrogenic and independent of Na^+, Cl^-, and Ca^{2+}. Although many of the properties displayed by oPepT1 are similar to those of PepT1 from other species, we have identified some important differences. First, the isoelectric point of oPepT1 is lower than that of others, but the oPepT1 protein seems to have the same functional conformation as that of others at physiological pH based on their titration curves. Second, more phosphorylation sites for protein kinases exist in oPepT1, which may mean that oPepT1 is likely regulated by protein kinases in a more complex manner. Third, compared with PepT1 from other species, oPepT1 has more negatively charged amino acids at its C-terminus. The effect of this on its function is unclear at the moment.

Implications

This is the first report of a cloned peptide transporter in ruminant animals. The structural information will help researchers to develop antibodies in the future in order to study the localization of the peptide transporter in sheep, which should provide valuable information for evaluating the role of peptide transport in sheep. Also more potential protein kinase phosphorylation sites and N-glycosylation sites were revealed in this study. If this proves to be true, then an important regulation method of the peptide transporter may have been identified. The information from the *in vitro* characterization of this peptide transporter will help in the formulation of better animal diets to improve efficiency and performance.

Table 4.1. Kinetics of oPepT1 in oocytes injected with oPepT1 cRNA.

Substrate	MW	Charge[a]	Hydrophobicity[b]	K_t (m*M*)	V_{max} (nA)
Dipeptide					
Glu-Glu	270	negative	-7.0	.029	51
Gly-Sar	164	neutral	- .8	.607	50
Leu-Val	230	neutral	8.0	.164	39
Lys-Lys	342	positive	-7.8	.020	33
Met-Glu	278	negative	-1.6	.048	43
Met-Gly	206	neutral	1.5	.184	44
Met-Leu	262	neutral	5.7	.073	37
Met-Lys	323	positive	-2.0	.450	37
Met-Met	280	neutral	3.8	.027	41
Val-Leu	266	neutral	8.0	.143	38
Tripeptide					
Leu-Gly-Gly	245	neutral	3.0	.647	42
Lys-Trp-Lys	460	positive	-8.7	3.02	48
Met-Leu-Phe	409	neutral	8.5	.15	38
Thr-Ser-Lys	334	positive	-5.4	.68	33
TetraPeptide					
Met-Gly-Met-Met	468	neutral	5.3		
Pro-Phe-Gly-Lys	501	positive	-3.1	No response	
Val-Gly-Asp-Glu	472	negative	-3.2		
Val-Gly-Ser-Glu	444	negative	- .5		

[a] Charge: calculated at pH 5.5.

[b] Hydrophobicity: calculated as the average of the value of the constituent amino acids according to Kyte and Doolittle (1982).

Table 4.2. Comparison result of amino acid sequences of transmembrane domains (TM) of sheep (oPepT1), human (hPepT1), rat, and rabbit PepT1.

	TM1	TM2	TM3
oPepT1	PKSC**FGYPLSIFFIV**V**NEFC**	**IYHTFVALCYLTPILGALI**	**TIV**S**LSIVYTIGQ**V**V**IAV
hPepT1	SHSF**FGYPLSIFFIV**V**NEFC**	**IYHTFVALCYLTPILGALI**	**TIV**S**LSIVYTIGQ**A**V**TSV
rat	SRGC**FGYPLSIFFIV**V**NEFC**	**IYHTFVALCYLTPILGALI**	**TIV**S**LSIVYTIGQ**A**V**ISV
rabbit	SLSC**FGYPLSIFFIV**V**NEFC**	**IYHTFVALCYLTPILGALI**	**TIV**W**LSIVYTIGQ**A**V**TSL

	TM4	TM5	TM6
oPepT1	SV**H**VALSMI**GL**V**LIALGTGG**	**FFSIFYL**A**INAGSLLSTIITP**	**PLAFG**V**PA**A**LMAV**S**LIVF**V**I**GS**
hPepT1	PV**H**VVLSLI**GL**A**LIALGTGG**	**FFSIFYL**A**INAGSLLSTIITP**	**PLAFG**V**PA**A**LMAV**A**LIVF**V**L**GS**
rat	PL**H**VALSMI**GL**A**LIALGTGG**	**FFSIFYL**A**INAGSLLSTIITP**	**PLAFG**V**PA**A**LMAV**A**LIVF**V**L**GS**
rabbit	PV**H**VAVCMI**GL**L**LIALGTGG**	**FFSIFYL**A**INAGSLLSTIITP**	**PLAFG**I**PA**I**LMAV**S**LIVF**II**GS**

	TM7	TM8	TM9
oPepT1	I**K**MVTR**V**M**FLYIPLPMFWALF**	**VN**A**ILI**VVM**VP**IV**DAV**V**YPLI**	TV**GM**F**LA**SM**AFV**A**AA**IV**QV**D**I**
hPepT1	I**K**MVTR**V**M**FLYIPLPMFWALF**	**VN**A**ILI**VIM**VP**IF**DAV**L**YPLI**	AV**GM**V**LA**SM**AFV**V**AA**IV**QV**E**I**
rat	I**K**IMTK**V**M**FLYIPLPMFWALF**	**VN**A**ILI**VIM**VP**IV**DAV**V**YPLI**	TV**GM**F**LA**SM**AFV**V**AA**IV**QV**E**I**
rabbit	I**K**MVTR**V**L**FLYIPLPMFWALF**	**VN**T**ILI**IIL**VP**IM**DAV**V**YPLI**	TI**GM**F**LA**SM**AFV**A**AA**IL**QV**E**I**

	TM10	TM11	TM12
oPepT1	**IPQYF**LL**TC**G**EVVFS**I**TGLEF**	**VLQAGWLLTVA**V**GNIIVLIVA**	**AEY**V**LFA**A**LL**LV**VC**I**IFA**I**MA**
hPepT1	**IPQYF**LL**TC**G**EVVFS**V**TGLEF**	**VLQAGWLLTVA**V**GNIIVLIVA**	**AEY**I**LFA**A**LL**LV**VC**V**IFA**I**MA**
rat	**IPQYF**LL**TC**G**EVVFS**V**TGLEF**	**VLQAGWLLTVA**I**GNIIVLIVA**	**AEY**V**LFA**S**LL**LV**VC**I**IFA**I**MA**
rabbit	**IPQYF**LI**TS**G**EVVFS**I**TGLEF**	**VLQAGWLLTVA**V**GNIIVLIVA**	**AEY**I**LFA**A**LL**LV**VC**V**IFA**I**MA**

Table 4.3. Comparison of Amino Acid Sequences and Protein Characteristics of oPepT1 to Other Mammalian Peptide Transporters.

Transporter	cDNA Size (kb)	Tissue Distribution	Protein	Topology	Ref.
oPepT1	2.8	Omasum Rumen Small intestine	707 aa MW 79 kDa pI 6.57	12 TM N-glycosylation sites: 6 PKC sites: 4 PKA sites: 3	The present study
Rabbit PepT1	2.7	Liver Kidney Small intestine	707 aa MW 79 kDa pI 7.47	12 TM N-glycosylation sites: 3 PKC sites: 1 PKA sites: 1	Fei et al., 1994
Human PepT1	3.1	Liver Kidney Small intestine Placenta Pancreas	708 aa, MW 79 kDa pI 8.58	12 TM N-glycosylation sites: 7 PKC sites: 2 PKA sites: none	Liang et al., 1995
Rat PepT1	3.0	Kidney Small intestine	710 aa, MW 79 kDa pI 7.39	12 TM N-glycosylation sites: 5 PKC sites: 1 PKA sites: 1	Saito et al., 1995; Miyamoto et al, 1996
Human PepT2	2.7	Kdey Small intestine	729 aa MW 82 kDa pI 8.26	12 TM N-glycosylation sites: 3 PKC sites: 5 PKA sites: 1	Liu et al., 1995
Rabbit PepT2	4.2	Kidney Brain Lung Liver Heart	729 aa MW 82 kDa pI 7.39	12 TM N-glycosylation sites: 5 PKC sites: 4 PKA sites: none	Boll et al., 1996
Rat PepT2	3.9	Kidney Brain Lung Spleen	729 aa MW 82 Kda pI 7.99	12 TM N-glycosylation sites: 4 PKC sites: 3 PKA sites: none	Saito et al., 1996
HPT1	3.3	Caco-2 cells	832 aa MW 92 kDa pI unknown	1 TM others unknown	Dantzig et al., 1994
PTH1	2.7	Brain Eye	572 aa MW 65 kDa pI unknown	12 TM N-glycosylation sites: 4 PKC sites: 11 PKA sites: none	Yamashita et al., 1997

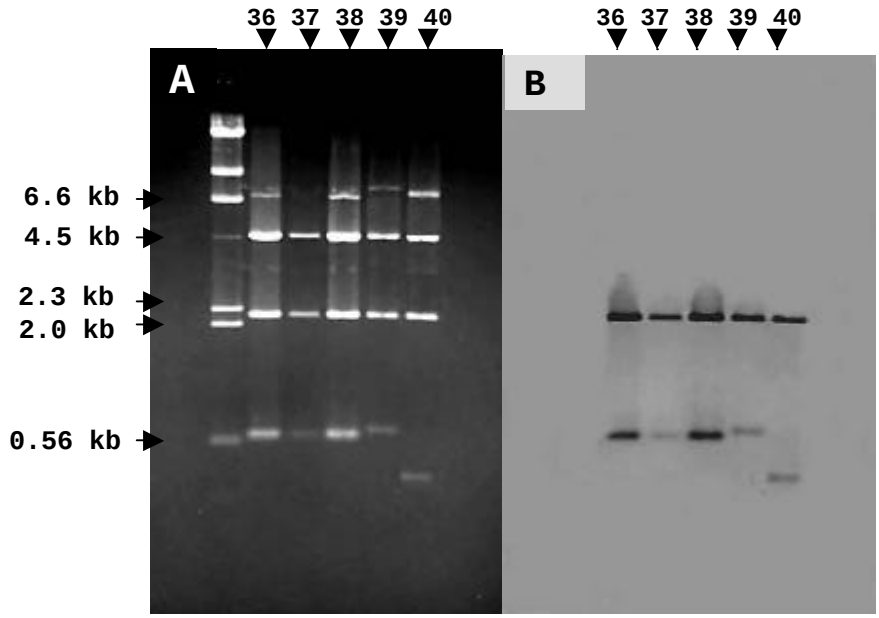

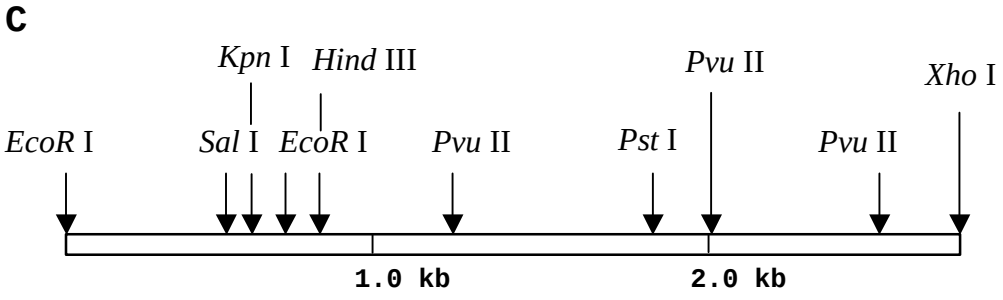

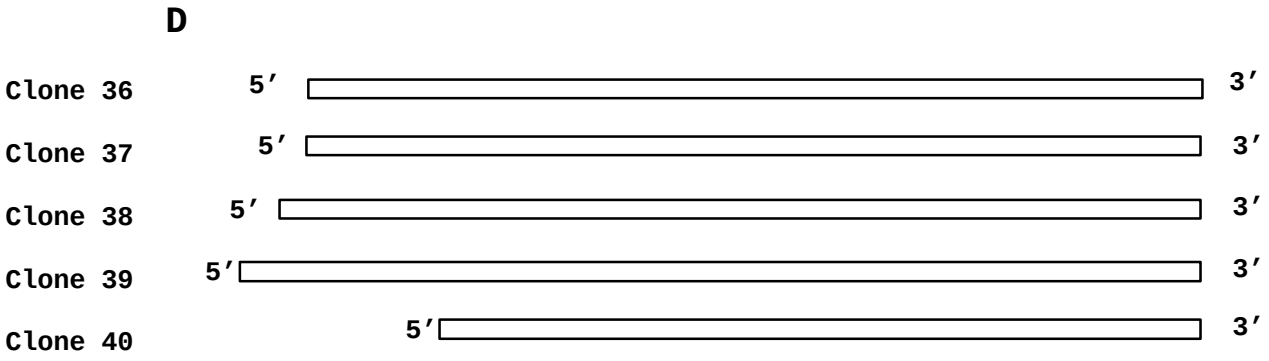

Figure. 4.1. Restriction enzyme *EcoR* I/*Xho* I digestion pattern (A) of all of the positive clones, Southern blot analysis (B) of the digestion results, restriction map (C), and sizes of all clones (D) are shown.

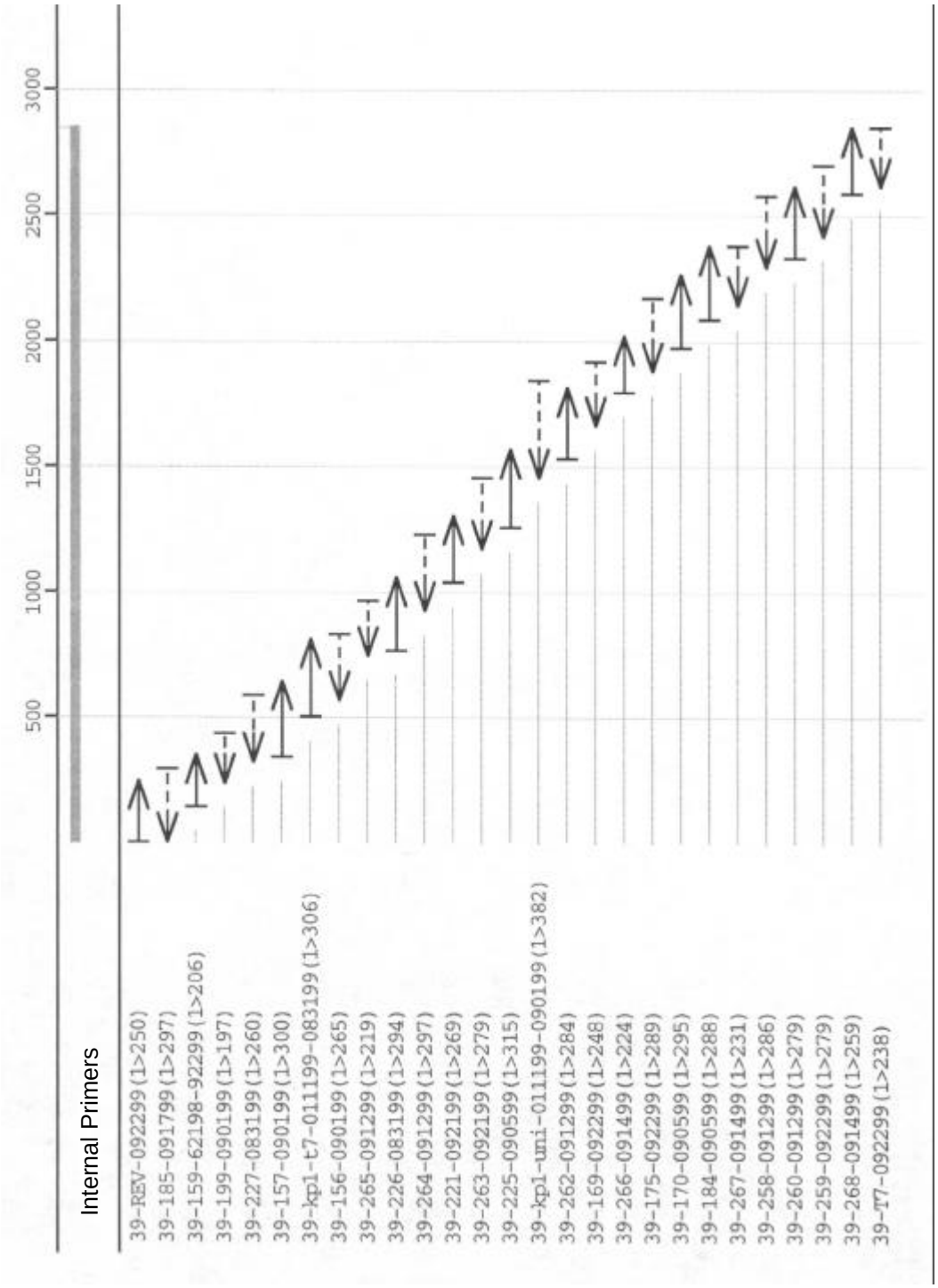

Figure 4.2. Sequence strategy of oPepT1.

```
                                                                  * Start of clone oPepT1-38
   1 - GAAACAACATCTTTAGCACGGATTCCTCCCACCTGGACTCCTCGCTCGCCAGTCGCAGGG - 60
     -

  61 - AGCCCTCGGAGCCGCCAGCATGGGAATGTCCGTGCCGAAGAGCTGCTTCGGTTACCCCTT - 120
     -                      M  G  M  S  V  P  K  S  C  F  G  Y  P  L
       G
 121 - AAGCATCTTCTTCATCGTGGTCAATGAGTTCTGCGAAAGGTTCTCTTACTATGGAATGAG - 180
     -  S  I  F  F  I  V  V  N  E  F  C  E  R  F  S  Y  Y  G  M  R

 181 - AGCACTCCTGATCCTGTACTTCCAACGTTTCCTGGGCTGGAACGACAACCTGGGCACCGC - 240
     -  A  L  L  I  L  Y  F  Q  R  F  L  G  W  N  D  N  L  G  T  A
              A
 241 - CATCTATCACACGTTCGTCGCCCTGTGCTACCTGACGCCCATCCTCGGAGCTCTCATCGC - 300
     -  I  Y  H  T  F  V  A  L  C  Y  L  T  P  I  L  G  A  L  I  A

 301 - CGACTCCTGGCTGGGGAAGTTCAAGACGATCGTGTCGCTGTCCATCGTCTACACCATTGG - 360
     -  D  S  W  L  G  K  F  K  T  I  V  S  L  S  I  V  Y  T  I  G
                                                 G
 361 - GCAGGTAGTCATCGCTGTGAGCTCAATTAATGACCTCACTGACTTCAACCATGATGGAAC - 420
     -  Q  V  V  I  A  V  S  S  I  N  D  L  T  D  F  N  H  D  G  T
                                    G
 421 - CCCAAACAATATTTCTGTGCACGTGGCACTCTCCATGATTGGCCTGGTCCTGATAGCTCT - 480
     -  P  N  N  I  S  V  H  V  A  L  S  M  I  G  L  V  L  I  A  L

 481 - GGGTACCGGAGGGATAAAGCCTTGCGTGTCTGCATTTGGCGGAGATCAGTTTGAAGAGGG - 540
     -  G  T  G  G  I  K  P  C  V  S  A  F  G  G  D  Q  F  E  E  G

 541 - CCAGGAAAAGCAAAGGAACAGATTTTTTTCCATCTTTTATTTGGCCATTAATGCTGGAAG - 600
     -  Q  E  K  Q  R  N  R  F  F  S  I  F  Y  L  A  I  N  A  G  S

 601 - TTTGCTTTCTACTATCATCACCCCCATGCTCAGAGTTCAGGTATGCGGAATTCACAGTAA - 660
     -  L  L  S  T  I  I  T  P  M  L  R  V  Q  V  C  G  I  H  S  K

 661 - GCAAGCTTGTTACCCCCTGGCCTTTGGGGTTCCTGCTGCACTCATGGCTGTATCTCTGAT - 720
     -  Q  A  C  Y  P  L  A  F  G  V  P  A  A  L  M  A  V  S  L  I

 721 - CGTGTTTGTCATTGGCAGTGGAATGTACAAGAAGGTCCAGCCCCAGGGTAACATCATGTC - 780
     -  V  F  V  I  G  S  G  M  Y  K  K  V  Q  P  Q  G  N  I  M  S

 781 - TAAAGTTGCCAGGTGCATTGGGTTTGCCATCAAAAATAGGATTAGCCATCGGAGTAAGAA - 840
     -  K  V  A  R  C  I  G  F  A  I  K  N  R  I  S  H  R  S  K  K

 841 - ATTTCCTAAGAGGGAGCACTGGCTGGACTGGGCTAGCGAGAAATATGATGAGCGGCTCAT - 900
     -  F  P  K  R  E  H  W  L  D  W  A  S  E  K  Y  D  E  R  L  I

 901 - CTCTCAAATTAAGATGGTTACAAGGGTGATGTTCCTGTACATTCCTCTCCCCATGTTCTG - 960
     -  S  Q  I  K  M  V  T  R  V  M  F  L  Y  I  P  L  P  M  F  W

 961 - GGCCTTGTTTGATCAGCAGGGCTCCAGGTGGACACTGCAAGCAACGACCATGAGTGGGAA - 1020
     -  A  L  F  D  Q  Q  G  S  R  W  T  L  Q  A  T  T  M  S  G  K

1021 - GATTGGAATCATTGAAATCCAGCCGGATCAGATGCAGACGGTGAACGCCATCCTGATCGT - 1080
     -  I  G  I  I  E  I  Q  P  D  Q  M  Q  T  V  N  A  I  L  I  V

1081 - CGTCATGGTCCCCATCGTGGATGCCGTGGTATATCCTCTGATCGCAAAGTGTGGTTTAAA - 1140
```

```
     -  V  M  V  P  I  V  D  A  V  V  Y  P  L  I  A  K  C  G  L  N

1141 - TTTCACCTCCCTGAAGAAGATGACCGTCGGCATGTTTCTGGCCTCCATGGCTTTCGTGGC - 1200
     -  F  T  S  L  K  K  M  T  V  G  M  F  L  A  S  M  A  F  V  A

1201 - AGCTGCCATCGTGCAGGTGGACATTGACAAAACTCTGCCCGTCTTCCCCAAAGGAAATGA - 1260
     -  A  A  I  V  Q  V  D  I  D  K  T  L  P  V  F  P  K  G  N  E

1261 - AGTCCAAATCAAAGTCCTGAATATAGGAAATAATAGCATGACCGTGTCTTTTCCCGGAAC - 1320
     -  V  Q  I  K  V  L  N  I  G  N  N  S  M  T  V  S  F  P  G  T

1321 - GACAGTGACATGTGACCAGATGTCTCAAACAAACGGATTTCTGACTTTCAACGTAGACAA - 1380
     -  T  V  T  C  D  Q  M  S  Q  T  N  G  F  L  T  F  N  V  D  N

1381 - CCTAAGTATAAACATTTCTTCTACTGGAACACCAGTCACTCCAGTAACTCATAACTTTGA - 1440
     -  L  S  I  N  I  S  S  T  G  T  P  V  T  P  V  T  H  N  F  E

1441 - GTCCGGCCATCGCCATACCCTTCTCGTCTGGGCCCCAAGTAACTACCAAGTGGTAAAAGA - 1500
     -  S  G  H  R  H  T  L  L  V  W  A  P  S  N  Y  Q  V  V  K  D

1501 - TGGCCTTAACCAGAAGCCAGAAAAAGGGAGAAATGGAATCAGATTCGTTAATGCTTTTGG - 1560
     -  G  L  N  Q  K  P  E  K  G  R  N  G  I  R  F  V  N  A  F  G

1561 - CGAGAGCTTCGGCGTCACAATGGATGGGGAAGTTTACAACAATGTCTCCGGTCACAATGC - 1620
     -  E  S  F  G  V  T  M  D  G  E  V  Y  N  N  V  S  G  H  N  A

1621 - CAGTGAATATCTTTTTTTCTCTTCTGGCGTAAAGAGCTTCACAATAAACTCACCAGAGAT - 1680
     -  S  E  Y  L  F  F  S  S  G  V  K  S  F  T  I  N  S  P  E  I

1681 - TTCACAACAGTGTGAAAAACAGTTCAAAACATCCTACCTTGAATTTGGTAGTGCGTTTAC - 1740
     -  S  Q  Q  C  E  K  Q  F  K  T  S  Y  L  E  F  G  S  A  F  T

1741 - CTATGTAATCAGCAGAAAGAGTGACGGTTGCCCCGAACCAAAGATTTTCGAAGACATCTC - 1800
     -  Y  V  I  S  R  K  S  D  G  C  P  E  P  K  I  F  E  D  I  S

1801 - CCCCAACACAGTCAGCATGGCTCTGCAGATCCCCCAGTACTTCCTCCTCACCTGTGGCGA - 1860
     -  P  N  T  V  S  M  A  L  Q  I  P  Q  Y  F  L  L  T  C  G  E

1861 - GGTGGTCTTCTCCATCACCGGCCTGGAGTTCTCCTATTCTCAGGCTCCTTCCAACATGAA - 1920
     -  V  V  F  S  I  T  G  L  E  F  S  Y  S  Q  A  P  S  N  M  K
                                                C
1921 - GTCGGTACTTCAGGCAGGATGGCTGTTGACCGTGGCCGTTGGCAACATCATCGTGCTTAT - 1980
     -  S  V  L  Q  A  G  W  L  L  T  V  A  V  G  N  I  I  V  L  I

1981 - TGTGGCAGGAGCAGGCCAGTTCAGTGAACAGTGGGCCGAGTACGTTCTGTTTGCGGCATT - 2040
     -  V  A  G  A  G  Q  F  S  E  Q  W  A  E  Y  V  L  F  A  A  L

2041 - GCTTCTGGTCGTCTGCATAATATTTGCCATCATGGCTCGATTCTATACGTATGTCAACCC - 2100
     -  L  L  V  V  C  I  I  F  A  I  M  A  R  F  Y  T  Y  V  N  P

2101 - CGCAGAGATTGAAGCTCAGTTTGATGAGGATGACAAGGAGGATGACCTGGAAAAGAGTAA - 2160
     -  A  E  I  E  A  Q  F  D  E  D  D  K  E  D  D  L  E  K  S  N

2161 - CCCATACGCCAAGCTGGACTTCGTCTCACAGACACAAATGTGAATGTCAGGAAGCAAGCG - 2220
     -  P  Y  A  K  L  D  F  V  S  Q  T  Q  M  *

2221 - GACGCGGGGCTGGGCCAGGGTGTGCCCAGGGGTCTGTCCCATGGGGGCAGGACACTCTGT - 2280
```

2281 - TGGGTGGCCTCTGATGGGGAAGACTTCAGAACTGTGGACCAAACCAAGACAGCTGCTTTC - 2340

2341 - TCAGCAGCCGGCAATGAACCTGAAACTCCAAAAGACGTCCTTTTGTTTGTTTGTTTTTAG - 2400

2401 - AGAAGTCTTATTTAAAGCGCACACACACGCACACGCACACACATGCACACACACACACTT - 2460

2461 - TTATAAGAGTCCATACTCTGCCTGAACTCCTTTTCCTAACACACAAATAAAGTTATTTTG – 2520

2521 - GACTAACTTGAATTTTTGAAATGGTGGCCAAGCTCCATACGTGCATTCGCACACTCTGTG – 2580

2581 - CAAACAATGTTAAAGGAGGCAAAAAGTGAATGGTTGGGGCTTTTGAATAGTACGTGTTCA – 2640

2641 - TAATAAGGACCGGCTGGTATTAACTGATAACTCTACCTTCTGTTTTTAGTTCTGTTTTTC – 2700

2701 - CATTCCCTACCTCTTTGTAAATTATGGATTAACCTTTGAAAAACCACTCAGGTAAAGGCA – 2760

2761 - AGTCATGATTTTTGGAGTCTCAACGGTATGAAATAAACTCTCATTCTCAAGAAAAAAAAA - 2820

2821 - AAAAAAAAA - 2829

Figure. 4.3. Nucleotide (upper row) and deduced amino acid (lower row) sequences of sheep oPepT1-39 cDNA. Differences in oPepT1-38 are indicated above the corresponding nucleotide sequence of oPepT1-39. The predicted 12 transmembrane domains are *underlined*. The polyadenylation signal is boxed.

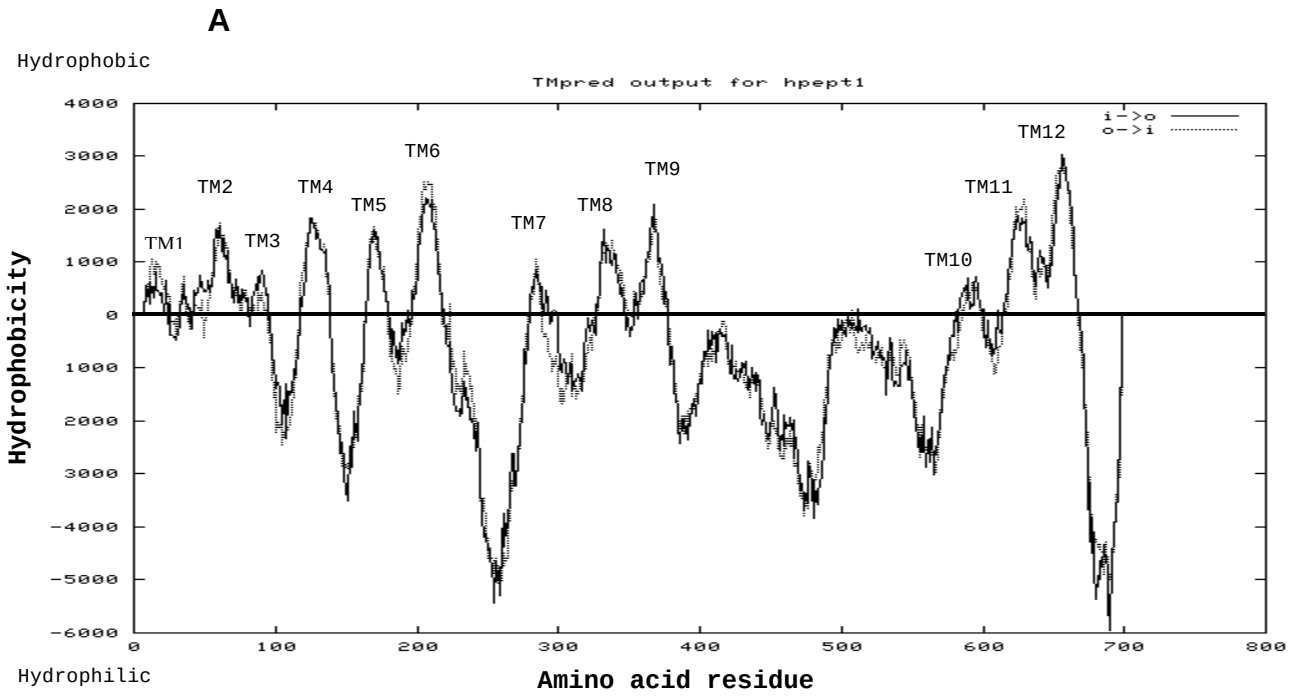
A
Hydrophobic
TMpred output for hpept1
i->o
o->i
TM1
TM2
TM3
TM4
TM5
TM6
TM7
TM8
TM9
TM10
TM11
TM12
Hydrophobicity
Hydrophilic
Amino acid residue

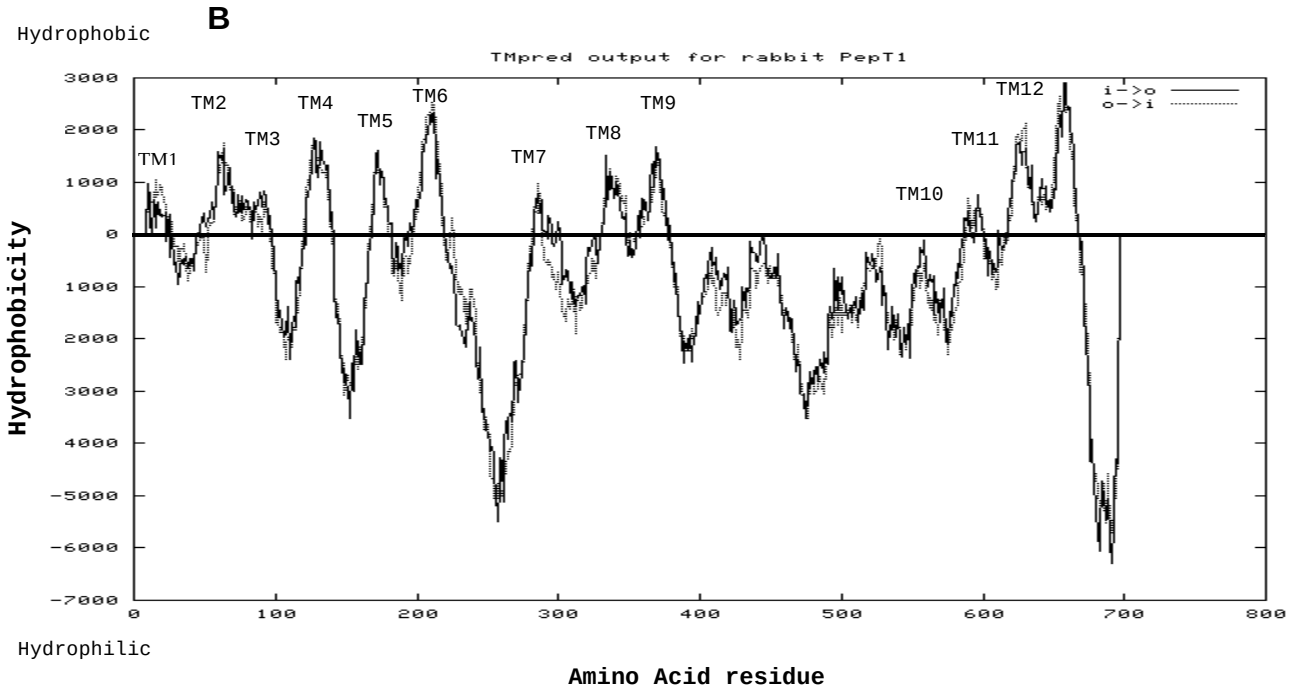
B
Hydrophobic
TMpred output for rabbit PepT1
i->o
o->i
TM1
TM2
TM3
TM4
TM5
TM6
TM7
TM8
TM9
TM10
TM11
TM12
Hydrophobicity
Hydrophilic
Amino Acid residue

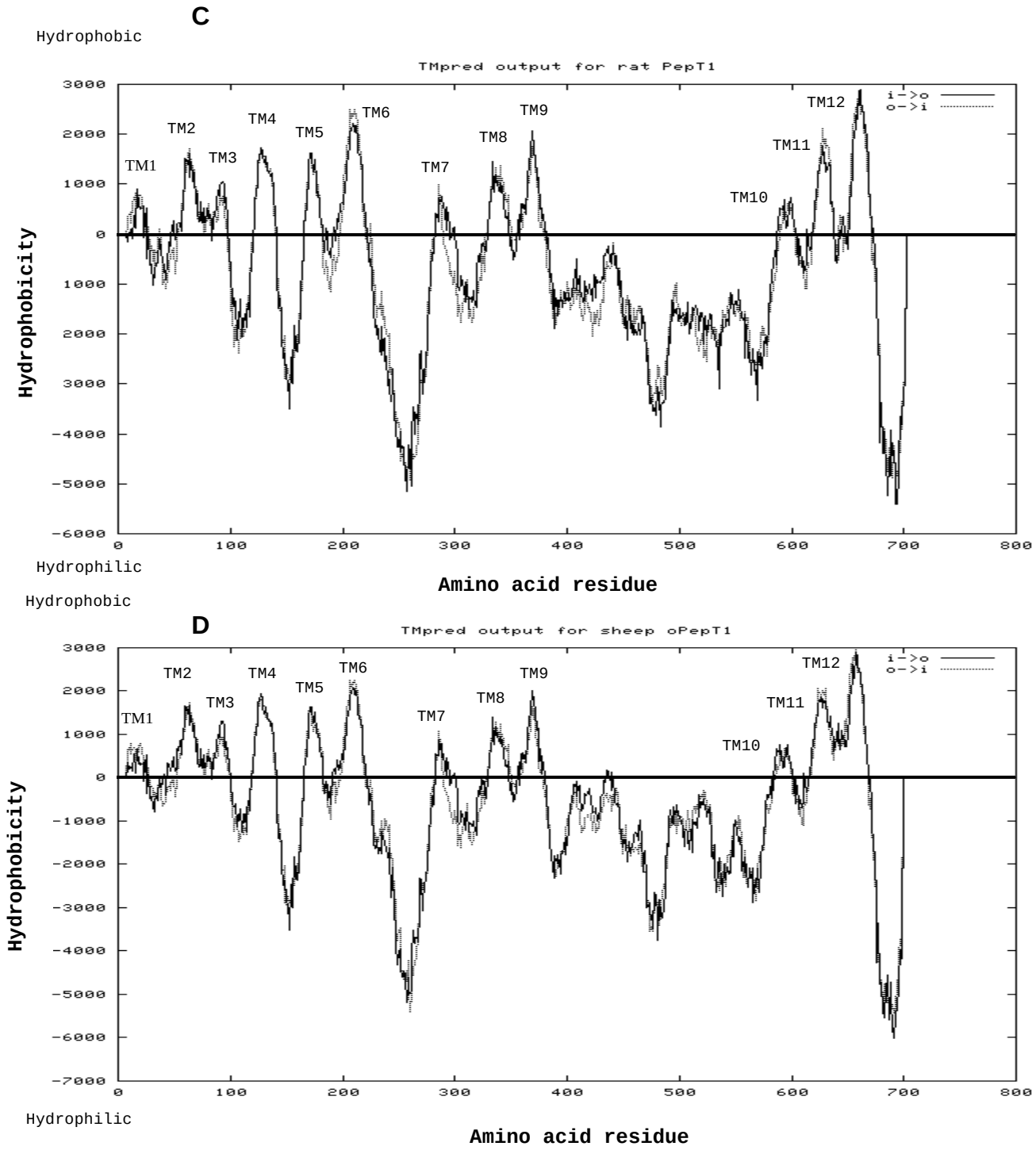

Figure. 4.4. Comparison of deduced amino acid hydrophobicity plot of human (A), rabbit (B), rat (C), and sheep (D) PepT1. TM: transmembrane domain as indicated by peaks in the plot.

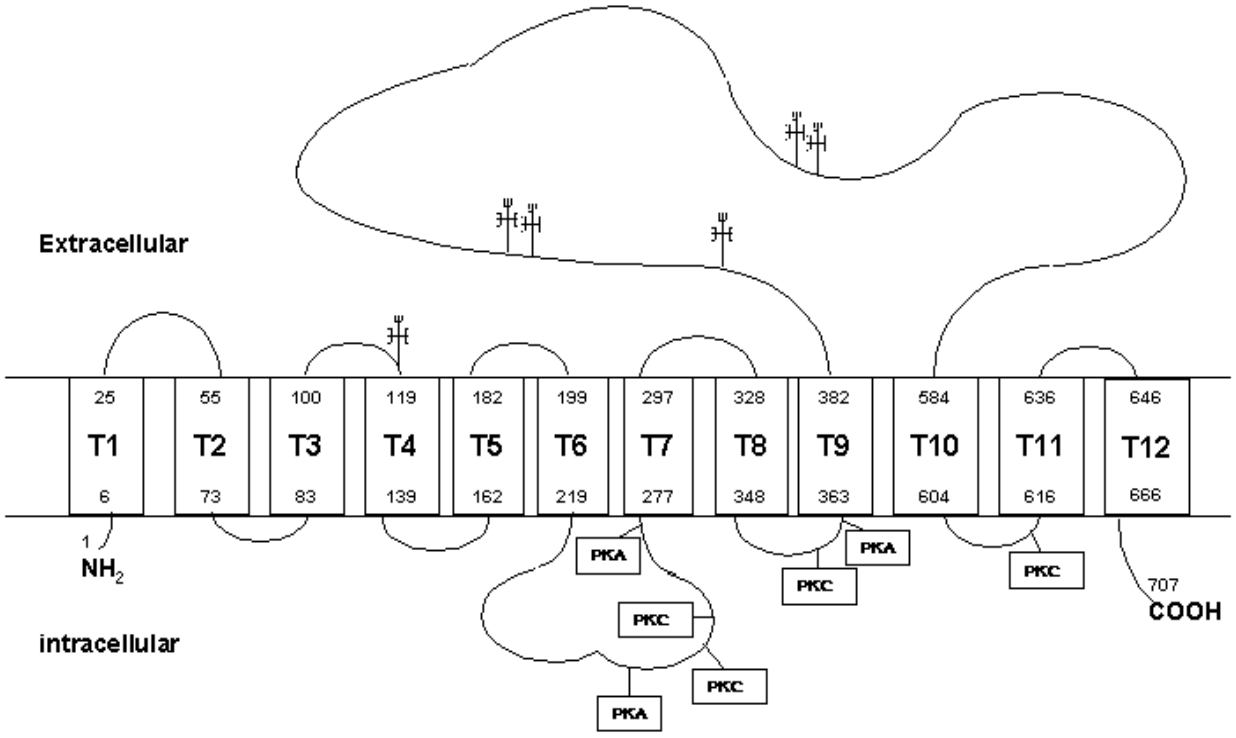

Figure 4.5. Membrane model of oPepT1. Potential N-linked glycosylation sites are indicated by the symbol (). Potential protein kinase C phosphorylation sites (PKC) and protein kinase A phosphorylation sites (PKA) are also indicated.

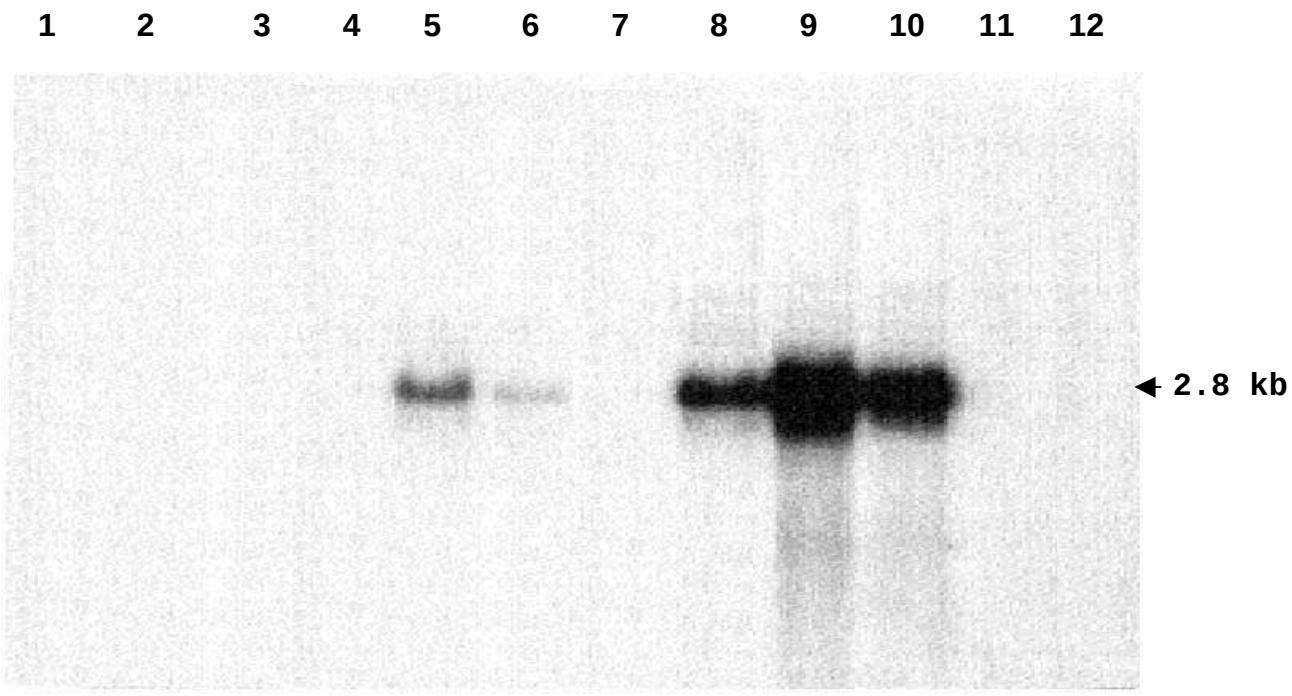

Figure 4.6. Northern blot analysis of oPepT1 mRNA in sheep tissues. Tissue-specific expression of the mRNA corresponding to oPepT1 was examined by high stringency northern analysis using full-length oPepT1 as the probe. Each lane contained 10 μg of poly(A)$^+$ RNA, and lanes 1 to 12 represent the liver, kidney, semitendinosus muscle, longissimus muscle, omasum, rumen, abomasum, duodenum, jejunum, ileum, cecum, colon, respectively.

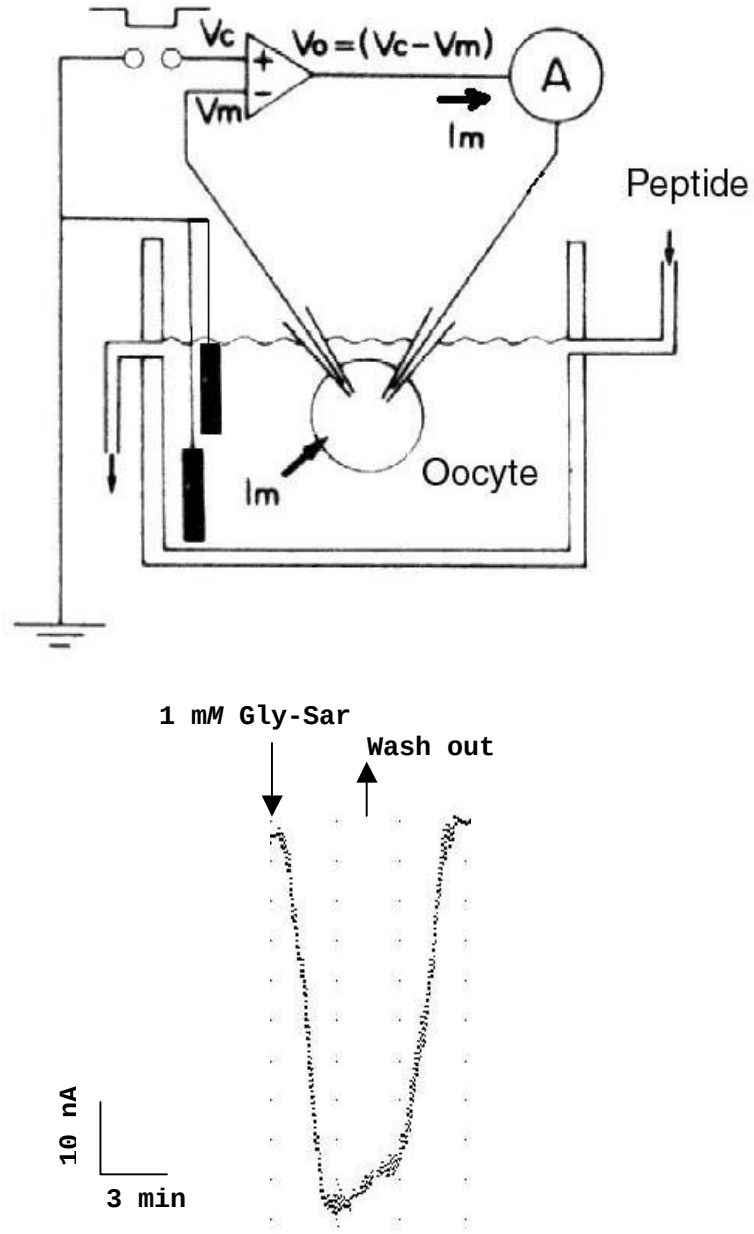

Figure 4.7. Voltage clamp technique (a, adapted from Masu et al., 1987) and a representative recording trace of oPepT1 (b). Vc: Command potential; V_m: membrane potential; I_m: current.

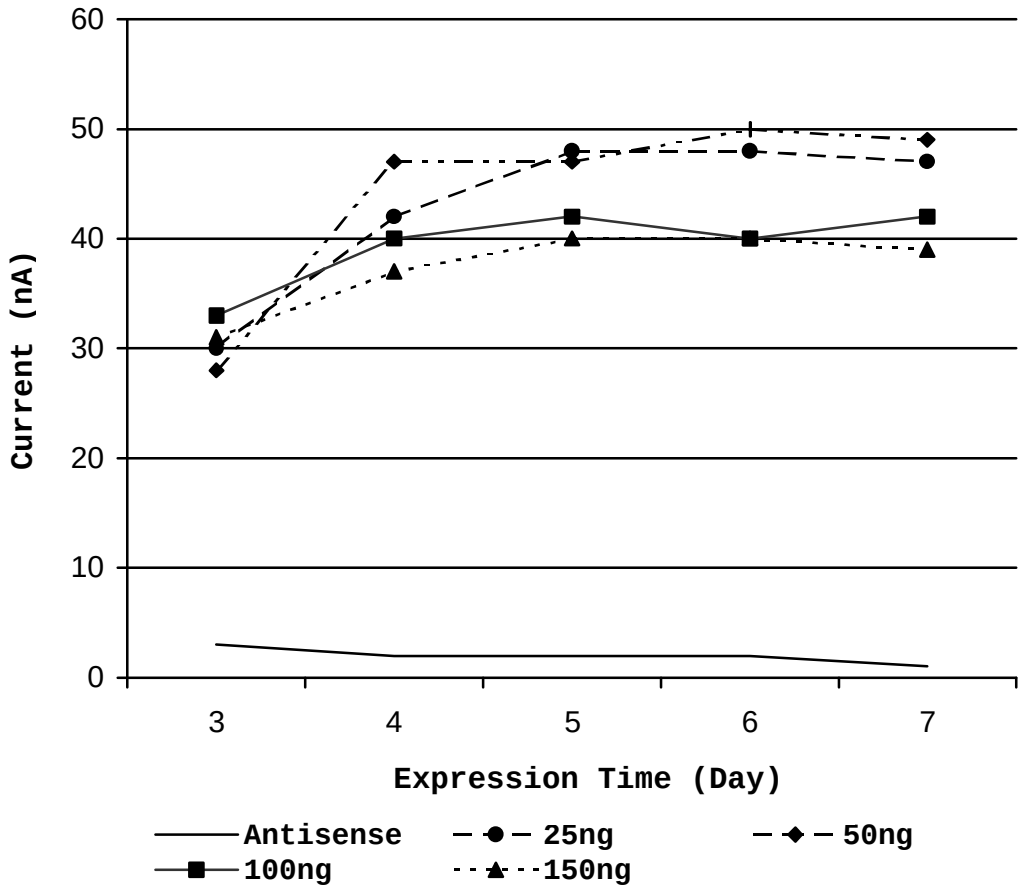

Figure 4.8. Dependence of peptide transport on the expression time and the amount of injected cRNA. Current responses in oocytes injected with different amounts of oPepT1 cRNA (25 ng, 50 ng, 100ng, and 150 ng) were recorded when perfused with 1 m*M* Gly-Sar at pH 5.5.

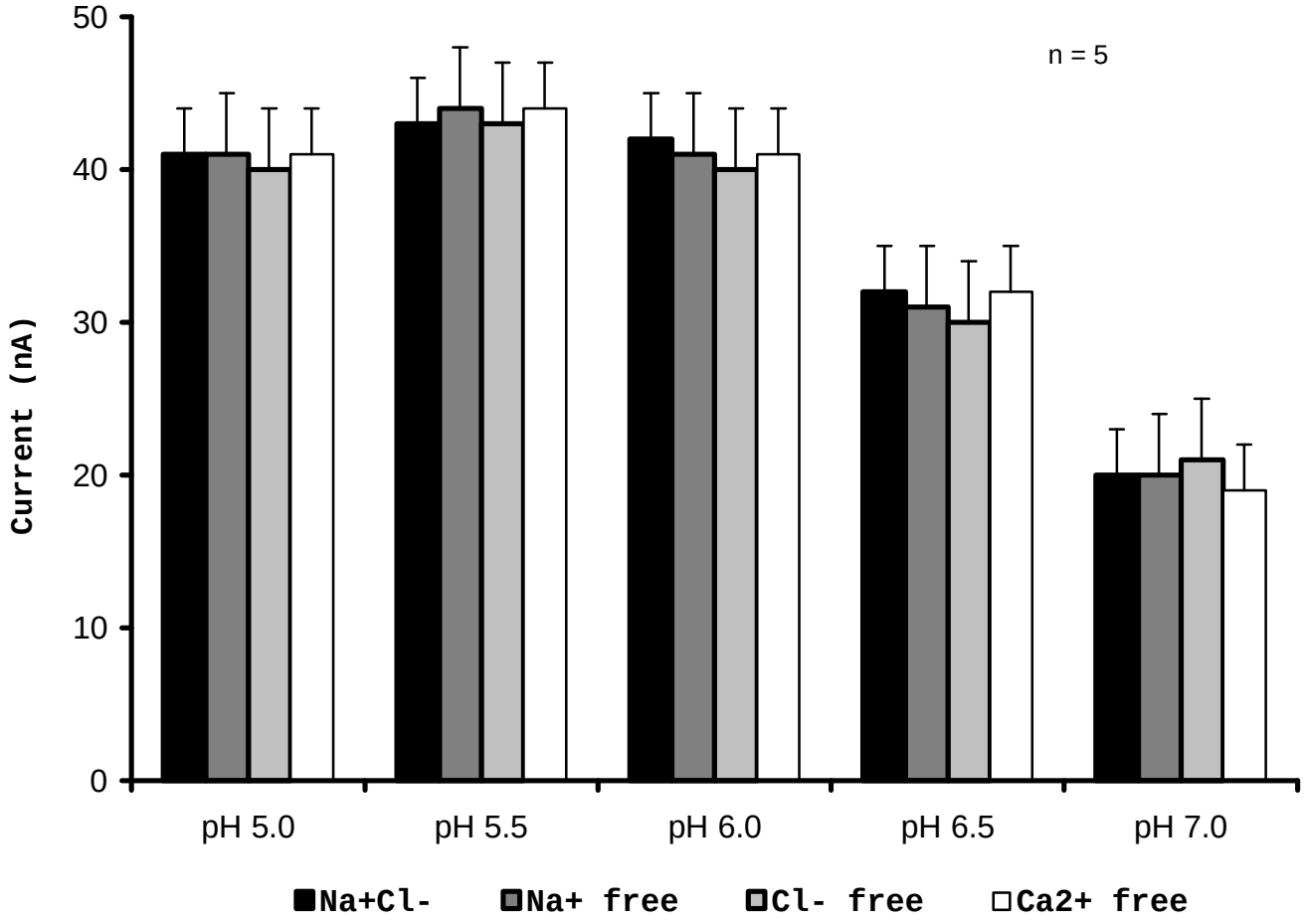

Figure 4.9. Influence of ions on current responses in oocytes injected with oPepT1 cRNA when perfused with 1 m*M* Gly-Sar at different pH (5.0, 5.5, 6.0, 6.5 and 7.0).

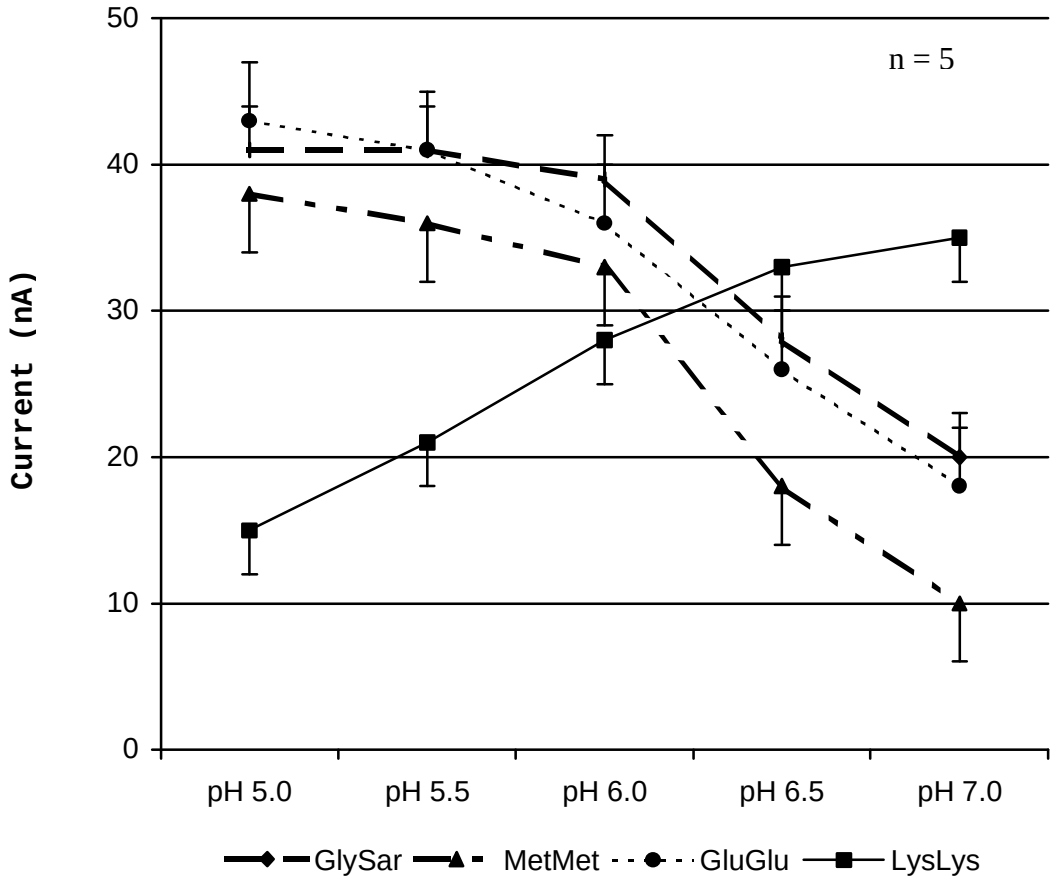

Figure 4.10. Influence of net charge of substrates on current responses in oocytes injected with oPepT1 cRNA when perfused with 5 m*M* Gly-Sar, Met-Met, Glu-Glu, Lys-Lys at different pH.

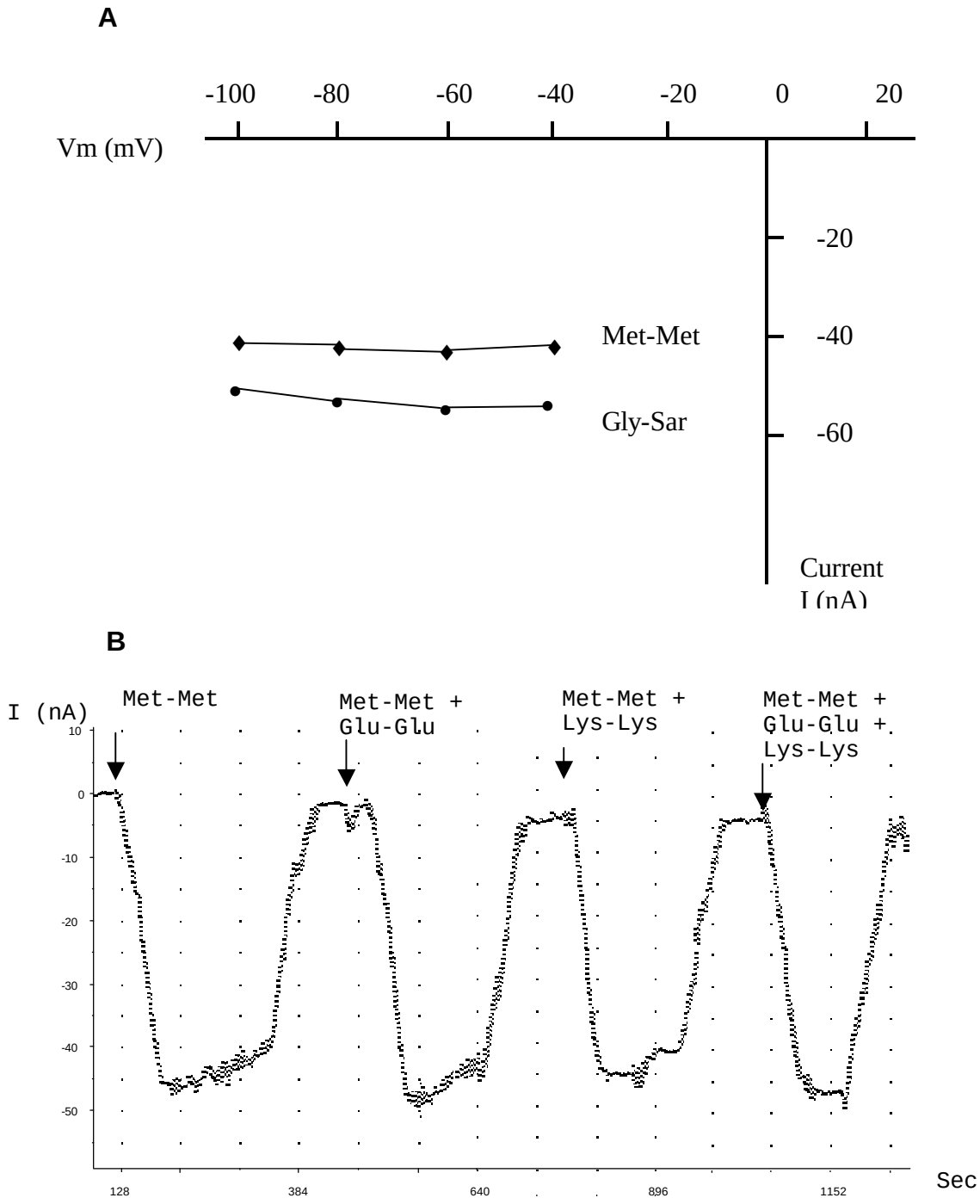

Figure. 4.11. The effects of different membrane potentials (A) and combined dipeptide perfusion (B) to the current responses were determined in cRNA-injected oocytes recorded at pH 5.5 using two electrode voltage clamp.

Dipeptides

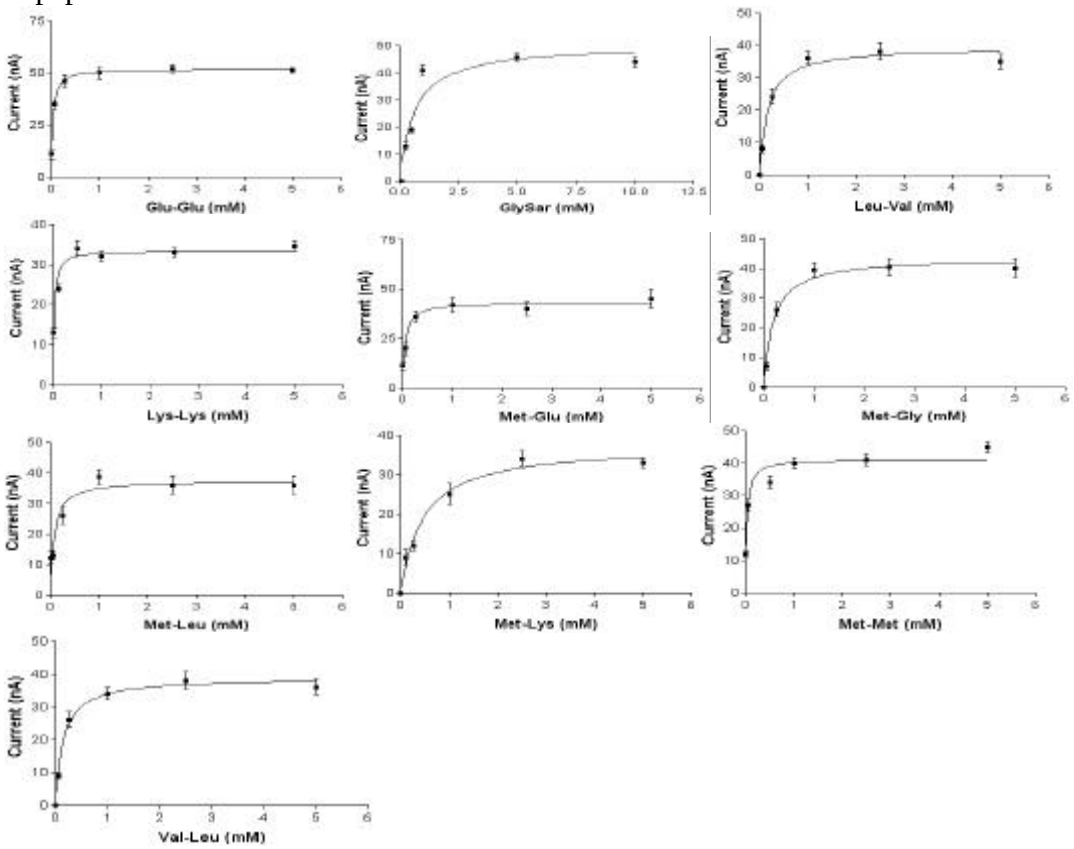

Tripeptide

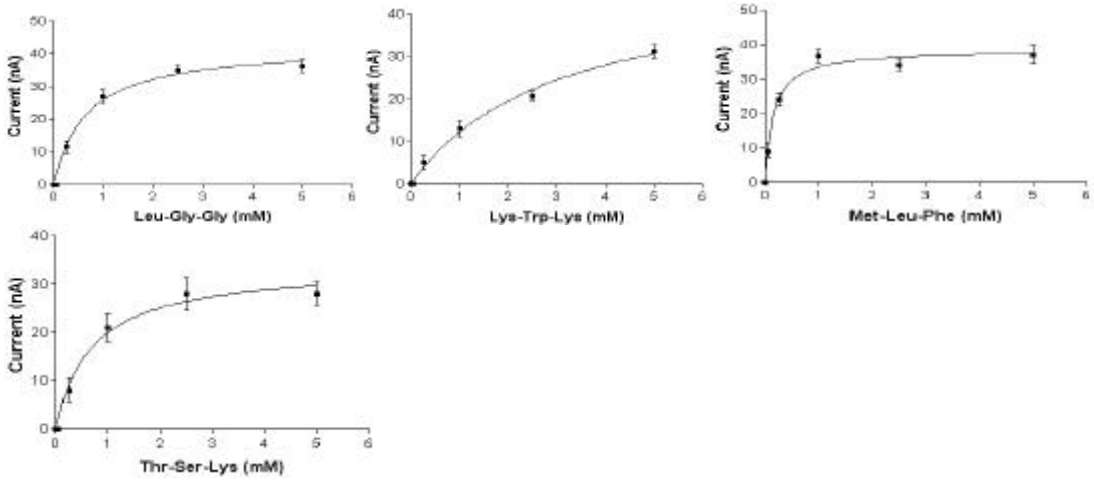

Figure 4.12. Saturation curve of all peptide substrates examined in the kinetic study. Oocytes were clamped to –60 mV using the two-electrode voltage-clamp technique and perfused with .01, .05, .25, .5, 1.0, 2.5, and 5.0 m*M* di- to tetrapeptides in standard measurement buffer at pH 5.5.

```
           1                                                   50
    sheep  MGMSVPKSCF GYPLSIFFIV VNEFCERFSY YGMRALLILY FQRFLGWNDN
    Human  MGMSKSHSFF GYPLSIFFIV VNEFCERFSY YGMRAILILY FTNFISWDDN
      Rat  MGMSKSRGCF GYPLSIFFIV VNEFCERFSY YGMRALLVLY FRNFLGWDDD
   Rabbit  MGMSKSLSCF GYPLSIFFIV VNEFCERFSY YGMRALLILY FRNFIGWDDN
Consensus  mgMSks.scF GYPLSIFFIV VNEFCERFSY YGMRAlL!LY FrnFigW#D#

           51                                                  100
    sheep  LGTAIYHTFV ALCYLTPILG ALIADSWLGK FKTIVSLSIV YTIGQVVIAV
    Human  LSTAIYHTFV ALCYLTPILG ALIADSWLGK FKTIVSLSIV YTIGQAVTSV
      Rat  LSTAIYHTFV ALCYLTPILG ALIADSWLGK FKTIVSLSIV YTIGQAVISV
   Rabbit  LSTVIYHTFV ALCYLTPILG ALIADAWLGK FKTIVWLSIV YTIGQAVTSL
Consensus  LsTaIYHTFV ALCYLTPILG ALIADsWLGK FKTIVsLSIV YTIGQaVtsv

           101                                                 150
    sheep  SSINDLTDFN HDGTPNNISV HVALSMIGLV LIALGTGGIK PCVSAFGGDQ
    Human  SSINDLTDHN HDGTPDSLPV HVVLSLIGLA LIALGTGGIK PCVSAFGGDQ
      Rat  SSINDLTDHD HDGSPNNLPL HVALSMIGLA LIALGTGGIK PCVSAFGGDQ
   Rabbit  SSVNELTDNN HDGTPDSLPV HVAVCMIGLL LIALGTGGIK PCVSAFGGDQ
Consensus  SS!N#LTD.# HDGtP#slpv HVals$IGL. LIALGTGGIK PCVSAFGGDQ

           151                                                 200
    sheep  FEEGQEKQRN RFFSIFYLAI NAGSLLSTII TPMLRVQVCG IHSKQACYPL
    Human  FEEGQEKQRN RFFSIFYLAI NAGSLLSTII TPMLRVQQCG IHSKQACYPL
      Rat  FEEGQEKQRN RFFSIFYLAI NAGSLLSTII TPILRVQQCG IHSQQACYPL
   Rabbit  FEEGQEKQRN RFFSIFYLAI NAGSLLSTII TPMVRVQQCG IHVKQACYPL
Consensus  FEEGQEKQRN RFFSIFYLAI NAGSLLSTII TPmlRVQqCG IHskQACYPL

           201                                                 250
    sheep  AFGVPAALMA VSLIVFVIGS GMYKKVQPQG NIMSKVARCI GFAIKNRISH
    Human  AFGVPAALMA VALIVFVLGS GMYKKFKPQG NIMGKVAKCI GFAIKNRFRH
      Rat  AFGVPAALMA VALIVFVLGS GMYKKFQPQG NIMGKVAKCI RFAIKNRFRH
   Rabbit  AFGIPAILMA VSLIVFIIGS GMYKKFKPQG NILSKVVKCI CFAIKNRFRH
Consensus  AFG!PAaLMA VsLIVF!iGS GMYKKfkPQG NI$sKVakCI .FAIKNRfrH

           251                                                 300
    sheep  RSKKFPKREH WLDWASEKYD ERLISQIKMV TRVMFLYIPL PMFWALFDQQ
    Human  RSKAFPKREH WLDWAKEKYD ERLISQIKMV TRVMFLYIPL PMFWALFDQQ
      Rat  RSKAFPKRNH WLDWAKEKYD ERLISQIKIM TKVMFLYIPL PMFWALFDQQ
   Rabbit  RSKQFPKRAH WLDWAKEKYD ERLIAQIKMV TRVLFLYIPL PMFWALFDQQ
Consensus  RSK.FPKR.H WLDWAkEKYD ERLIsQIKmv TrV$FLYIPL PMFWALFDQQ

           301                                                 350
    sheep  GSRWTLQATT MSGKIGIIEI QPDQMQTVNA ILIVVMVPIV DAVVYPLIAK
    Human  GSRWTLQATT MSGKIGALEI QPDQMQTVNA ILIVIMVPIF DAVLYPLIAK
      Rat  GSRWTLQATT MTGKIGTIEI QPDQMQTVNA ILIVIMVPIV DAVVYPLIAK
   Rabbit  GSRWTLQATT MSGRIGILEI QPDQMQTVNT ILIIILVPIM DAVVYPLIAK
Consensus  GSRWTLQATT MsGkIGilEI QPDQMQTVNa ILI!!$VPI. DAVvYPLIAK

           351                                                 400
    sheep  CGLNFTSLKK MTVGMFLASM AFVAAAIVQV DIDKTLPVFP KGNEVQIKVL
    Human  CGFNFTSLKK MAVGMVLASM AFVVAAIVQV EIDKTLPVFP KGNEVQIKVL
      Rat  CGFNFTSLKK MTVGMFLASM AFVVAAIVQV EIDKTLPVFP SGNQVQIKVL
   Rabbit  CGLNFTSLKK MTIGMFLASM AFVAAAILQV EIDKTLPVFP KANEVQIKVL
Consensus  CGlNFTSLKK Mt!GMfLASM AFVaAAIvQV #IDKTLPVFP kgN#VQIKVL
           401                                                 450
    sheep  NIGNNSMTVS FPGTTVTCDQ MSQTNGFLTF NVDNL.SINI SSTGTP.VTP
    Human  NIGNNTMNIS LPGEMVTLGP MSQTNAFMTF DVNKLTRINI SSPGSP.VTA
      Rat  NIGNNDMAVY FPGKNVTVAQ MSQTDTFMTF DVDQLTSINV SSPGSPGVTT
   Rabbit  NVGSENMIIS LPGQTVTLNQ MSQTNEFMTF NEDTLTSINI TSGSQ..VTM
Consensus  N!Gn#.M.!s lPG.tVTl.q MSQT#.F$TF #v#.LtsIN! sS.g.p.VT.
```

```
           451                                                  500
    sheep  VTHNFESGHR HTLLVWAPSN YQVVKDGLNQ KPEKGRNGIR FVNAFGESFG
    Human  VTDDFKQGQR HTLLVWAPNH YQVVKDGLNQ KPEKGENGIR FVNTFNELIT
      Rat  VAHEFEPGHR HTLLVWGPNL YRVVKDGLNQ KPEKGENGIR FVSTLNEMIT
   Rabbit  ITPSLEAGQR HTLLVWAPNN YRVVNDGLTQ KSDKGENGIR FVNTYSQPIN
Consensus  !t..fe.GqR HTLLVWaPnn YrVVkDGLnQ Kp#KGeNGIR FVnt..#.i.

           501                                                  550
    sheep  VTMDGEVYNN VSGHNASEYL FFSSGVKSFT INSPEISQQC EKQFKTSYLE
    Human  ITMSGKVYAN ISSYNASTYQ FFPSGIKGFT ISSTEIPPQC QPNFNTFYLE
      Rat  IKMSGKVYEN VTSHSASNYQ FFPSGQKDYT INTTEIAPNC SSDFKSSNLD
   Rabbit  VTMSGKVYEH IASYNASEYQ FFTSGVKGFT VSSAGISEQC RRDFESPYLE
Consensus  !tMsGkVYen !.synASeYq FF.SGvKg%T !ss.eIs.#C ..#F.s.yL#

           551                                                  600
    sheep  FGSAFTYVIS .RKSDGCPEP KIFEDISPNT VSMALQIPQY FLLTCGEVVF
    Human  FGSAYTYIVQ .RKNDSCPEV KVFEDISANT VNMALQIPQY FLLTCGEVVF
      Rat  FGSAYTYVIR SRASDGCLEV KEFEDIPPNT VNMALQIPQY FLLTCGEVVF
   Rabbit  FGSAYTYLIT SQAT.GCPQV TEFEDIPPNT MNMAWQIPQY FLITSGEVVF
Consensus  FGSA%TY.!. sra.dgCp#v keFEDIppNT vnMAlQIPQY FLlTcGEVVF

           601                                                  650
    sheep  SITGLEFSYS QAPSNMKSVL QAGWLLTVAV GNIIVLIVAG AGQFSEQWAE
    Human  SVTGLEFSYS QAPSNMKSVL QAGWLLTVAV GNIIVLIVAG AGQFSKQWAE
      Rat  SVTGLEFSYS QAPSNMKSVL QAGWLLTVAI GNIIVLIVAE AGHFDKQWAE
   Rabbit  SITGLEFSYS QAPSNMKSVL QAGWLLTVAV GNIIVLIVAG AGQINKQWAE
Consensus  S!TGLEFSYS QAPSNMKSVL QAGWLLTVA! GNIIVLIVAg AGqf.kQWAE

           651                                                  700
    sheep  YVLFAALLLV VCIIFAIMAR FYTYVNPAEI EAQFDEDDKE DDLEKSNPYA
    Human  YILFAALLLV VCVIFAIMAR FYTYINPAEI EAQFDEDEKK NRLEKSNPYF
      Rat  YVLFASLLLV VCIIFAIMAR FYTYINPAEI EAQFDEDEKK KGVGKENPYS
   Rabbit  YILFAALLLV VCVIFAIMAR FYTYVNPAEI EAQFEEDEKK KNPEKNDLYP
Consensus  Y!LFAaLLLV VC!IFAIMAR FYTY!NPAEI EAQF#ED#Kk k..eK.#pY.

           701    710
    sheep  KLDFVSQTQM
    Human  MSGANSQKQM
      Rat  SLEPVSQTNM
   Rabbit  SLAPVSQTQM
Consensus  sl.pvSQt#M
```

Figure. 4.13. Comparison of deduced amino acid sequences of sheep (oPepT1-39), human (hPepT1), rat, and rabbit PepT1. The predicted 12 transmembrane domains are *underlined.*

Consensus symbols: ! is either I or V; $ is either L or M
% is either F or Y; # is either N, D, Q, E, B, or Z

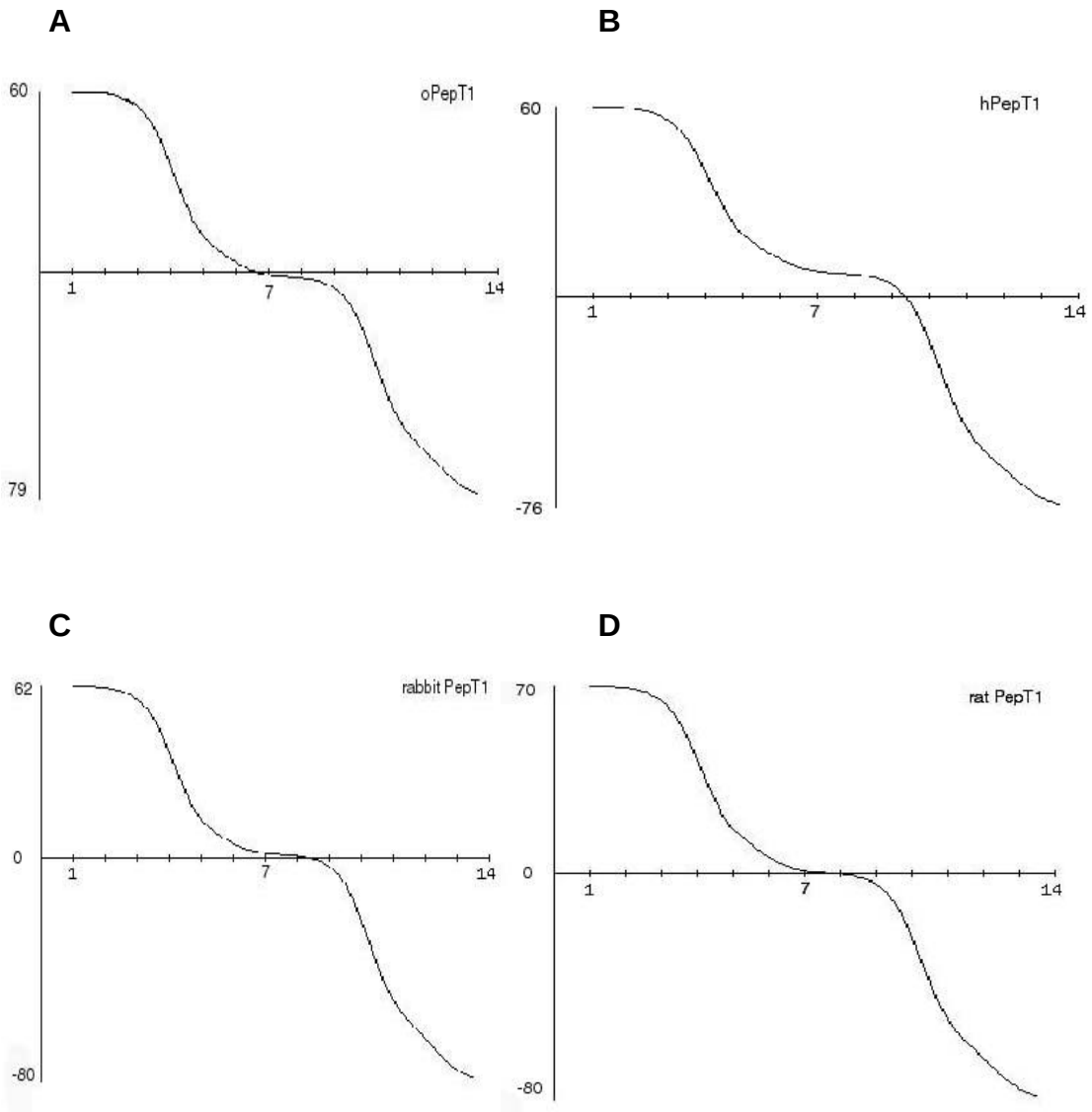

Figure 4.14. Comparison of the titration curves of all PepT1 proteins, oPepT1 (A); Human PepT1 (B), rabbit PepT1 (C), and rat PepT1 (D).

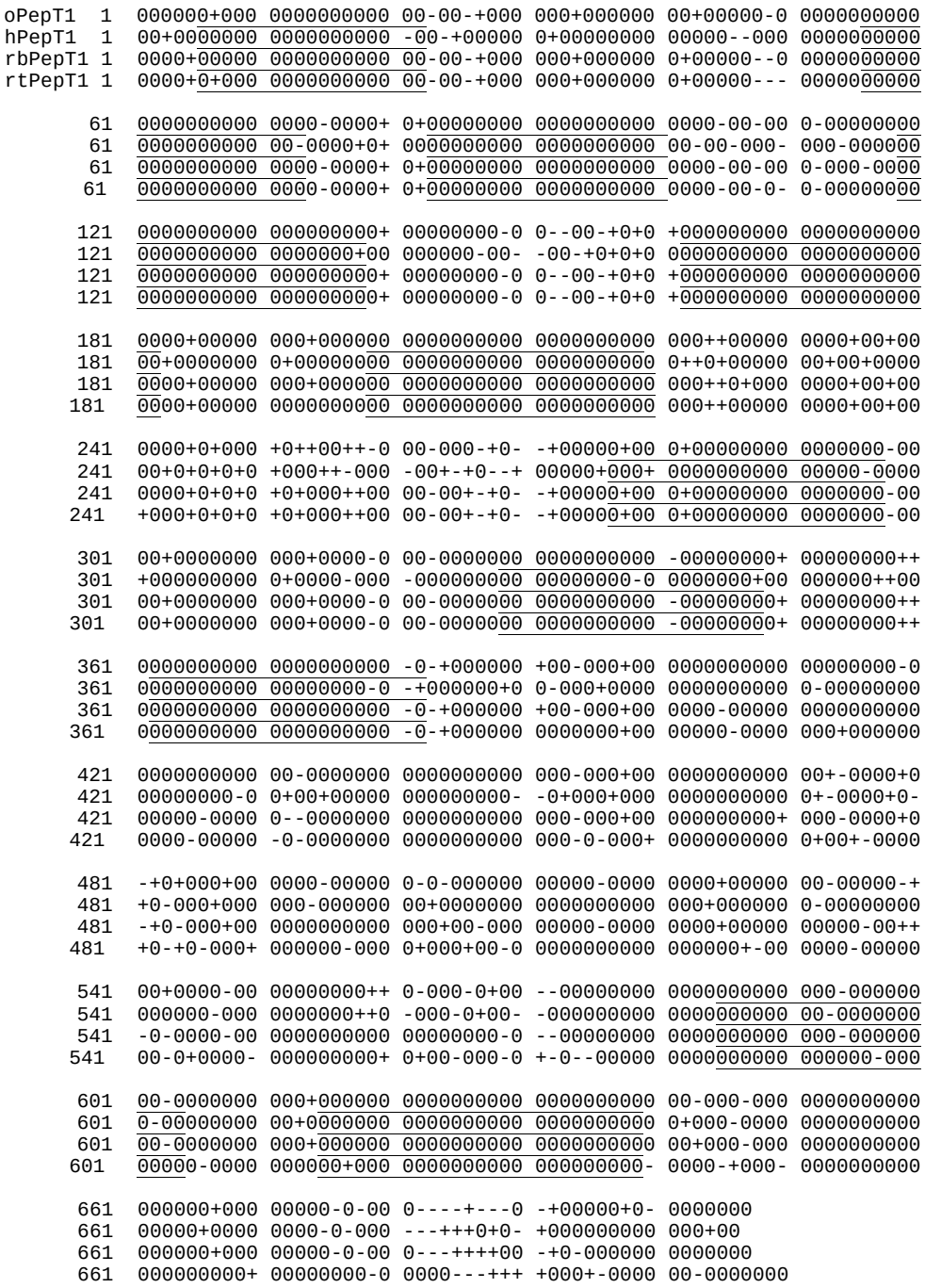

Figure. 4.15. Charge distributional analysis of PepT1 protein sequences was evaluated by SAPS (Brendel et al., 1992). The predicted 12 transmembrane domains are *underlined*.

Chapter V

Epilogue

The cloning and *in vitro* expression of oPepT1 in *Xenopus* oocytes in the present study provide primary information on the molecular structure and basic functions of this peptide transporter. These data make it possible to further understand the role of peptide transport in sheep. Traditionally, it was believed that only free amino acids entered the portal blood from intestinal epithelial cells (Matthews, 1991). However, recent studies demonstrated that ~50% of circulating plasma amino acids were peptide bound, and the majority were in the form of di- and tripeptides (Seal and Parker, 1991). This suggests that the existence of a basolateral peptide transporter in the small intestine. The research data from our laboratory suggest that peptide transport occurs in the ruminant forestomach and intestine (Matthews et al., 1996; Pan et al., 1997; Chen et al., 1999). However, because of controversial data regarding portal flux of peptides in ruminants (Koeln et al., 1993; Seal and Parker, 1996; Backwell et al., 1997), it became important to demonstrate the presence, cellular membrane location, and surface expression of a peptide transporter protein in sheep. An understanding of the distribution of the peptide transporter protein in the gastrointestinal tract of sheep is now emerging.

Anti-PepT1 antibodies have been successfully developed against synthetic peptides corresponding to the C-terminal 15 amino acids of the peptide transporter (Saito et al., 1995; Ogihara et al., 1996). The C-termini were selected not only because of the

complete lack of homology between PepT1 and PepT2 in this region but also the lack of homology among species. Polyclonal antibodies were also generated against fusion proteins containing the large extracellular loop of the peptide transporter (Shen et al., 1999), since there was little amino acid identity among peptide transporters in this region. Although similar results were observed with antisera prepared from fusion proteins compared with C-terminal synthetic peptides, the signals were much weaker with antisera prepared from fusion proteins. Therefore, the C-terminal 15 amino acids (SNPYA KLDFV SQTQM, amino acids 693-707) of oPepT1 likely can be used to develop anti-oPepT1 antibodies. The cellular localization of oPEPT1 proteins can then be further investigated by immunofluorescence using affinity-purified antibodies. Definitive evidence will be provided regarding the distribution of oPepT1 proteins in sheep tissues. They will provide yet further information regarding the physiological and pharmacological significance of this transporter in sheep. These are critical data for protein absorption in the sheep forestomach. Although our data continue to support the existence of a peptide transporter in the sheep forestomach and possible involvement of the forestomach in the appearance of peptides in portal flux, we have not shown evidence of the site of peptide transporter function in the four-layed forestomach cell strata. Therefore, the cloning of oPepT1 in the present study should greatly facilitate these future studies.

We found that all dipeptides and tripeptides transported by oPepT1 in *Xenopus* oocytes obeyed Michaelis-Menten-type kinetics. The estimated K_t values for peptides range from 20 μ*M* to 3 m*M*. One of the controversial issues regarding peptide transport is that the difference in substrate recognition and affinity might exist among different

experimental models. Therefore, the data from *Xenopus* oocytes might not reflect the real situation in animals. Comparison of the apparent affinity constants in different expression systems is listed in Table 5.1. Some dipeptides (Gly-Sar and Phe-Ala) and peptidomimetics (cefadroxil, ceftibuten, cephradine, and cyclacillin) have been examined in multiple experimental models. Generally, in the same expression system, the apparent K_t value of one certain substrate uptake by the PepT1-expressing model is 10 times or more lower than that by the PepT2-expressing model. However, the apparent K_t value of most of the substrates studied in different systems seems consistent in different experimental models. In fact, most of the key functional features, including the ionic dependence, proton to peptide stoichiometry, substrate specificity, substrate affinities, are found to be similar for peptide transporters expressed in different systems. Some small variations are probably due to peptide transporters in different species rather than the expression systems. This suggests that the expression models in which they are heterologously expressed may not affect the functional characteristics of peptide transporters. Expression of oPepT1 in a mammalian cell line should be able to confirm the data from the present study.

We cannot preclude the possibility of the existence of any other peptide transporter in sheep. The cloning of oPepT1 may help us identify more peptide transporters. Yamashita et al. (1997) reported the cloning of a brain peptide/histidine transporter (PHT1) from rat brain cDNA library using a 55-bp fragment homologous to rabbit PepT1 under medium stringency conditions. Interestingly, the amino acid sequence of PHT1 showed only low similarity with other mammalian peptide transporters (32% similarity and

17% identity with PepT1, 27% similarity and 12% identity with PepT2), but PHT1 did transport the dipeptide carnosine in a proton-dependent manner. Therefore, we may employ the same method to design some short primers based on the oPepT1 sequence and screening the ovine cDNA library with these short primers may isolate new peptide transporters.

Little is known about the regulation of peptide transporters, even though they contain potential target sites for phosphorylation by protein kinases. To answer the question about the role of protein kinases in the regulation of oPepT1, we can employ the oocyte expression system to express different isoforms of oPepT1. Different oPepT1 isoforms will be constructed using site-directed mutagenesis to alter the number of potential target sites for phosphorylation by protein kinases. The cytoplasmic loops of oPepT1 which are located between transmembrane domains 6 and 7, and 8 and 9 and include almost all the consensus sites for protein kinases, will be the primary target region for site-directed mutagenesis. The electrophysiological methods provide sensitive assays for both the kinetics and number of transporters in the plasma membrane. The major advantages are that these parameters can be determined in a single cell before and after activation of protein kinases. Standard protocols can be used to activate PKA and PKC in oocytes (Corey et al., 1994). Phorbol esters have been used to activate PKC (Zhu et al., 1997) and 8-Br-cAMP has been used to activate PKA (Blumenthal and Kaczmarek. 1992) in oocytes expressing cloned membrane proteins. These activators can rapidly, and reversibly, modulate the functional expression of oPepT1 in oocytes. Changes in transport rate can be recorded after adding the membrane permeable protein kinase activators to the

bath. Therefore, the effect of a protein kinase depending on the transporter and the isoform being expressed can be revealed. These data should be valuable if we decide to alter the peptide transport process in sheep.

The selective expression of oPepT1 in different tissues suggests that characterization of the gene encoding this peptide transporter may provide insight into regulatory elements responsible for tissue-specific gene expression and potential regulatory factors. An ovine genomic library can be constructed and screened with the oPepT1 cDNA to identify the gene. Construction of reporter gene plasmids containing various 5`-flanking region of the oPepT1 gene can be transfected into a cell line, such as HeLa, CHO, or Caco-2, and the mechanism of transcriptional activation of oPepT1 gene by different factors can then be investigated. Once the gene is identified, knocking out the gene may help us to finally understand the important role of peptide transporters in animals.

In summary, we have cloned the first peptide transporter, oPepT1, in ruminants. The tissue distribution and characterization of oPepT1 *in vitro* has demonstrated both similarities and differences of oPepT1 to PepT1 from other species. These data should facilitate future research on peptide transport in sheep.

Table 5.1. Comparison of the apparent K_t in different experimental models.

Substrate	Expression system	Transporter	K_t	Reference
Ala-Asp	*Xenopus* oocytes	PepT1	143 μ*M*, pH 5.5	Fei et al., 1994
	Xenopus oocytes	PepT1	140 μ*M*, pH 5.5	Steel et al., 1997
Ala-Lys	*Xenopus* oocytes	PepT1	.30 m*M*, pH 5.5	Steel et al., 1997
Gly-Asp	*Xenopus* oocytes	PepT1	.14 m*M*, pH 5.5	Amesheh et al., 1997a
	Xenopus oocytes	PepT2	4.4 μ*M*, pH 6.5	Amesheh et al., 1997b
Gly-Gln	*Xenopus* oocytes	PepT1	.14 m*M*, pH 5.5	Amesheh et al., 1997a
	Xenopus oocytes	PepT2	7.6 μ*M*, pH 6.5	Amesheh et al., 1997b
	Xenopus oocytes	PepT2	16 μ*M*, pH 6.5	Chen et al., 1999a
Gly-Glu	*Xenopus* oocytes	PepT1	.22 m*M*, pH 5.5	Steel et al., 1997
Gly-Gly	*Xenopus* oocytes	PepT1	2.5 m*M*, pH 5.5	Fei et al., 1994
	Xenopus oocytes	PepT1	2.5 m*M*, pH 5.5	Steel et al., 1997
Gly-Leu	*Xenopus* oocytes	PepT1	81 μ*M*, pH 5.5	Fei et al., 1994
	Xenopus oocytes	PepT1	80 μ*M*, pH 5.5	Steel et al., 1997
	Xenopus oocytes	PepT2	4 μ*M*, pH 6.0	Chen et al., 1999a
Gly-Lys	*Xenopus* oocytes	PepT1	2.9 m*M*, pH 5.5	Amesheh et al., 1997a
	Xenopus oocytes	PepT1	2.4 m*M*, pH 5.5	Steel et al., 1997
	Xenopus oocytes	PepT2	86 μ*M*, pH 5.5	Amesheh et al., 1997b
	Xenopus oocytes	PepT2	51 μ*M*, pH 5.5	Chen et al., 1999a
Gly-Sar	*Xenopus* oocytes	PepT1	1.9 m*M*, pH 5.5	Fei et al., 1994
	Xenopus oocytes	PepT1	0.7 m*M*, pH 5.5	Mackenzie et al., 1996
	Xenopus oocytes	PepT1	1.7 m*M*, pH 5.5	Fei et al., 1998
	Xenopus oocytes	PepT2	70 μ*M*, pH 5.5	Fei et al., 1998
	Xenopus oocytes	PepT2	50 μ*M*, pH 5.5	Ramamoorthy et al., 1995
	BBMV	PepT1	1.2 m*M*, pH 5.5	Takahashi et al., 1998
	BBMV	PepT2	50 μ*M*, pH 5.5	Takahashi et al., 1998
	Caco-2	PepT1	1.0 m*M*, pH 6.0	Brandsch et al., 1997
	Caco-2	PepT1	.5 m*M*, pH 5.5	Ganapathy et al., 1998
	Caco-2	PepT1	2.1 m*M*, pH 6.0	Han et al., 1998
	Caco-2	PepT2	67 μ*M*, pH 6.0	Ganapathy et al., 1998
	SKPT	PepT2	67 μ*M*, pH 6.0	Brandsch et al., 1995
	SKPT	PepT2	48 μ*M*, pH 6.0	Ganapathy et al., 1995
	SKPT	PepT2	74 μ*M*, pH 6.0	Brandsch et al., 1997
	SKPT	PepT2	75 μ*M*, pH 6.0	Ganapathy et al., 1997
	LLC-PK_1	PepT1	1.1 m*M*, pH 6.0	Terada et al., 1997
	LLC-PK_1	PepT2	.1 m*M*, pH 6.0	Terada et al., 1997
	HeLa	PepT1	.3 m*M*, pH 5.5	Liang et al., 1995
	HeLa	PepT1	1.9 m*M*, pH 5.5	Steel et al., 1997
	HeLa	PepT2	35 μ*M*, pH 6.0	Steel et al., 1997
	SK-N-SH	PepT2	84 μ*M*, pH 6.0	Wang et al., 1998
Phe-Ala	*Xenopus* oocytes	PepT1	1.2 m*M*, pH 5.5	Amesheh et al., 1997
	Xenopus oocytes	PepT1	1.2 m*M*, pH 5.5	Doring et al., 1997
	Xenopus oocytes	PepT2	51 μ*M*, pH 6.0	Doring et al., 1997
	Xenopus oocytes	PepT2	75 μ*M*, pH 6.0	Chen et al., 1999a
	LLC-PK_1	PepT2	22 μ*M*, pH 6.0	Wenzel et al., 1998;
	LLC-PK_1	PepT2	22 μ*M*, pH 6.0	Wenzel et al., 1999
Phe-Glu	*Xenopus* oocytes	PepT1	.94 m*M*, pH 5.5	Steel et al., 1997
	Xenopus oocytes	PepT2	48 μ*M*, pH 6.0	Chen et al., 1999a
Phe-Lys	*Xenopus* oocytes	PepT2	135 μ*M*, pH 6.0	Chen et al., 1999a
Gly-Gly-Gly	*Xenopus* oocytes	PepT1	5.1 m*M*, pH 5.5	Fei et al., 1994
	Xenopus oocytes	PepT1	5.1 m*M*, pH 5.5	Steel et al., 1997
Cefadroxil	*Xenopus* oocytes	PepT1	1.1 m*M*, pH 5.5	Boll et al., 1994
	Xenopus oocytes	PepT2	26 μ*M*, pH 6.0	Boll et al., 1996
	Caco-2	PepT1	5.1 m*M*, pH 6.0	Ganapathy et al., 1995
	HeLa	PepT1	.87 m*M*, pH 5.5	Ganapathy et al., 1997
	HeLa	PepT2	66 μ*M*, pH 6.0	Ganapathy et al., 1997
	SKPT	PepT2	66 μ*M*, pH 6.0	Ganapathy et al., 1995
Ceftibuten	*Xenopus* oocytes	PepT1	.9 m*M*, pH 6.0	Saito et al., 1995
	Caco-2	PepT1	.9 m*M*, pH 6.0	Matsumoto et al., 1994
Cephalexin	*Xenopus* oocytes	PepT1	4.2 m*M*, pH 5.5	Fei et al., 1994
	SKPT	PepT2	49 μ*M*, pH 6.0	Ganapathy et al., 1995
Cephradine	*Xenopus* oocytes	PepT1	12.4 m*M*, pH 6.0	Saito et al., 1995
	Caco-2	PepT1	8.3 m*M*, pH 6.0	Inui et al., 1992b
Cyclacillin	*Xenopus* oocytes	PepT1	.137 m*M*, pH 5.5	Fei et al., 1994
	Caco-2	PepT1	.6 m*M*, pH 6.0	Ganapathy et al., 1995
	HeLa	PepT1	.35 m*M*, pH 5.5	Ganapathy et al., 1997
	HeLa	PepT2	50 μ*M*, pH 6.0	Ganapathy et al., 1997
	SKPT	PepT2	39 μ*M*, pH 6.0	Ganapathy et al., 1995

Literature Cited

Adibi, S.A., and Y.S. Kim. 1981. Peptide absorption and hydrolysis. 2:1073-1095. In: Johnson LR, eds. Physiology of the gastrointestinal tract. New York: Raven.

Adibi, S.A. 1997. The oligopeptide transporter (Pept-1) in human intestine: biology and function. Gastroenterology 113:332-340.

Akarawut, W., C-J. Lin, and E. David. 1998. Noncompetitive inhibition of glycylsarcosine transport by quinapril in rabbit renal brush border membrane vesicles: effect on high-affinity peptide transporter. J. Pharmacol. Exp. Ther. 287:684-690.

Alting-Mees, M. A., J. A. Sorge, and J. M. Short. 1992. pBluesscriptII: Multifunctional cloning and mapping vectors. Methods in Enzymology. 216:483-495.

Amasheh, S., U. Wenzel, M. Boll, D. Dorn, W.-M. Weber, W. Clauss, and H. Daniel. 1997a. Transport of charged dipeptides by the intestinal H+/peptide symporter PepT1 expressed in Xenopus laevis oocytes. J. Membrane Biol. 155:247-256.

Amasheh, S., U. Wenzel, W-M. Weber, W. Clauss, and H. Daniel 1997b. Electrophysiological analysis of the function of the mammalian renal peptide transporter expressed in Xenopus laevis oocytes. J. Physiol. 504:169-174.

Ames, G. F.-L., C. S. Mimura, and V. Shyamala. 1990. Bacterial periplasmic permeases belong to a family of transport proteins operating from Escherichia to human: traffic ATPases. FEMS Microbiol. Rev. 75:429-438.

Backwell, F.R.C., M. Hipolito-Reis, D. Wilson, L.A. Bruce, V. Buchan, and J.C. MacRea. 1997. Quantification of circulating peptides and assessment of peptide uptake across the gastrointestinal tract of sheep. J. Anim. Sci. 75:3315-3322.

Baker, R. D., and M. J. George. 1971. Pattern of neutral amino acid uptake along rat small intestine. Biochem. Biophys. Acta. 225:315-325.

Beauchamp, L.M., Orr G.F., de Miranda P., Doucette M., Burnette T. and W. Krenitsky. 1992. Amino acid ester prodrugs of acyclovir. Antiviral Chem. Chemother. 3**:**157-164.

Ben-Ghedalia, D., H. Tagari, and A. Bondi. 1974. Protein digestion in the intestine of sheep. Br. J. Nutr. 31:125-130.

Benson, D. A., M. Boguski, D. J. Lipman, and J. Ostell. 1996. GenBank. Nucleic Acids Res. 24:1-5.

Berger, U. V., and M. A. Hediger. 1999. Distribution of peptide transporter PepT2 mRNA in the rat nervous system. Anat. Embryol. 199:439-449.

Berlioz, F., S. Julien, A. Tsocas, J. Chariot, C. Carbon, R. Farinotti, and C. Rozé. 1999. Neural modulation of cephalexin intestinal absorption through the di- and tripeptide brush border transporter of rat jejunum in vivo. J. Pharmacol. Exp. Ther. 288:1037-1044.

Bismuth, Y., M. P. Kavanaugh, and B. I. Kanner. 1997. Tyrosine of the aminobutyric acid transporter gat-1 plays a critical role in neurotransmitter recognition. J. Biol. Chem. 272:16096-16102.

Blumenthal, E. M., and L. K. Kaczmarek. 1992. Modulation by cAMP of a slowly activating potassium channel expressed in Xenopus oocytes. J. Neurosci. 12:290-296.

Bockman D.E., V. Ganapathy, T.G. Oblak, and F.H. Leibach 1997. Localization of peptide transporter in nuclei and lysosomes of the pancreas. Int. J. Pancreatol. 22:221-5

Boll, M., D. Markovich, W.-M. Weber, H. Korte, H. Daniel, and H. Murer. 1994. Expression cloning of a cDNA from rabbit small intestine related to proton-coupled transport of peptides, β-lactam antibiotics and ACE-inhibitors. Eur. J. Physiol. 429:146-149.

Boll, M., M. Herget, M. Wagener, W.-M. Weber, D. Markovich, J. Biber, W. Clauss, H. Murer, and H. Daniel. 1996. Expression cloning and functional characterization of the kidney cortex high-affinity proton-coupled transporter. Proc. Natl. Acad. Sci. USA. 93:284-289.

Borner, V., Y.J. Fei, B. Hartrodt, V. Ganapathy, F.H. Leibach, K. Neubert, and M. Brandsch. 1998. Transport of amino acid aryl amides by the intestinal H+/peptide cotransport system, PepT1. Eur. J. Biochem. 255:698-702.

Brandsch, M., Y. Miyamoto, V.Ganapathy, and F. H. Leibach. 1994. Expression and protein kinase C-dependent regulation of peptide/H^+ co-transport system in the Caco-2 human colon carcinoma cell line. Biochem. J. 299:253-260.

Brandsch, M., V.Ganapathy, and F. H. Leibach. 1995. H^+-peptide cotransport in Madin-Darby canine kidney cells: expression and calmodulin-dependent regulation. Am. J. Physiol. 368:F391-F398.

Brandsch, M., C. Brandsch, P. D. Prasad, V. Ganapathy, U. Hopfer, and F. H. Leibach. 1995. Identification of a renal cell line that constitutively expresses the kidney-specific high-affinity H^+/ peptide cotransporter. FASEB J. 9:1489-1496.

Brandsch, M. C. Brandsch, M. E. Ganapathy, C. S. Chew, V. Ganapathy, and F. H. Leibach. 1997. Influence of proton and essential histidyl residues on the transport kinetics of the H^+/peptide cotransport systems in intestine (PepT1) and kidney (PepT2). Biochim. Biophys. Acta. 1324:251-262.

Brandsch, M., F. Thunecke, G. Küllertz, M. Schutkowski, G. Fischer, and K. Neubert. 1998. Evidence for the absolute conformational specificity of the intestinal H^+/peptide symporter, PepT1. J. Biol. Chem. 273:3861-3864.

Brendel, V., P.Bucher, I. Nourbakhsh, B.E. Blaisdell, and S. Karlin. 1992. Methods and algorithms for statistical analysis of protein sequences. Proc. Natl. Acad. Sci. USA. 89:2002-2006.

Buddington R.K., and J.M. Diamond. 1989. Ontogenetic development of intestinal nutrient transporters. Annu. Rev. Physiol. 51:601-619.

Caple, I. W. and T.J. Heath. 1975. Biliary and pancreatic secretions in sheep: Their regulation and roles. Digestion and metablism in the ruminant. pp 91-100. Univ. New England Publ. Univ. Armidale, Australia.

Casado, M., A. Bendahan, F. Zafra, N.C. Danbolt, C. Aragon, C. Gimenez, and B.I. Kanner. 1993. Phosphorylation and modulation of brain glutamate transporters by protein kinase C. J. Biol. Chem. 268:27313-27317.

Chen Q and P. H. Pekala. 1999. The influence of mRNA stability on glucose transporter (GLUT1) gene expression. Biochem. Biophys. Res. Commun. 263:265-269

Chen, X-Z, T. Zhu, D. E. Smith, and M.A. Hediger. 1999a. Stoichiometry and kinetics of the high-affinity H^+-coupled peptide transporter PepT2**.** J. Biol. Chem. 274:2773-2779.

Chen, H., E.A. Wong, and K.E. Webb, Jr. 1999b. Tissue distribution of a peptide transporter mRNA in sheep, dairy cows, pigs, and chickens. J. Anim. Sci. 77:1277-1283.

Corey, J.L., N. Davidson, H.A. Lester, N. Brecha, and M.W. Quick**.** 1994**.** Protein kinase C modulates the activity of a cloned gamma-aminobutyric acid transporter expressed in Xenopus oocytes via regulated subcellular redistribution of the transporter**.** J. Biol. Chem. 269:14759-14767.

Corpet, F. 1988. Multiple sequence alignment with hierarchical clustering. Nucleic Acids Res. 16:10881-10890.

Daniel, H., E.L. Morse, and S.A. Adibi. 1992. Determinants of substrate affinity for the oligopeptide/H^+ symporter in the renal brush border membrane. J. Biol. Chem. 267:9565-9573.

Daniel, H., and S.A. Adibi. 1994. Functional separation of dipeptide transport and hydrolysis in kidney brush border membrane vesicles. FASEB. J. 8:753-759.

Daniel, H. and S. A. Adibi. 1995. Selective effect of zinc on uphill transport of oligopeptides into kidney brush border membrane vesicles. FASEB J. 9:1112-1117.

Daniel, H. 1996. Function and molecular structure of brush border membrane peptide/H^+ symporters. J. Membrane Biol. 154:197-203.

Daniel, H. and M. Herget. 1997. Cellular and molecular mechanisms of renal peptide transport. Am. J. Physiol. 273:F1-F8.

Dantzig, A. H., J. Hoskins, L. B. Tabas, S. Bright, R. L. Shepard, I. L. Jenkins, D. C. Duckworth, J. R. Sportsman, D. Mackensen, P. R. Rosteck, Jr., and P. L. Skatrud. 1994. Association of intestinal peptide transport with a protein related to the cadherin superfamily. Science. 264:430-433.

Doring, F., D. Dorn, U. Bachfischer, S. Amasheh, M. Herget, and H. Daniel. 1997. Functional analysis of a chimeric mammalian peptide transporter derived from the intestinal and renal isoforms. J. Physiol. 497:773-779.

Döring, F., J. Walter, J. Will, M. Föcking, M. Boll, S. Amasheh, W. Clauss, and H. Daniel. 1998a. Delta-aminolevulinic acid transport by intestinal and renal peptide transporters and its physiological and clinical implications. J. Clin. Invest. 101:2761-2767.

Döring, F., Will, J., Amasheh, S., Clauss, W., Ahlbrecht, H., Daniel, H. 1998b. Minimal molecular determinants of substrates for recognition by the intestinal peptide transporter. J. Biol. Chem. 273: 23211-23218.

Dringen, R., B. Hamprecht, and S. Broer. 1998. The peptide transporter PepT2 mediates the uptake of the glutathione precursor CysGly in astrogila-rich primary cultures. J. Neurochem. 71:388-393.

Enjoh, M., K. Hashimoto, and S. Arai. 1996. Inhibitory effect of arphamenine A on intestinal dipeptide transport. Biosci. Biotechnol. Biochem. 60:1893-1895.

Erickson, R. H., J. R. Gum, Jr., M. M. Lindstrom, D. McKean, and Y. S. Kim. 1995. Regional expression and dietary regulation of rat small intestinal peptide and amino acid transporter mRNAs. Biochem. Biophys. Res. Commun. 216:249-257.

Ferraris RP, Diamond J, Kwan WW. 1988. Dietary regulation of intestinal transport of the dipeptide carnosine. Am. J. Physiol. 255:G143-G150.

Ferraris R.P., and J.M. Diamond. 1989. Specific regulation of intestinal nutrient transporters by their dietary substrates. Annu. Rev. Physiol. 51:125-141.

Fei, Y.-J., Y. Kanal, S. Nussberger, V. Ganapathy, F. H. Leibach, M. F. Romero, S. K. Singh, W. F. Boron, and M. A. Hediger. 1994. Expression cloning of a mammalian proton-coupled oligopeptide transporter. Nature. 368:563-566.

Fei, Y.-J., W. Liu, P. D. Prasad, R. Kekuda, T. G. Oblak, V. Ganapathy, and F. H. Leibach. 1997. Identification of the histidyl residue obligatory for the catalytic activity of the human H+/peptide cotransporters PepT1 and PepT2. Biochemistry. 36:452-460.

Fei, Y-J., J-C. Liu, T. Fujita, R. Liang, V. Ganapathy, F. H. Leibach. 1998. Identification of a potential substrate binding domain in the mammalian peptide transporters

PepT1 and PepT2 using PepT1-PepT2 and PepT2-PepT1 chimeras. Biochem. Biophys. Res. Commun. 246:39-44.

Fei, Y.J., E. Nara, J.C. Liu, C.A. Boyd, V. Ganapathy, and F.H. Leibach. 1999. Preferential recognition of zwitterionic dipeptides as transportable substrates by the high-affinity peptide transporter PepT2. Biochim. Biophys. Acta. 1418:344-351.

Freeman, T. C., A. J. Collins, R. P. Heavens, and D. R. Tivey. 1993. Genetic regulation of enterocyte function: a quantitative in situ hybridization study of lactase-phlorizin hydrolase and Na+-glucose cotransporter mRNAs in rabbit small intestine. Pflugers Arch. 422:570-576.

Freeman, T. C., B. S. Bentsen, D. T. Thwaites, and N. L. Simmons. 1995a. H^+/di-tripeptide transporter (PepT1) expression in the rabbit intestine. Eur. J. Physiol. 430:394-400.

Freeman, T. C., A. Howard, B. S. Bentsen, S. Legon, and J. R. F. Walters. 1995b. Cellular and regional expression of transcripts of the plasma membrane calcium pump PMCA1 in rabbit intestine. Am. J. Physiol. 269:G126-G131.

Fuhrman, S., M. Palkovits, M. Cassidy, and J. H. Neale. 1994. The regional distribution of N-acetyl aspartyl glutamate (NAAG) and peptidase activity against NAAG in the rat nervous system. J. Neurochem. 62:275-281.

Fujita, T., Y. Majikawa, S. Umehisa, N. Okada, A. Yamamoto, V. Ganapathy, and F.H. Leibach. 1999. Sigma receptor ligand-induced up-regulation of the H^+/peptide

transporter PepT1 in the human intestinal cell line Caco-2. Biochem Biophys Res Commun 261:242-246.

Ganapathy, V. and F.H. Leibach. 1983. Role of pH gradient and membrane potential in dipeptide transport in intestinal and renal brush-border membrane vesicles from the rabbit. Studies with L-carnosine and glycyl-L-proline. J. Biol. Chem. 258:14189-14192.

Ganapathy, M. E., M. Grandsch, P. D. Prasad, V. Ganapathy, and F. H. Leibach. 1995. Differential recognition of beta-lactam antibiotics by intestinal and renal peptide transporters, PepT1 and PepT2. J. Biol. Chem. 270:25672-25677.

Ganapathy, M. E., P. D. Prasad, B. Mackenzie, V. Ganapathy, and F. H. Leibach. 1997. Interaction of anionic cephalosporins with the intestinal and renal peptide transporters PepT1 and PepT2. Biochim. Biophys. Acta. 1324:296-308.

Ganapathy, M.E., H. Wei, H. Wang, V. Ganapathy, F. H. Leibach. 1998. Valacyclovir: A substrate for the intestinal and renal peptide transporters PepT1 and PepT2. Biochem. Biophys. Res. Commun. 246:470-475.

Goldin, A.L. 1992. Maintenance of Xenopus laevis and oocyte injection. Methods Enzymol. 207:266-279.

Grimble, G.K., and D.B.A. Silk. 1989. Peptides in human nutrition. Nutr. Res. Rev. 2:87-108.

Guillaume, G., M. Vanhove, J. Lamotte-Brasseur, P. Ledent, M. Jamin, B. Joris, J.-M. Frère. 1997. Site-directed mutagenesis of glutamate in two beta-lactamases: Kinetic and molecular modeling studies. J. Biol. Chem. 272:5438-5444.

Guo, A., P. Hu, P. V. Balimane, F. H. Leibach, and P. J Sinko. 1999. Interactions of a nonpeptidic drug, valacyclovir, with the human intestinal peptide transporter (hPEPT1) expressed in a mammalian cell line. J. Pharmacol. Exp. Ther. 289:448-454.

Gurdon, J. B., C. D. Lane, H. R. Woodland, and G. Marbaix. 1971. Use of frog eggs and oocytes for the study of messenger RNA and its translation in living cells. 233:177-182.

Hagting, A., E.R. Kunji, K.J. Leenhouts, B. Poolman, and W.N. Konings. 1994. The di- and tripeptide transport protein of Lactococcus lactis. A new type of bacterial peptide transporter. J. Biol. Chem. 269:11391-11399.

Han, H.K., D.M. Oh, and G.L. Amidon. 1998. Cellular uptake mechanism of amino acid ester prodrugs in Caco-2/hPEPT1 cells overexpressing a human peptide transporter. Pharm. Res. 15:1382-1386.

Han, H.K., J.K. Rhie, D.M. Oh, G. Saito, C.P. Hsu, B.H. Stewart, and G.L. Amidon. 1999. CHO/hPEPT1 cells overexpressing the human peptide transporter (hPEPT1) as an alternative in vitro model for peptidomimetic drugs. J. Pharm. Sci. 88:347-350.

Harcouët L., D. Lebrec, C. Rozé, C. Carbon, and R. Farinotti 1997. Increased intestinal absorption of cefixime by nifedipine in the rat intestinal perfusion model: evidence for a neural regulation. Pharmacol. Exp. Ther. 281:738-745.

Hediger, M.A., and D.B. Rhoads. 1994. Molecular physiology of sodium-glucose cotransporters. Physiol. Rev. 74:993-1026.

Henize, M.W. 1991. Determinants and regulation of cytoplasmic mRNA stability in eukaryotic cells. Biochem. Biophys. Acta. 1090:281-292.

Hirsch, J. R., D. D.F. Loo, and E. M.Wright. 1996. Regulation of Na^+/glucose cotransporter expression by protein kinases in *Xenopus laevis* oocytes. J. Biol. Chem. 271:14740-14746.

Hofmann K., and W. Stoffel. 1993. TMbase-A database of membrane spanning proteins segments. Biol. Chem. **347:**166-180

Inui, K. I., Y. Tomita, T. Katsura, T. Okano, M. Takano, and R. Hori. 1992. H^+-coupled active transport of bestatin via the dipeptide transport system in rabbit intestinal brush-border membranes. J. Pharmacol. Exp. Ther. 260:482-486.

Inui, K., M. Yamamoto, and H. Saito. 1992b. Transepithelial transport of oral cephalosporins by monolayers of intestinal epithelial cell line Caco-2: specific transport systems in apical and basolateral membranes. J. Pharmacol. Exp. Ther. 261:195-201.

Kennelly P. J. and E. G. Krebs. 1991. Consensus sequences as substrate specificity determinants for protein kinases and protein phosphatases. J. Biol. Chem. 266:15555-15558.

Koeln, L.L. and K.E. Webb, Jr. 1982. Peptide, erythrocyte and plasma amino acid transport across the gastrointestinal tract and liver of calves. Fed. Proc. 41:948-953.

Kozak, M. 1987. An analysis of 5'-noncoding sequences from 699 vertebrate messenger RNAs. Nucleic Acids Res. 15:8125-8148.

Kramer, W.; F. Girbig; U. Bewersdorf; S. Kohlrautz; and C. Weyland. 1998. Structural studies of the H+/oligopeptide transport system from rabbit small intestine. Biochim. Biophys. Acta. 1373:179-194.

Kyte, J., and R.F. Doolittle. 1982. A simple method for displaying the hydropathic character of a protein. J. Mol. Biol. 157:105-132.

Leibach, F. H., and V. Ganapathy. 1996. Peptide transporters in the intestine and the kidney. Annu. Rev. Nutr. 16:99-119.

Lin, C-J, W. Akarawut, and D. E. Smith. 1999. Glycylsarcosine transport by enalapril in rabbit renal brush border membrane vesicles: interaction of ACE inhibitors with high-affinity H+/peptide symporter. Pharm. Res. 16:609-615.

Lister, N., P. D. Bailey, I. D. Collier, C. A. R. Boyd, and J. R. Bronk. 1997. The influence of luminal pH on transport of neutral and charged dipeptides by rat small intestine, *in vitro*. Biochim. Biophys. Acta. 1324:245-250.

Liu, W., R. Liang, S. Ramamoorthy, Y.-J. Fei, M. E. Ganapathy, M. A. Hediger, V. Ganapathy, and F. H. Leibach. 1995. Molecular cloning of PEPT 2, a new member of the H^+/ peptide cotransporter family, from human kidney. Biochim. Biophys. Acta. 1235:461-466.

Liang, R., Y.-J. Fei, P. D. Prasad, S. Ramamoorthy, H. Han, T. L. Yang-Feng, M. A. Hediger, V. Ganapathy, and F. H. Leibach. 1995. Human intestinal H+/peptide cotransporter cloning, functional expression, and chromosomal localization. J. Biol. Chem. 270:6456-6463.

Lochs, H., P. E. Williams, E. L. Morse, N. N. Abumrad, and S. A. Adibi. 1988. Metabolism of dipeptides and their constituent amino acids by liver, gut, kidney and muscle. Am. J. Physiol. 254:E588-E594.

Mackenzie, B., Y. J. Fei, V. Ganapathy, and F. H. Leibach**.** 1996. The human intestinal H^+/oligopeptide cotransporter hPEPT1 transports differently-charged dipeptides with identical electrogenic properties. Biochim. Biophys. Acta 1284:125-128.

Mackenzie, B., D. D. F. Loo, Y-J. Fei, W. Liu, V. Ganapathy, F. H. Leibach, and E. M. Wright. 1996b. Mechanisms of the human intestinal H^+-coupled oligopeptide transporter hPepT1. J. Biol. Chem. 271:5430-5438.

Matsumoto, S., H. Saito, and K. Inui. 1994. Transcellular transport of oral cephalosporins in human intestinal epithelial cells, Caco-2: interaction with dipeptide transport systems in apical and basolateral membranes. J. Pharmacol. Exp. Ther. 270:498-504.

Matthews, D. M., and S. A. Adibi. 1976. Peptide absorption. Gastroenterology. 71:151-161.

Matthews, D. M. 1991. Protein Absorption: Development and Present State of the Subject. Wiley-liss, Inc. New York.

Matthews, J. C., E. A. Wong, P. K. Bender, J. R. Bloomquist, and K. E. Webb, Jr. 1996. Demonstration and characterization of dipeptide transport system activity in sheep omasal epithelium by expression of mRNA in *Xenopus laevis* oocytes. J. Anim. Sci. 74:1720-1727.

Meredith, D., and C. A. R. Boyd. 1995. Oligopeptide transport by epithelial cells. J. Membrane Biol. 145:1-12.

Meredith, D., C. A. R. Boyd, J. R. Bronk, P. D. Bailey , K. M. Morgan , I. D. Collier & C. S. Temple 1998. 4-Aminomethylbenzoic acid is a non-translocated competitive inhibitor of the epithelial peptide transporter PepT1. J. Physiol. 512:629-634

Miyamoto, K.-I., T. Shiraga, K. Morita, H. Yamamoto, H. Haga, Y. Taketani, I. Tamai, Y. Sai, A. Tsuji, and E. Takeda. 1996. Sequence, tissue distribution and developmental changes in rat intestinal oligopeptide transporter. Biochim. Biophys. Acta. 1305:34-38.

Moffett, J. R., L. Williamson, M. Palkovits, and M. A. A. Namboodiri. 1990. N-acetyl aspartyl glutamate: a transmitter candidate for the retinohypothalamic tract. Proc. Natl. Acad. Sci. USA. 87:8065-8069.

Muller, U., M. Brandsch, P. D. Prasad, Y.-J. Fei, V. Ganapathy, and F. H. Leibach. 1996. Inhibition of the H^+/peptide cotransporter in the human intestinal cell line Caco-2 by cyclic AMP. Biochem. Biophys. Res. Commun. 218:461-465.

Newton, A. C., and J. E. Johnson. 1998. Protein kinase C: a paradigm for regulation of protein function by two membrane-targeting modules. Biochim. Biophys. Acta. 1376:155-172.

Nunez, E. and C. Aragon. 1994. Structural analysis and functional role of the carbohydrate component of glycine transporter. J. Biol. Chem. 269:16920-16924.

Nussberger, S. A. Steel, D. Trotti, M. F. Romero, W. F. Boron, and M. A. Hediger. 1997. Symmetry of H+ binding to the intra and extracellular side of the H+-coupled oligopeptide cotransporter PepT1. J. Biol. Chem. 272:7777-7785.

Ogihara, H., H. Saito, B.-C. Shin, T. Terada, S. Takenoshita, Y. Nagamachi, K.-I. Inui, and K. Takata. 1996. Immuno-localization of H+/peptide cotransporter in rat digestive tract. Biochem. Biophys. Res. Commun. 220:848-852.

Olivares, L., Aragón, C., Giménez, C., Zafra, F. 1995. The role of N-glycosylation in the targeting and activity of the GLYT1 glycine transporter. J. Biol. Chem. 270:9437-9442

Oser, B.L. 1965. Hawk's physiological chemistry. (14 th Ed.). McGraw Hill Book Co., New York. p. 511-521.

Pan, Y., P. K. Bender, R. M. Akers, and K. E. Webb, Jr. 1996. Methionine-containing peptides can be used as methionine sources for protein accretion in cultured C_2C_{12} and MAC-T cells. J. Nutr. 126:232-241.

Pan, Y.-X., E. A. Wong, J. R. Bloomquist, and K. E. Webb, Jr. 1997. Poly(A)$^+$ RNA from sheep omasal epithelium induces expression of a peptide transport protein(s) in *Xenopus laevis* oocytes. J. Anim. Sci. 75:3323-3330.

Pan, Y., and K. E. Webb, Jr. 1998. Peptide-bound methionine as methionine sources for protein accretion and cell proliferation in primary cultures of ovine skeletal muscle. J. Nutr. 128:251-256.

Pantanowitz, S., A. Bendahan, and B.I. Kanner. 1993. Only one of the charged amino acids located in the transmembrane alpha- helices of the gamma-aminobutyric acid transporter (subtype A) is essential for its activity. J. Biol. Chem. 268:3222-3225.

Paulsen, I. T., and Skurray, R. A. 1994. The POT family of transport proteins. Trends Biochem. Sci. 19: 404-404.

Payne, J. W., and M. W. Smith. 1994. Peptide transport by micro-organisms. Adv. Microbiol. Physiol. 36:1-15.

Peng, H. and J. E. Lever. 1995. Post-Transcriptional Regulation Of Na^+-Glucose Cotransporter (*SGTL1*) Gene Expression In LLC-PK_1 Cells. J. Biol. Chem. 270:20536-20542.

Perry, J.R., M.A. Basrai, H-Y. Steiner, F. Naider, and J.M. Becker. 1994. Isolation and characterization of a Saccharomyces cerevisiae peptide transport gene. Mol. Cell. Biol. 14:104-115.

Phillips, W. A., K. E. Webb, Jr., and J. P. Fontenot. 1976. In vitro absorption of amino acid by the small intestine of sheep. J. Anim. Sci. 42:201-207.

Phillips, W. A., K. E. Webb, Jr., and J. P. Fontenot. 1979. Characteristics of threonine, valine, and methionine absorption in the jejunum and ileum of sheep. J. Anim. Sci. 48:926-933.

Puissant, C., and L.-M. Houdebine. 1990. An improvement of the single-step method of RNA isolation by acid guanidinium thiocyanate-phenol-chloroform extraction. BioTechniques 8:148-149.

Ramamoorthy, S., W. Liu, Y-Y. Ma, T. L. Yang-Feng, V. Ganapathy, F.H. Leibach. 1995. Proton/peptide cotransporter (PepT2) from human kidney: Functional characterization and chromosomal location. Biochim. Biophys. Acta. 1240:1-4.

Rothman, J. E. and L. Orci. 1992. Molecular dissection of the secretory pathway. Nature. 355:409-415.

Rothman, J. E. 1994. Mechanisms of intracellular protein transport. Nature 372:55-64.

Sachs, A.B. 1993. Messenger RNA degradation in eukaryotes. Cell 74:413-421.

Saier, Jr. M. H. 1994. Computer-aided analyses of transport protein sequences: Gleaning evidence concerning function, structure, biogenesis, and evolution. Microbiol. Rev. 58:71-93.

Saier Jr., M. H., B. H. Eng, S. Fard, J. Garg, D. A. Haggerty, W. J. Hutchinson, D. L. Jack, E. C. Lai, H. J. Liu, D. P. Nusinew, A. M. Omar, S. S. Pao, I. T. Paulsen, J. A. Quan, M. Sliwinski, T-T. Tseng, S. Wachi, G. B. Young. 1999. Phylogenetic characterization of novel transport protein families revealed by genome analyses. Biochim. Biophys. Acta. 1422:1-56.

Saito, H., M. Okuda, T. Terada, S. Sasaki, and K.-I. Inui. 1995. Cloning and characterization of a rat H^+/peptide cotransporter mediating absorption of beta-lactam antibiotics in the intestine and kidney. J. Pharmacol. Exp. Therap. 275:1631-1637.

Saito, H., T. Terada, M. Okuda, S. Sasaki, and K.-I. Inui. 1996. Molecular cloning and tissue distribution of rat peptide transporter PepT2. Biochim. Biophys. Acta. 1280:173-177.

Sambrook, J., E. F. Fritsch, and T. Maniatis. 1989. Molecular cloning: a laboratory manual (2nd Ed.). Cold Spring Harbor, NY.

Sawada, K., Terada, T., Saito, H., Hashimoto, Y., Inui, K.-I. (1999). Recognition of L-amino acid ester compounds by rat peptide transporters PepT1 and PepT2. J. Pharmacol. Exp. Ther. 291:705-709.

Seal, C. J., and D. S. Parker. 1991. Isolation and characterization of circulating low molecular weight peptides in steer, sheep and rat portal and peripheral blood. Comp. Biochem. Physiol. 99B:679-685.

Seal, C. J., and D. S. Parker. 1996. Effect of intraruminal propionic acid infusion on metabolism of mesenteric- and portal-drained viscera in growing steers fed a forage diet: II. Ammonia, urea, amino acid, and peptides. J. Anim. Sci. 74:245-256.

Shen, H.; D.E. Smith, T. Yang, Y.G. Huang, J.B. Schnermann, and F.C. Brosius, 3rd. 1999. Localization of PepT1 and PepT2 proton-coupled oligopeptide transporter mRNA and protein in rat kidney. Am. J. Physiol. 276:F658-65.

Shiraga, T., Miyamoto, K.-I., Tanaka, H., Yamamoto, H., Taketani, Y., Morita, K., Tamai, I., Tsuji, A., Takeda, E. (1999). Cellular and molecular mechanisms of dietary regulation on rat intestinal H^+/peptide transporter PepT1. Gastroenterology. 116:354-362.

Sinko, P.J. and P.V. Balimane. 1998. Carrier-mediated intestinal absorption of valacyclovir, the L-valyl ester prodrug of acyclovir: 1. Interactions with peptides, organic anions, and organic cations in rats. Biopharm. Drug Dispos. 19**:**209-217.

Smith, D.E., A. Pavlova, U.V. Berger, M.A. Hediger, T, Yang, Y.G. Huang, and J.B. Schnermann. 1998. Tubular localization and tissue distribution of peptide transporters in rat kidney. Pharm. Res. 15:1244-1249.

Snyder, N.J.; L.B. Tabas,; D.M. Berry,; D.C. Duckworth, D.O. Spry, and A.H. Dantzig. 1997. Structure-activity relationship of carbacephalosporins and cephalosporins: Antibacterial activity and interaction with the intestinal proton-dependent dipeptide transport carrier of Caco-2 cells. Antimicrob. Agents Chemother. 41:1649-1657.

Soderlund, D.M., J.R. Bloomquist, F. Wong, L.L. Payne, and D.C. Knipple. 1989. Molecular neurobiology: Implications for insecticide action and resistance. Pestic. Sci. 26:359-374.

Steel, A., S. Nussberger, M. F. Romero, W. F. Boron, C. A. R. Boyd, and M. A. Hediger. 1997. Stoichiometry and pH dependence of the rabbit proton-dependent oligopeptide transporter PepT1. J. Physiol. 498:563-569.

Steiner, H.Y.,W.Song, L. Zhang, F. Naider, J.M. Becker, G. Stacey. 1994. An Arabidopsis peptide transporter is a member of a new class of membrane transport proteins. Plant Cell. 6:1289-1299.

Swaan, P. W., M. F. C. Stehouwer, and J. J. Tukker. 1995. Molecular mechanisms for the relative binding affinity to the intestinal peptide carrier: Comparison of three ACE inhibitors: enalapril, enalaprilat, and lisinopril. Biochim. Biophys. Acta. 1236:31-38.

Swaan, P.W., and J.J. Tukker. 1997. Molecular determinants of recognition for the intestinal peptide carrier. J. Pharm. Sci. 86:596-602.

Swaan, P.W., B. C. Koops, E. E. Moret, and J. J. Tukker. 1998. Mapping the binding site of the small intestinal peptide carrier (PepT1) using comparative molecular field analysis. Receptors Channels 6:189-200.

Tacnet, F., F. Lauthier, and P. Ripoche. 1993. Mechanisms of zinc transport into pig small intestine brush-border membrane vesicles. J. Physiol. 465:57-72.

Takahashi, K., Nakamura, N., Terada, T., Okano, T., Futami, T., Saito, H., Inui, K.-I. (1998). Interaction of beta-lactam antibiotics with H^+/peptide cotransporters in rat renal brush-border membranes. J. Pharmacol. Exp. Ther. 286:1037-1042.

Tam, R., and M.H. Saier, Jr. 1993. Structural, functional, and evolutionary relationships among extracellular solute-binding receptors of bacteria. Microbiol. Rev. 57:320-46.

Taylor, R.B. 1962. Pancreatic secretion in the sheep. Res. Vet. Sci. 3:63-69.

Tamai, I, T. Nakanishi, H. Nakahara, Y. Sai, V. Ganapathy, F. H. Leibach, and A. Tsuji. 1998. Improvement of L-dopa absorption by dipeptidyl derivation, utilizing peptide transporter PepT1. J. Pharm. Sci. 87:1542-1546.

Tanaka, H., Miyamoto, K.-I., Morita, K., Haga, H., Segawa, H., Shiraga, T., Fujioka, A., Kouda, T., Taketani, Y., Hisano, S., Fukui, Y., Kitagawa, K., Takeda, E. 1998. Regulation of the PepT1 peptide transporter in the rat small intestine in response to 5-fluorouracil-induced injury. Gastroenterology 114:714-723.

Temple CS; Bronk JR; Bailey PD; Boyd CA 1995. Substrate-charge dependence of stoichiometry shows membrane potential is the driving force for proton-peptide cotransport in rat renal cortex. Pflugers Arch. 430:825-829.

Temple, C.S. and C.A.R. Boyd. 1998. Proton-coupled oligopeptide transport by rat renal cortical brush border membrane vesicle: a functional analysis using ACE inhibitors to determine the isoform of the transporter. Biochim. Biophys. Acta 1373:277-281.

Temple, C. S., A. K. Stewart, D. Meredith, N. A. Lister, K. M. Morgan, I. D. Collier, R. D. Vaughan-Jones, C. A. R. Boyd, P. D. Bailey, and J. R. Bronk. 1998. Peptide mimics as substrates for the intestinal peptide transporter. J. Biol. Chem. 273:20-22.

Terada T, H. Saito, M. Mukai, and K. Inui. 1996. Identification of the histidine residues involved in substrate recognition by a rat H^+/peptide cotransporter, PepT1. FEBS Lett. 394:196-200

Terada T, H. Saito, M. Mukai, and K. Inui 1997. Recognition of β-lactam antibiotics by rat peptide transporters, PepT1 and PepT2, in LLC-PK_1 cells. Am. J. Physiol. 273:F706-F711.

Terada, T., H. Saito, and K. Inui. 1998. Interaction of β-lactam antibiotics with histidine residue of rat H^+/peptide cotransporters, PepT1 and PepT2. J. Biol. Chem. 273:5582-5585.

Terada T., K. Sawada, H. Saito, Y. Hashimoto, and K-I. Inui. 1999. Functional characteristics of basolateral peptide transporter in the human intestinal cell line Caco-2. Am. J. Physiol. 276:G1435-G1441.

Tsuji, A., I. Tamai, M. Nakannishi, and G.L. Amidon. 1990. Mechanism of absorption of the dipeptide α-methyldopa-phe in intestinal brush border membrane vesicles. Pharm. Res. 7:308-309.

Vilner, B. J., C. S. John, and W. D. Bowen. 1995a. Sigma-1 and sigma-2 receptors are expressed in a wide variety of human and rodent tumor cell lines. Cancer Res. 55:408–413.

Vilner, B. J., B. R. De Costa, and W. D. Bowen. 1995b. Cytotoxic effects of sigma ligands: Sigma receptor-mediated alterations in cellular morphology and viability. J. Neurosci. 15:117–134.

Walker, D., D. T. Thwaites, N. L. Simmons, H. J. Gilbert, and B. H. Hirst. 1998. Substrate upregulation of human small intestinal peptide transporter, hPEPT1. J. Physiol. 507:696-706.

Wang, H.P., H.H. Lu, J.S. Lee, C.Y. Cheng, J.R. Mah, C.Y. Ku, W. Hsu, C.F. Yen, C.J. Lin, and H.S. Kuo. 1996. Intestinal absorption studies on peptide mimetics α-methyldopa prodrug. J. Pharm. Pharmacol. 48:270-276.

Wang, H., Y-J. Fei, V. Ganapathy, and F. H. Leibach. 1998. Electrophysiological characteristics of the proton-coupled peptide transporter PepT2 cloned from rat brain. Am. J. Physiol. 275: C967-C975.

Wenzel, U., D. T. Thwaites, and H. Daniel. 1995. Stereoselective uptake of β-lactam antibiotics by the intestinal peptide transporter. Br. J. Pharmacol. 116:3021-3027.

Wenzel, U., I. Gebert, H. Weintraut, W.-M. Weber, W. Claub, and H. Daniel. 1996. Transport characteristics of differently charged cephalosporin antibiotics in oocytes expressing the cloned intestinal peptide transporter PepT1 and in human intestinal Caco-2 cells. J. Pharmacol. Exp. Therap. 277:831-839.

Wenzel, U., D. Diehl, M. Herget, and H. Daniel. 1998. Endogenous expression of the renal high-affinity H^+-peptide cotransporter in LLC-PK_1 cells. Am. J. Physiol. 275:C1573-C1579.

Wenzel U., D. Diehl, M. Herget, S. Kuntz, and H. Daniel. 1999. Regulation of the high-affinity H+/peptide cotransporter in renal LLC-PK1 cells. J. Cell Physiol. 178:341-348

Wilson, J. W., and K. E. Webb, Jr. 1990. Lysine and methionine transport by bovine jejunal and ileal brush border membrane vesicles. J. Anim. Sci. 68:504-514.

Wright, E. M., K. M. Hager, and E. Turk. 1992. Sodium cotransport proteins. Current Opin. Cell Biol. 4:696-702.

Wright, E.M., J.R. Hirsch, D.D.F. Loo, and G. A. Zampighi. 1997. Regulation of Na+/glucose cotransporters. J. Exp. Biol. 200:287-293.

Yamashita, T., S. Shimada, W. Guo, K. Sato, E. Kohmura, T. Hayakawa, T. Takagi, and M. Tohyama. 1997. Cloning and functional expression of a brain peptide/histidine transporter. J. Biol. Chem. 272:10205-10211.

Yeung, A.K., S.K. Basu, S.K. Wu, C. Chu, C.T. Okamoto, S.F. Hamm-Alvarez, H. von Grafenstein, W-C. Shen, K-J. Kim, M.B. Bolger, I.S. Haworth, D.K. Ann, and V.H.L. Lee. 1998. Molecular identification of a role for tyrosine 167 in the

function of the human intestinal proton-coupled dipeptide transporter (hPEPT1). Biochem. Biophys. Res. Comm. 250:103-107.

Zhu, S.-J., Kavanaugh, M. P., Sonders, M. S., Amara, S. G., Zahniser, N. R. 1997. Activation of protein kinase c inhibits uptake, currents and binding associated with the human dopamine transporter expressed in *Xenopus* oocytes. J. Pharmacol. Exp. Ther. 282:1358-1365

Vita

YuanXiang Pan, son of Guangyan Pan and Deyin Luo, was born in October 1967, in Lanzhou, Gansu, P. R. of China. He was graduated from Lanzhou University, with a Bachelor of Science degree in Cell Biology in July 1990. He married Hong Chen in August 1992. He came to Virginia Tech in August 1994 and initiated his program of graduate study in Protein Nutrition. He received financial support from the John Lee Pratt Animal Nutrition Program for five years.

He is a member of the American Society of Animal Science, American Society of Nutritional Sciences, Gamma Sigma Delta, and Sigma Xi.